
This item was submitted to [Loughborough's Research Repository](#) by the author.
Items in Figshare are protected by copyright, with all rights reserved, unless otherwise indicated.

An investigation into vibration-testing techniques for aero-engine accessories

PLEASE CITE THE PUBLISHED VERSION

PUBLISHER

Loughborough University of Technology

LICENCE

CC BY-NC 4.0

REPOSITORY RECORD

Holme, Anthony H.E.. 2020. "An Investigation into Vibration-testing Techniques for Aero-engine Accessories".
Loughborough University. <https://doi.org/10.26174/thesis.lboro.13089404.v1>.

LOUGHBOROUGH
UNIVERSITY OF TECHNOLOGY
LIBRARY

AUTHOR/FILING TITLE

HOLME, AHE

ACCESSION/COPY NO.

001032/02

VOL. NO.

CLASS MARK

~~date due:-~~

~~LOAN COPY~~

~~- 9 DEC 1994~~

~~- 9 JUL 1983~~

~~LOAN 1 MTH + 2~~
~~UNLESS RECALLED~~
~~EDINBURGH~~

~~date due:-~~

~~- 9 DEC 1994~~

~~- 5 AUG 1992~~

~~LOAN 3 WKS. + 3~~
~~UNLESS RECALLED~~

~~- 5 JUL 1991~~

~~SOLICITORS~~

~~DEBBY~~
~~date due:~~

~~10-9-92.~~

~~- 3 NOV 1992~~

000 1032 02



AN INVESTIGATION INTO VIBRATION TESTING TECHNIQUES FOR

AERO - ENGINE ACCESSORIES

by

Anthony Hugh Edward Holme

A Master's Thesis

Submitted in partial fulfilment of the requirements for the award
of Master of Science of the Loughborough University of Technology
January 1983

Loughborough University	
of Technology	
Date	14 June 83
Class	
Acc. No.	001033/02

An Investigation into Vibration Testing Techniques for Aero-Engine Accessories

by A H E Holme

Abstract

The design of an aero-engine accessory requires a statement of its functional objectives and a knowledge of its operational environment. Achievement of these design objectives is the subject of its development programme. However, experience has shown that in spite of successful completion of development testing this has not always resulted in acceptable Service performance. In particular this has been true of the simulation of the engine vibration environment.

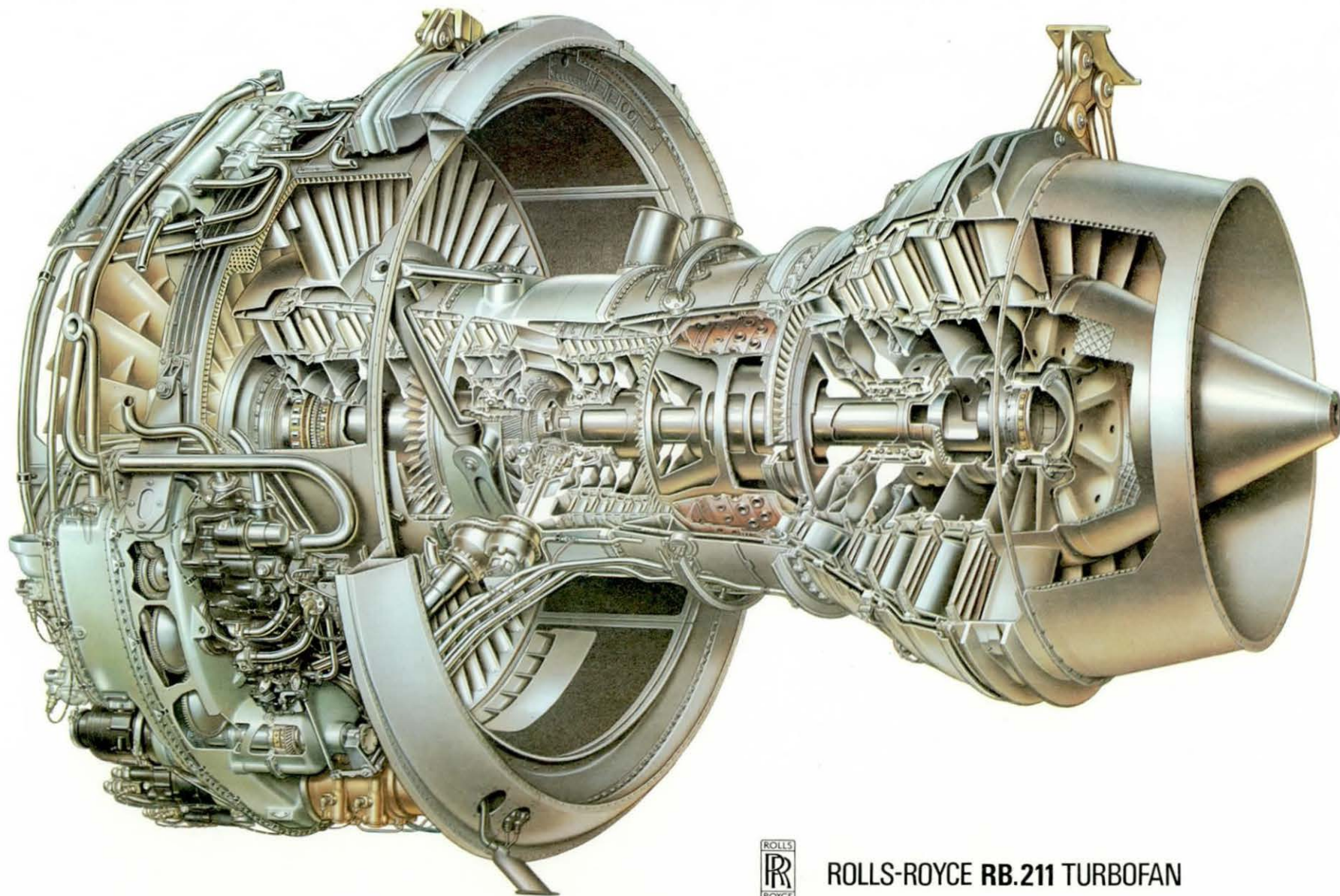
Based on a series of vibration tests a revised technique is developed for improved rig simulation of the engine based on a Spoke or Campbell Diagram and multi-sine endurance testing.

An extension of this revision to engine testing is given which advances the accuracy of service reliability predictions. This involves a Severity Criterion based on the resultant vibration velocity amplitude from three orthogonal measurement directions and augmented by a Mission Weighting.

A further investigation to improve reliability prediction is discussed based on structural dynamic modelling of the accessory. It is argued that this may be better achieved by modal testing than by purely theoretical methods although this depends on the accessory and degree of sophistication required.

Where relevant, case histories are cited to illustrate the arguments put forward.

Keywords Aero-engine, Accessory, Vibration Test, Reliability, Modelling.



ROLLS-ROYCE **RB.211** TURBOFAN

Acknowledgements

As with most industrial based projects there have been many personnel both at Rolls-Royce, Ltd, Derby and their accessory suppliers who have contributed in various ways to the work of this thesis and the author is grateful for their assistance which is acknowledged by reference to their reported work. In particular the involvement and guidance of D S Pearson, Project Development Engineer - Measurement Engineering - as instigator of this project and his successor P R Watts is gratefully acknowledged. Within the Accessory Development Group at Derby the help and comments of S G Smout, D G Goodall and A H Sherwood have been much appreciated.

The author is also pleased to acknowledge the assistance and encouragement in the completion of this work received from C A Foord of the Experimental Vibration Department.

The author is very appreciative of the comments, guidance and assistance received from his supervisors in the Transport Technology Department at Loughborough University, M G Milsted and E G Jenkins.

Finally, the author would like to thank Rolls-Royce Ltd for sponsoring this research project and for giving permission to publish the work contained within this thesis.

Preamble

A Being based on industrial experience this work has benefited from the contributions of many colleagues, especially those in the Measurement Engineering and Accessory Development Departments. As such, it is difficult for anyone to claim originality for any particular idea as it will have been argued and discussed by those involved before reaching the refinement illustrated in this thesis. However the author has provided continuity throughout this work and has been responsible for guiding it to a point where it is being applied by others. In particular while contributing to the original discussions on the Spoke Diagrams and Severity Criterion the author was responsible for developing their application to accessory engine testing together with the extension of this work to transfer function testing and modelling.

B Due to Rolls-Royce's involvement in the international aircraft industry the Company uses a mixture of units; American, Imperial and SI. Although there appears to be a slow drift towards the general adoption of SI units, in vibration work the aircraft industry still tends to use Imperial units. Therefore in this thesis the author has kept to existing Company practice while quoting SI equivalents in parantheses.

<u>Contents</u>	<u>Page No</u>
Abstract	2
Acknowledgements	4
Preamble	5
<u>1.0 Introduction</u>	10
1.1 Accessory Groupings	11
1.2 Accessory Design Specification	14
1.3 Accessory Environment - General	14
1.4 Accessory Environment - Vibration	15
1.5 Accessory Vibration Testing	16
1.6 Aims of Thesis	19
<u>2.0 Vibration Experience in Service</u>	20
2.1 Lower Teleflex Control Box Testing	21
2.2 Lower Teleflex Control Box Testing - Problem Solutions	28
2.3 Summary	29
<u>3.0 Accessory Test Revisions</u>	30
3.1 The Spoke Diagram	30
3.2 Derivation of the Spoke Diagram	32
3.3 Use of the Spoke Diagram in Endurance Testing	34
a) Endurance Period	34
b) Mission Weighting	38
c) Endurance Testing Levels	39
3.4 Use of the Spoke Diagram - Fuel Flow Regulator Case History	41
3.5 Summary	42
<u>4.0 Assessing the Vibration Environment</u>	44
4.1 Severity Criterion	46
4.2 Mission Weightings	50
4.3 Testing the Severity Criterion	52
4.4 Summary	53
<u>5.0 Modelling the Accessory</u>	58
5.1 Modal Test Results	62
5.2 Spring - Mass Sub-system Representation	66
5.3 Modal property Estimate using Vector Techniques	71
5.4 Summary	77

<u>Contents</u>	<u>Page No</u>
6.0 <u>Conclusions</u>	78
7.0 <u>References</u>	82
7.1 Introductory References	82
7.2 Vibration Experience References	83
7.3 Accessory Test Revision References	85
7.4 Environment Assessment References	89
7.5 Modelling References	93
7.6 Appendices References	94
Appendix A - Lower Teleflex Control Box - Problem Solution Testing	96
Appendix B - Fuel Flow Regulator - Testing the new technique	103
Appendix C - Fuel Flow Regulator Modelling	115
C.1 Modal Test Method	116
C.2 Partially Assembled FFR Results	119
C.3 FFR Fuel Side Body Results	122
C.4 Estimate of Dynamic Mass	124
C.5 Listing of Circle Fit Program	126
Appendix D - Signal Processing Techniques	132
Appendix E - Summary of Excitation Techniques	
E.1 Swept Sine	
E.2 Random	
E.3 Transient	
Appendix F - Use of RMS Velocity	136

List of Figures

RB 211 Turbofan	3
1.1 Engine Accessory Groupings	13
1.2 Frequency Spectrum of Typical Accessory	17
2.1 Detail of Throttle Control System	22
2.2 Vibration Associated Problems on lower Teleflex Box.	23
2.3 High Speed Gearbox Drive Orders	25
2.4 Teleflex Conduit Vibratory Stress Levels.	24
2.5 Locus of Teleflex Conduit	27
3.1 Spoke and Response Diagrams	33
3.2 Developed Spoke Diagram and Vibration Envelopes	35

<u>Contents</u>	<u>Page No</u>
<u>List of Figures continued</u>	
3.3 Assumed Accessory Fatigue Curve	37
4.1 Summary of Vibration Assessment	45
4.2 Peak Accessory Vibration Levels	47
4.3 Mission Profile and Weighting Factors	51
4.4 Severity Assessment from Vrms plots - Solenoid Valve	56
4.5 Severity Assessment from Vrms plots - FFR	57
5.1 Photograph of Test Fuel Flow Regulator	60
5.2 Photograph of Test Rig	61
5.3 Point Mobility Plot - FFR	65
5.4 Point Mobility Plot - FFR Fuel Side with Skeleton	67
5.5 Mass - Spring Subsystem Representation of FFR Fuel Side Body	68
5.6 Nyquist Plot of FFR Fuel Side Body	74
5.7 Nyquist Plot of Modal Circle	75
5.8 Schematic and Mode Shape of FFR Fuel Side Body	76
6.1 Summary of Vibration Severity Criterion	81
A.1 Coherence and Correlation Limitations	98
A.2 Comparison of Standard and Modified Teleflex Rack Modes	100
A.3 Effect of Balancing Gearbox Drive	101
A.4 'Bowstring' Teleflex Control Box	102
B.1 Fuel Flow Regulator - Detail	104
B.2 Frequency Spectrum - FFR Stirrup Assembly	105
B.3 Details of FFR Stirrup Transducer Location	107
B.4 10 KW Shaker Rig	109
B.5 20 KW Shaker Rig	110
B.6 Change in VMO position with time	111
B.7 Summary of Excitation Levels used in FFR Test	112
B.8 Change in Stirrup Frequency Spectrum - Original Unit	113
B.9 Change in Stirrup Frequency Spectrum - Modified Unit	114
C.1 SD 1002E Transfer Function Analyser Block Diagram	117
C.2 Point Mobility Plot - FFR with Fuel Side Internals removed	118
C.3 Point Mobility Plot - FFR Fuel Side Body only	120
C.4 As C3 - 1000 to 8000 Hz	121
C.5 Schematic of FFR for mass calculation	122

Contents

Page No

List of Figures Continued

D.1	Campbell Diagram Plot Formats	130
D.2	Campbell Diagram System Block Diagram	131
E.1	Random Signal Types	133
E.2	Time-Frequency Domain Consideration	134
E.3	Transient Signal Types	135

List of Tables

1.1	Accessory Groupings by Function	11
1.2	Accessory Groupings by Environment	12
3.1	Example of Possible Mission	38
3.2	Amplitude Factors and Endurance Periods	40
3.3	Vibration Specification Amplitude Factors	41
4.1	Severity Classification for Aero-engine Accessories	48
4.2	Severity Classification for Turbo Machinery	49
4.3	Summary of RB 211-535C Accessory Vibration Classifications	55

1.0 INTRODUCTION

The correct function and operation of a gas turbine aero-engine is monitored and controlled by various units. These are collected under the generic name of 'accessory' since they might be considered additional to the main engine components of compressors, combustion and turbines. However, the major engine components could not function correctly or safely without the various accessories and hence these latter items are an integral part of the whole engine.

In order to perform correctly there must be clear definition of what the particular accessory's function is likely to be, together with a knowledge of the environmental constraints imposed on the accessory by virtue of its function and location.

These two factors, function and environment, are defined in an accessory design specification (or similarly titled document). This specification is necessarily issued ahead of a new engine design, or derivative, and hence contains a certain amount of estimation, based on design predictions and past experience, of the actual requirements and environment of the installed accessory. Of various environmental parameters accessory vibration is arguably the least accurately predicted. The reasons for this are complex and are based on the difficulties inherent in modelling the structures involved. Hence to a large extent specification of the vibration environment relies on experience until representative hardware is available for test verification. This has led to vibration problems being discovered late in a development programme or after entry into aircraft service. Why this should be will become apparent from an understanding of existing techniques and requirements. This thesis will then present arguments for improvements in both test techniques and service reliability predictions. This prediction is based on extending existing severity standards to aero-engine accessories.

This approach has been summarized in references 7.1.1 - 7.1.3. Further, by looking at modal testing of a typical accessory structure a method of modelling the dynamic properties of the accessory is demonstrated which could be used when modelling whole engine responses.

These points will be illustrated by specific case histories where appropriate.

1.1 Accessory Groupings

Accessory functions can be broadly classified as those which control the operation of the engine and those which monitor this operation. In the former group would be included fuel pumps and metering systems, compressor Bleeds and variable vane controls. Typical examples of the latter group would be pressure and temperature sensors, thrust indicators and vibration monitors.

Further groupings of accessory types are made by the method used to perform their function. These groupings have comprised hydro-mechanical, electro-mechanical, electrical/electronic and 'others'. Examples of accessories within these groups are shown in Table 1.1 although it is probable that more functions will fall within the electrical/electronic grouping in future years.

TABLE 1.1 ACCESSORY GROUPINGS BY FUNCTION

HYDRO-MECHANICAL	ELECTRO-MECHANICAL	ELECTRICAL/ELECTRONIC	OTHERS
LP Fuel Pump	Solenoid Control Valve	Control Amplifiers	Air Starters
HP Fuel Pump	Constant Speed Drives And Alternators	Igniter Units	Thrust Reverser Drive Motors/Actuating Rams
Fuel Flow Regulator		Thrust Indicators	
Hydraulic Pumps	Variable Inlet Guide Vane Controllers	Pressure Transducers	Fuel/Oil Filters
Oil Delivery and Scavenge Pumps	Shut-Off Cocks	Temperature Indicators	Fuel/Oil Coolers
	Tachometers	Vibration Indicators	Bleed Valves
	Fuel Flow Meters	Junction Boxes	Throttle Linkage Control Boxes

As with accessory functions the environment too can be split into its various aspects; this commonly comprising pressure, temperature, vibration and 'miscellaneous'. This last mentioned containing such considerations as resistance to contaminants and fire.

The environmental aspects also result in a final sub-division of accessories namely those directly mounted on the engine casing and those which in addition require motive power from the engine and are usually mounted and driven from a gearbox. Typical examples are shown in Table 1.2

TABLE 1.2 ACCESSORY GROUPINGS BY ENVIRONMENT

NON-DRIVEN, CASING MOUNTED	DRIVEN, GEARBOX MOUNTED	MISCELLANEOUS
Solenoid Valves - Various	Fuel Pumps, LP and HP	Speed Probes
Thrust Indication Transmitter	Fuel Flow Regulator	Thrust Reverser Actuators
Amplifiers - Various	Hydraulic/Oil Pumps	
Fuel/Oil Coolers, Filters	Aircraft Electrical Generators	
Temp/Pressure Sensors	Starter Motor	
Vibration Transmitter		
Igniter System		
Fire Detector/Extinguisher		

It is important to note these various divisions since each needs to be taken into account when designing a particular accessory for use on an aero-engine which itself has to meet the aircraft operating environment. A summary of these groupings is given in figure 1.1.

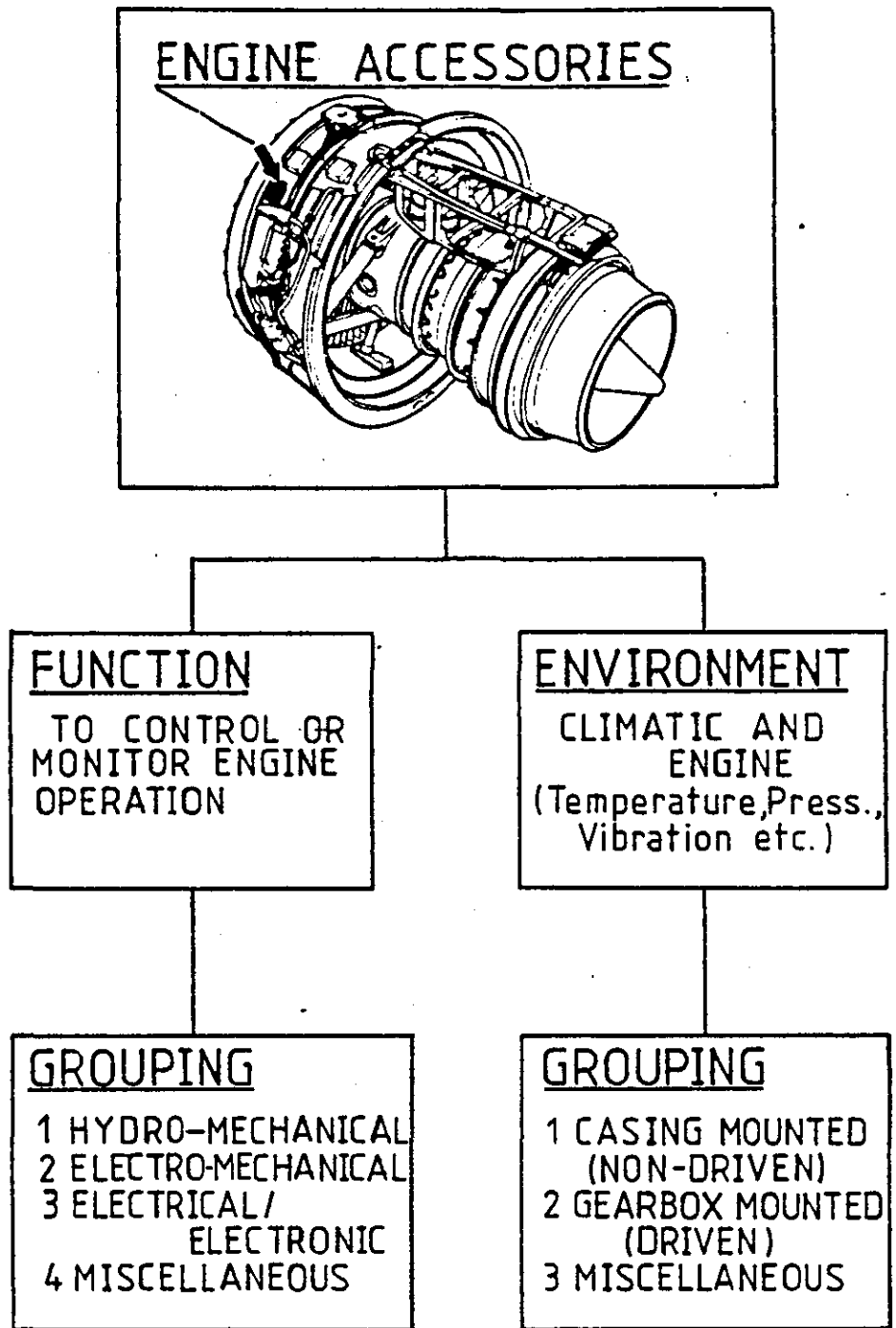


Fig. 1.1

1.2 Accessory Design Specification

It is essential when designing a new accessory to know the operational purpose of the function the accessory is required to perform. This is necessarily defined at the start of the design specification. Closely tied to this is the performance of the accessory. This could include its construction and method of operation together with any operating constraints. These last mentioned would include pressure and temperature ranges, input and/or output required together with response rates, tolerances and accuracies. As can be surmised from the accessory groupings there is a large variation in performance characteristics depending on the accessory's function.

A typical specification continues by defining general design and environmental requirements. The former includes such topics as life and reliability while the latter includes temperature and pressure regimes, a list of possible contaminants, climatic environment, operational loadings and the vibration environment.

Later sections deal with the whole gamut of development and production unit testing required to show compliance with the defined purpose.

1.3 Accessory Environment - General

Whatever the accessory it has to be capable of operating on the ground between -40°C (an Alaskan winter) and 50°C (summer in the Middle East). The effects of ambient pressure and temperature changes with altitude also need to be accounted for in the basic design with variations from 15.2 psi (1047 mbar) at 17°C to 2.1 psi (145 mbar) at -57°C for typical commercial flight operations. However although these temperatures and pressures may be considered to be extremes of our earthly environment the accessory in operation could well be subjected to a differing set of pressures and temperatures due to the operations of the engine. These engine generated environments will normally increase the pressures and temperatures well above their normal ambient levels. For example, core engine casing temperatures could reach $6-700^{\circ}\text{C}$ and HP Compressor delivery pressure could be of the order of 425 psi (29.3 bar). It is unlikely that any particular accessory would have to survive simultaneously

all these extremes of pressure and temperature, but not impossible e.g. compressor bleed valves.

In addition to pressure and temperature consideration an accessory shall be able to withstand contamination from fuel, oil or hydraulic fluid spillages or leaks. Further, various additives or cleaning fluids should not cause malfunctions when in contact with the accessory. Water in the form of rain or sea spray should not cause faults or corrosion, this being of particular concern with electrical equipment. All accessories should be able to withstand or contain fire to varying extents. It is far more important for units containing fuel to be fire resistant than for an amplifier.

These environmental considerations are set out for each accessory in its own design specification but a general statement of them is given in the British Standard Specification for General Requirements for Equipment in Aircraft, BS.36.100 (Reference 7.1.4). In addition the various tests necessary to show compliance with the above specifications are also detailed. Similar standards such as Reference 7.1.5 exist in America.

1.4 Accessory Environment - Vibration

Additional to the various constraints outlined previously the vibration environment in which the accessory will have to function is of great interest. As well as vibration resulting from normal engine operation mounting loads resulting from various landing and flight manoeuvres have to be specified in the design requirements.

Mounting loads are quoted as velocity or acceleration levels seen at the accessory mounts due to aircraft manoeuvres such as climb and descent, pitch or yaw, as well as those associated with taxiing, take-off and landing. These manoeuvres are assumed to be resulting in zero frequency loadings and hence it is only the basic rigid body modes of vibration which concern the designer.

During normal engine operation the rotor dynamic excitations generated by the engine are of prime concern as these encompass

frequencies from 10 to 10,000 Hz. However the effects of the very high frequencies which are generated by rotor blade passing orders (no of blades/stage multiplied by rotational speed) or gear meshing orders (no of gear teeth multiplied by gear rotational speed) are difficult to quantify and hard to measure experimentally. The effects are likely to be seen as fretting, wear or localised wall resonances of the accessory.

Design Specifications have therefore never exceeded 3000 Hz in this country or 2000 Hz in the USA. These frequency limits being considered reasonable to bound both basic accessory resonances and test constraints imposed by excitation and measurement systems.

A summary of vibration regions for a typical accessory is shown in the Campbell Diagram of figure 1.2. The derivation of this plot is described in Appendix D.

1.5 Accessory Vibration Testing

Having defined the accessory's functional objective and the environmental conditions in which it will have to operate it is necessary to show that it will meet these requirements. To wait until the finished article is available and then test it on the engine is likely to result in failure to meet the design requirements. This would necessarily result in delay and expense to both engine and accessory programmes. Depending on the particular accessory it is necessary to validate the operation of the various sub-systems as well as the complete accessory. Hence modifications can be incorporated as required before committing the design to full production.

This testing is performed on various rigs which are set up to try and simulate predicted engine operation, assuming a completely new accessory and engine design. However most accessory and engine designs are based to some extent on existing systems and hence some testing maybe curtailed or omitted, an engineering judgement being made by the responsible designer on what is necessary in agreement with his customer.

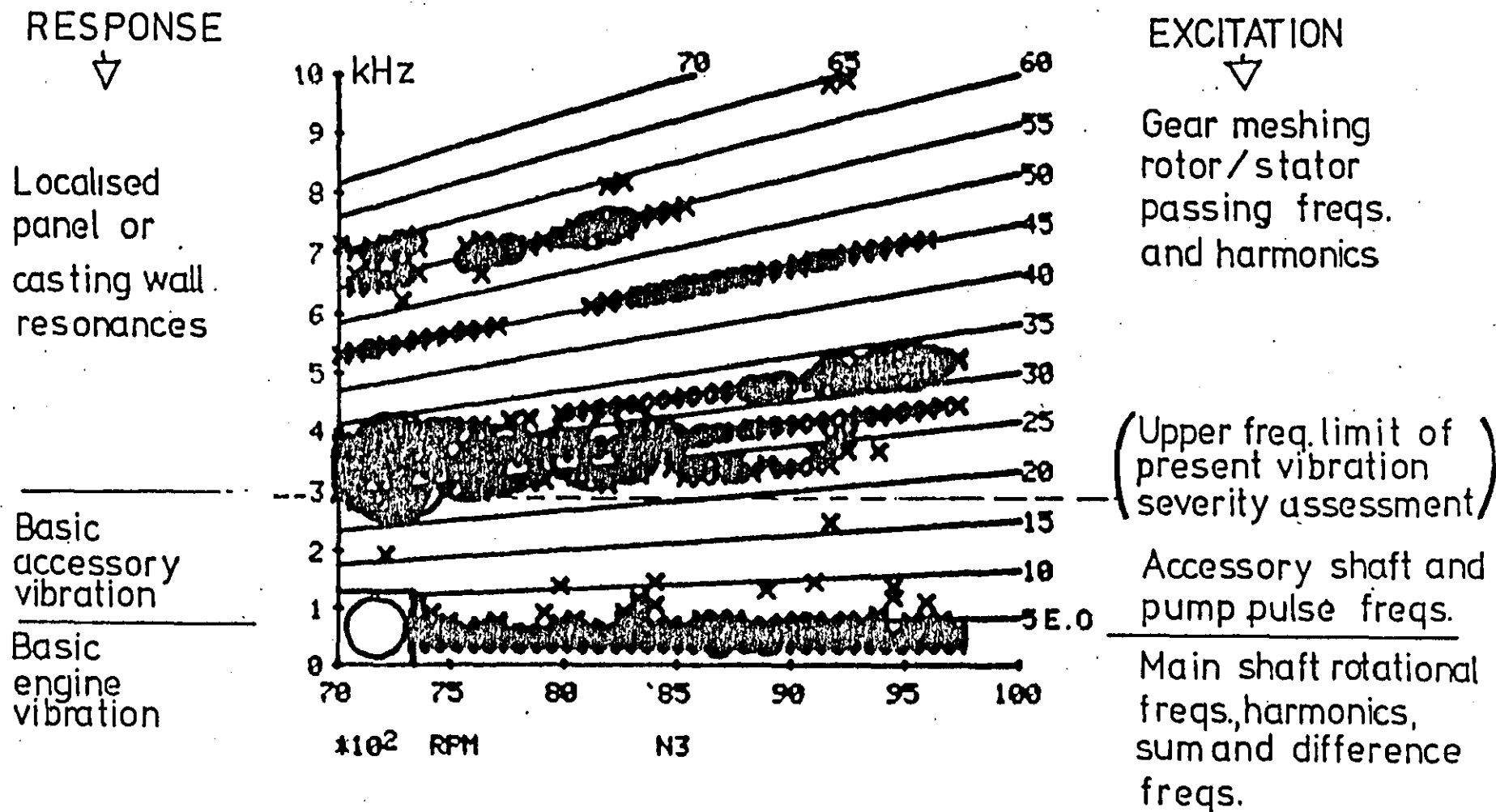


Fig. 1.2 FREQUENCY SPECTRUM OF TYPICAL ACCESSORY

A typical accessory will have to pass through several stages of test before acceptance for airline service. First, a minimum standard of testing is performed for early engine accessories to allow initial bench (or ground) running of the engine. Secondly a full type approval test is required to show full conformance with the design specification. Finally production conformance and acceptance tests are carried out to show that the initial Production standard accessories can be made and perform to the desired standard. Subsequently Quality assurance testing is performed on selected accessory units from Production batches to ensure that standards are maintained.

All accessories have to demonstrate conformance with the above tests. However each test is further divided depending on what aspects of its function or environment are being investigated. When investigating an accessory's response to its vibration environment it has to show that it will "withstand the dynamic vibrational stresses without structural failure" and that it will "perform satisfactorily throughout its declared life when subjected to a vibrational environment equivalent to the maximum anticipated "in service" levels". (Ref 7.1.6).

This conformance with vibration requirements is performed by two basically distinct types of rig test. These are the Resonance Search and the Endurance Test. In the former test the accessory sub-system or unit is subjected to an excitation and its response measured. This has consisted of slowly sweeping a sinusoid through the desired frequency range at amplitudes up to the specification limit.

More recently use is being made of band limited random noise which applies a random signal over the frequency range of interest. Whichever test method is used the objective is to determine the test system natural frequencies and obtain estimates of their damping usually expressed in terms of the Quality or Q Factor.

Conformance with the test objectives is then demonstrated by carrying out Endurance Testing at selected natural frequencies for 10^6 or 10^7 cycles. Successful completion of the Endurance Testing has been deemed to show conformance with the specification. 'Successful' here implies that on completion of the test the accessory was still performing within its functional limits without obvious signs of distress.

However, the final arbiter of acceptability is how the accessory performs on the engine in the aircraft. Prior to this, development engine testing will have served to give some indication of how correct the design specification estimates were and how accurately they were simulated on the rig by the way in which the accessory behaves during the Development Programme.

1.6 Aims of Thesis

Having detailed the types of aero-engine accessory and outlined the environment that they are designed to meet it will be shown that they do not in fact always give adequate service in spite of successful completion of their development programme.

It is the aim of this thesis to:

- a) Show why existing rig and engine test technique have not always revealed potential vibration problems subsequently discovered in service, and
- b) Argue for appropriate changes to these techniques to ensure that vibration associated problems are designed out or discovered as soon as possible.

2.0 VIBRATION EXPERIENCE IN SERVICE

The RB 211-22B entered service in the Lockheed L1011 Tristar on 6 April 1972 after a development programme containing more than its fair share of financial and technical traumas. Just over five years later the uprated -524 version of the RB 211 entered service on 28 May 1977. Between these two milestones was approximately 4 million hours of engine service experience. One of the customer irritants that became apparent in this period was the lack of reliability of certain accessories. For example, the gearbox mounted fuel flow regulator (FFR) was causing an in-flight shut-down rate of 0.005 in 1974 increasing to 0.009 in 1977. This compares with an engine shut-down rate from all causes which was reducing from 0.2 to 0.16 over the same period. These rates being based on incidents/1000 hours as quoted in the Summary of Operations statistics (7.2.1). Not all the problems experienced by the FFR could be attributed to vibration but those seen with the lower Teleflex Control Box were almost entirely vibration related. This latter unit is also gearbox mounted. It is not driven by the gearbox but is part of the linkage between the Cockpit Throttle Lever and the engine FFR. This accessory resulted in an in-flight shut-down rate of 0.004 in 1974 increasing to 0.008 in 1977.

Service statistics presented at the 1976 Operators Conference (7.2.2) showed that the FFR and Teleflex Control Box problems were the source of 10% of all in-flight shut-downs.

These statistics ignore accessory removals from the engine as a result of reported flight problems. Hence in order to improve what was basically an excellent aero-engine further detailed investigations were required as the reported faults had not been seen during the development testing programme outlined in the introductory chapter.

2.1 Lower Teleflex Control Box Testing

The engine end of the throttle linkage is shown in figure 2.1 and comprises an upper control box manufactured by the Teleflex Corporation which transmits rotary movement from the aircraft controls into linear movement of the engine controls. This is achieved by a toothed quadrant and rack. This upper control box also sequences reverse thrust engine operation.

A cable runs from the top control box round the engine fan casing to the lower control box which operates in the reverse sense to the upper and is mounted on the end of the gearbox input drive tower (figure 2.1). The output lever of the lower control box moves the input lever of the Fuel Flow Regulator (FFR) by means of a control rod. In this way the pilot is able to schedule his fuel flow requirement to meet any particular flight regimes.

The control boxes successfully passed both their specified rig and bench development engine tests but in service failures began to occur particularly on the lower control box as summarized in figure 2.2.

Vibration rig testing indicated that the control rod between the lower Teleflex Box and FFR had a natural frequency in the HP shaft frequency range and this was modified. Additional bracketry was introduced in an attempt to stiffen the input conduit. However, some engines continued to show wear of the rack and quadrant teeth. This wear was initially observed as throttle stagger, ie the need to have different throttle angle settings on each of the engines to achieve the same thrust. This had resulted in a Service Instruction to inspect the Boxes every 350 hours if not required sooner and in the worst instance a Box had to be changed after 84 hours.

Development Testing had not shown the cause of the problem and so it was decided to take measurements on Service engines that

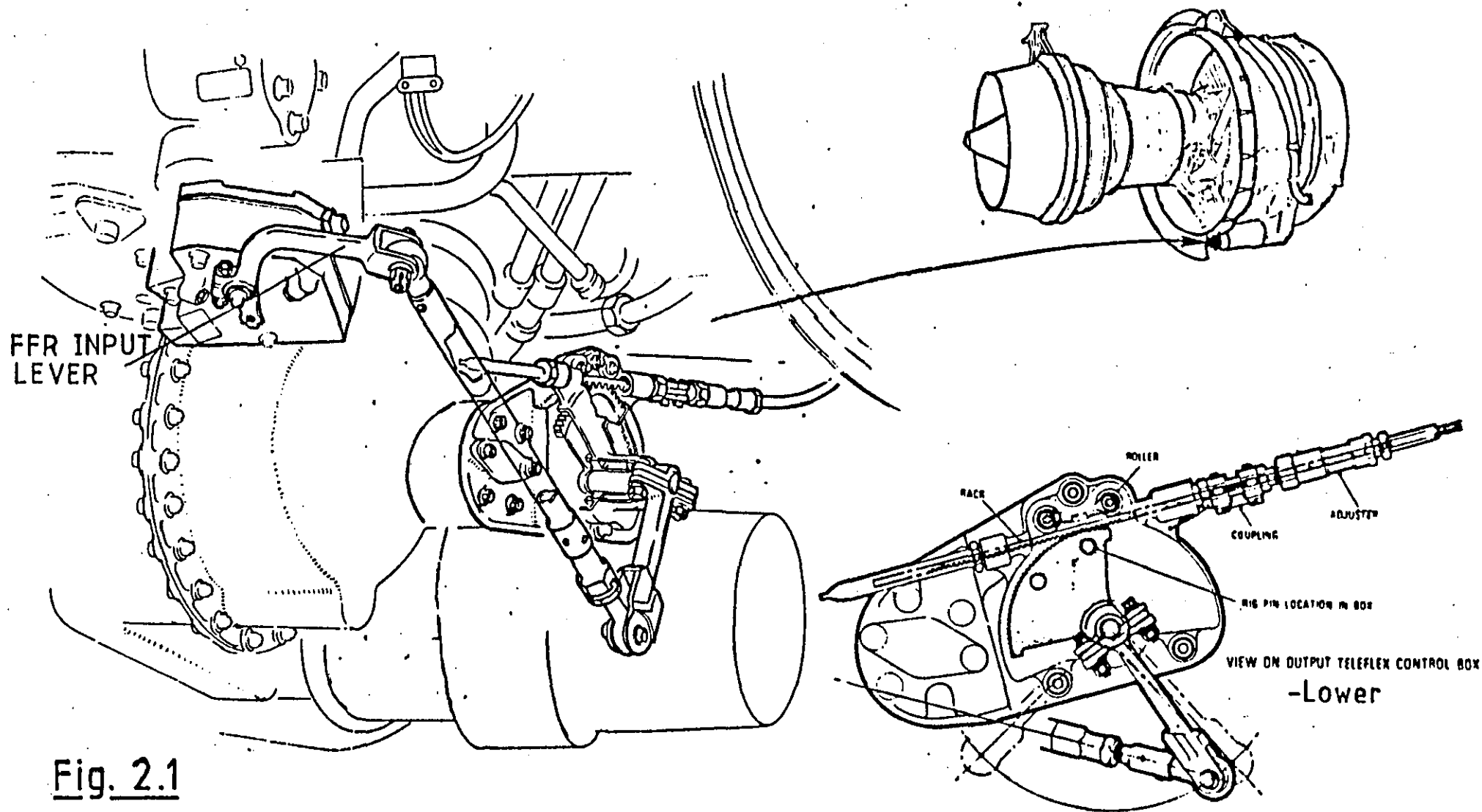


Fig. 2.1

DETAIL OF THROTTLE SYSTEM - EXTERNAL GEARBOX



RB211 THROTTLE CONTROL SYSTEM

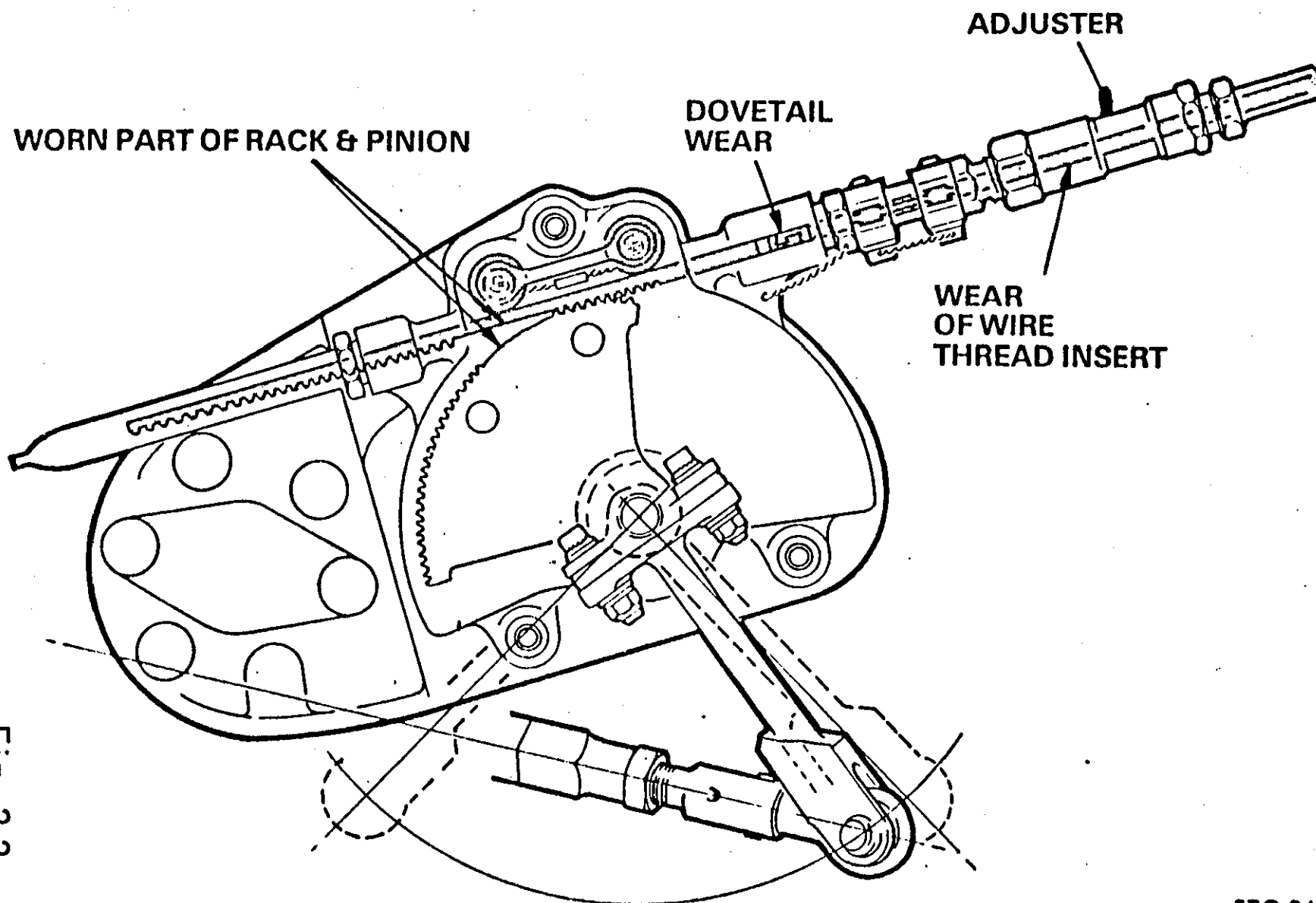


Fig. 2.2

exhibited the problem in order to determine what differences there were and obtain some indication of the possible cause. This testing showed that high levels of 1st HP order and external gearbox drive shaft orders (1.46 and 2.56 HP) were present. These excitation sources are shown relative to the lower Teleflex Box in figure 2.3.

On one of the test engines it was found that looking at the levels associated with these orders in the frequency domain strain gauge measurements on the throttle conduit showed stress levels of 11,000 psi pk - pk (756 MPa) at 160 Hz (1st HP) and at 400 Hz (2.56 HP) in an engine axial direction. Radial to the engine these levels were 1500 psi (10 MPa) and 4000 psi (27.6 MPa) respectively. This is shown in figure 2.4.

COMPARISON OF AXIAL & RADIAL STRESS COMPONENTS

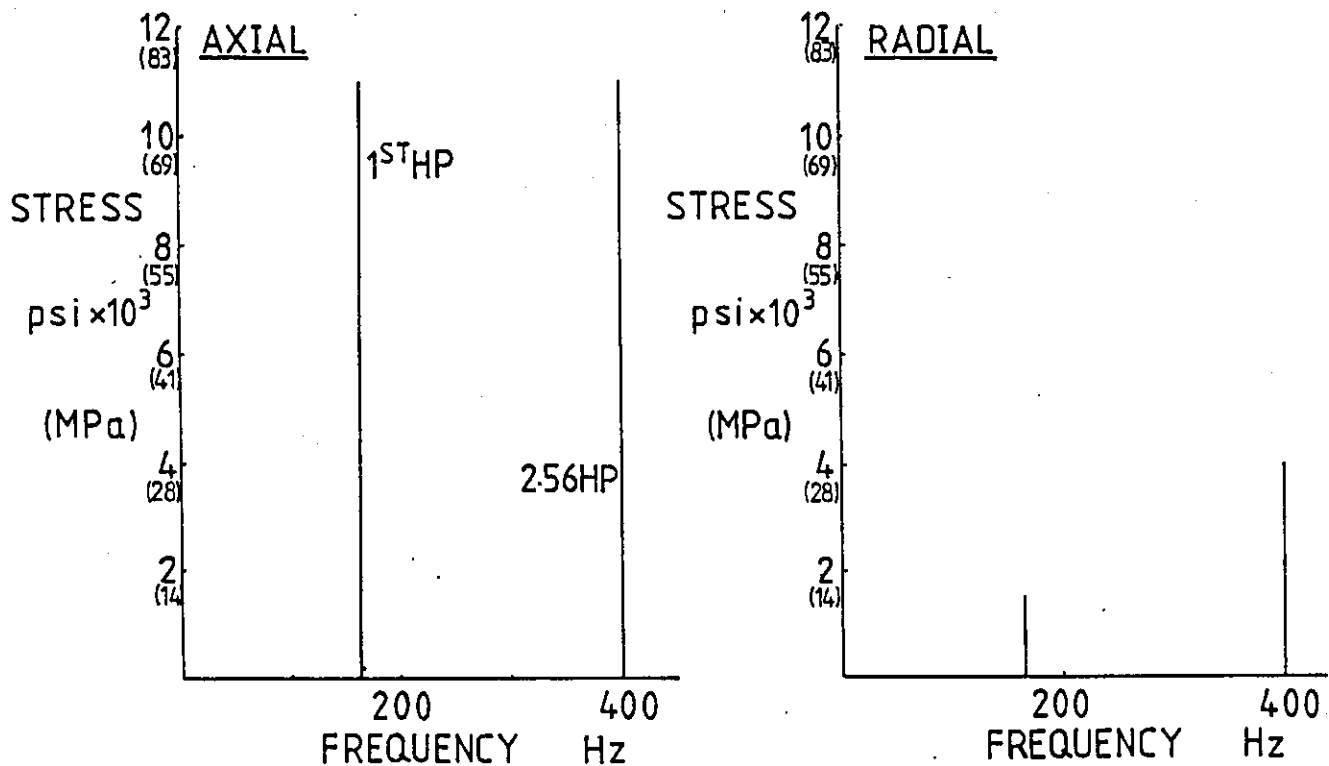


Fig. 2.4



RB211

THROTTLE CONTROL SYSTEM

H.S. Gearbox Drive — Vibration

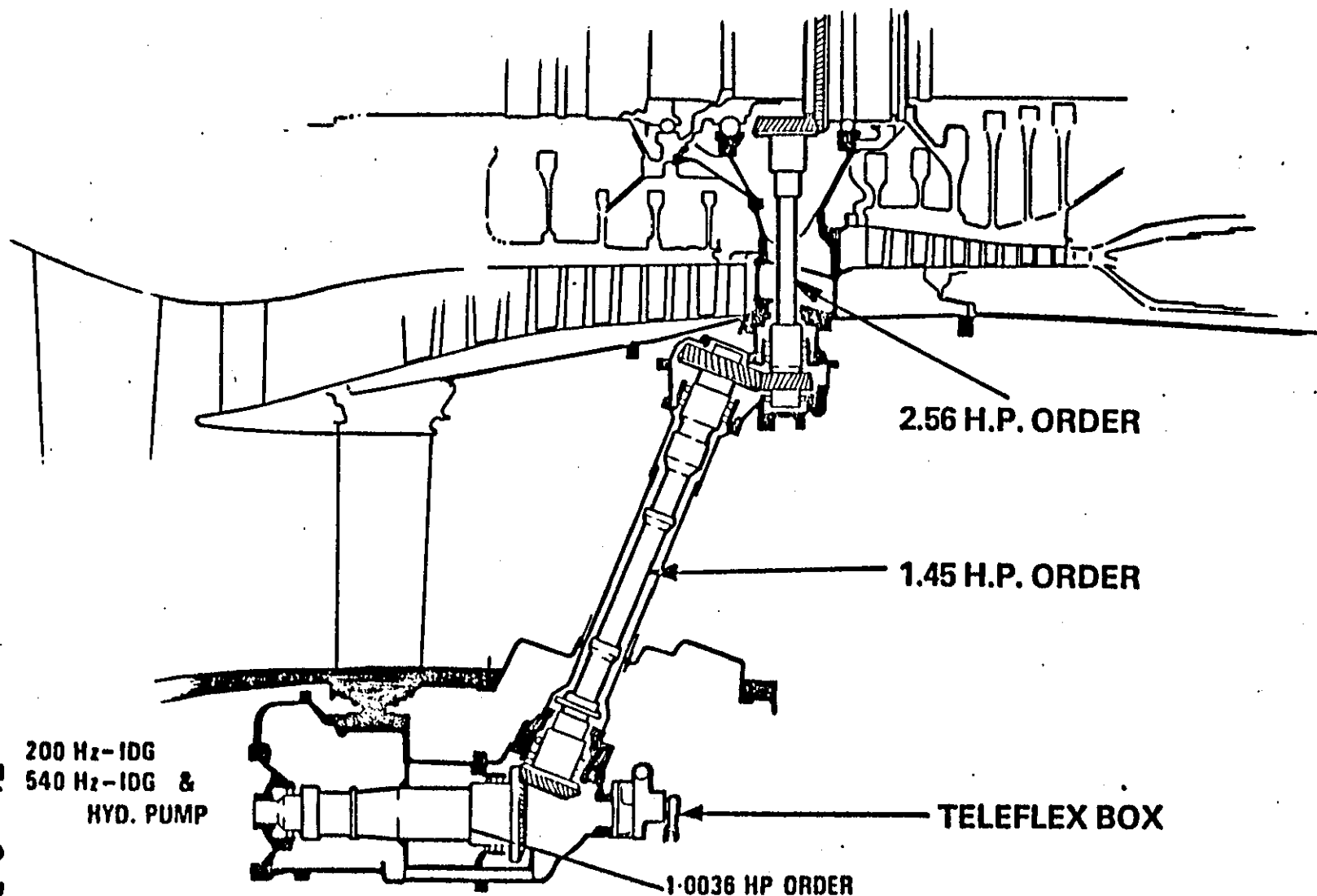
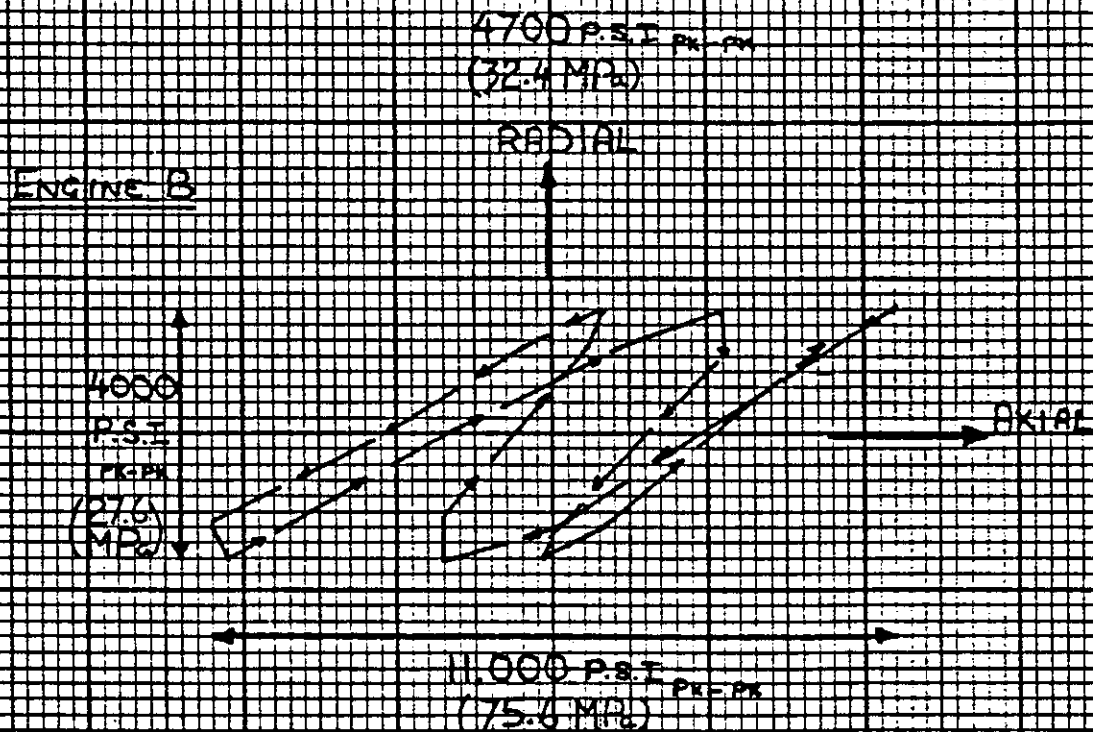
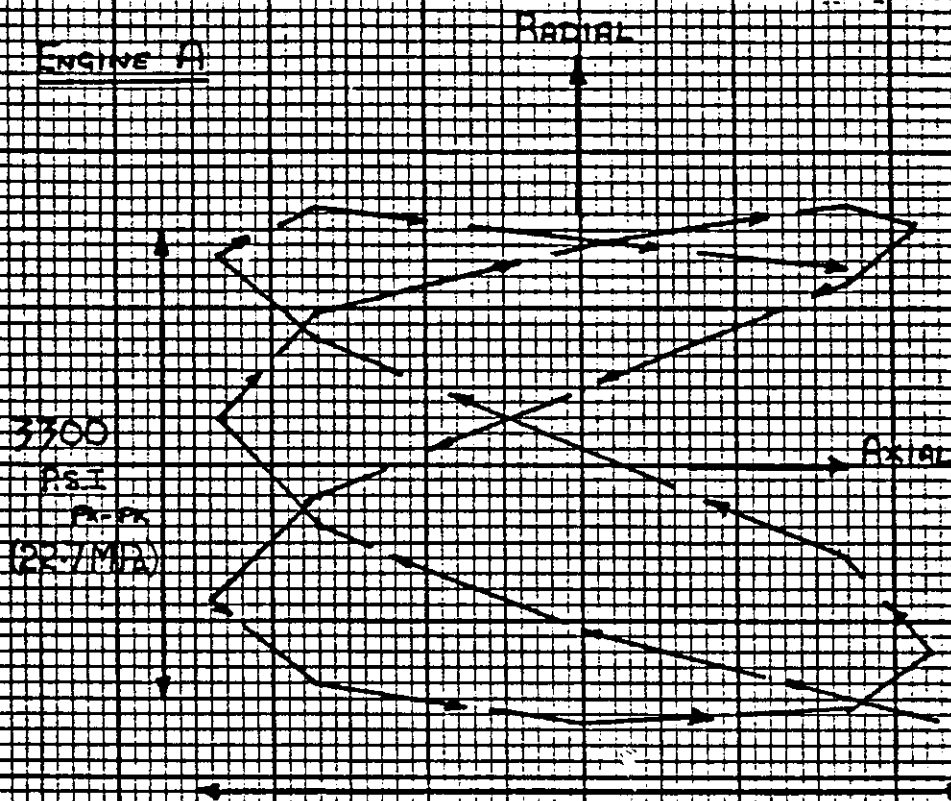


Fig. 2.3

In themselves these vibratory component stress levels could not account for the failures seen. However on looking at the time of occurrence of the spectral peak the locus plots of figure 2.5 were obtained which indicated that the gauge positions may not be showing the maximum resultant level, i.e. they were not in the optimum positions, and that the conduit was not vibrating in a simple mode. In fact it was realised that the various frequency components in occurring simultaneously in all three planes were giving a complex excitation not previously simulated in rig endurance testing. It was also found that these simultaneous excitations were occurring in the climb/cruise region, a region in which the service engine spends a considerable portion of its operating time unlike the development engine which is usually run at maximum ratings. Other conclusions were reached and tests performed which are detailed in 7.2.3, 7.2.4 but in the context of this work the above are the significant results.

The realisation that it was not necessarily correct to treat each resonant condition separately was a revolutionary if not a novel discovery. Previous vibration experience had been largely built up on blade vibrations where discrete modes are excited at various engine conditions and simultaneous excitation from several sources was not known to give rise to particular problems. Further consideration showed that on accessories high levels of forcing could occur from several sources even at non-resonant conditions especially in the critical cruise speed ranges. This in turn lead to the realisation that a high vibration level at take-off speeds might be tolerable for the relatively short time this occurred while lower levels at cruise occurring over several hours per flight could well lead to the types of problems experienced with the Teleflex Box.



LOCUS PLOT OF A POINT ON THE TELETYPE
CONDUIT

90° STRAIN GAUGE RESULTS TWO SERVICE ENGINES

Fig. 25

2.2 Lower Teleflex Control Box Testing - Problem Solutions

As a result of the lessons learnt in the above investigation the testing to obtain a solution concentrated on the following areas:

- a) forcing function transmission path analysis,
- b) investigation of Airline proposed solutions,
- c) improvement to the vibration environment, and
- d) investigation of an alternative control box construction.

Details of the testing involved in the above approaches are given in Appendix A and references 7.2.5 - 24, a summary only being given here. It was found that the transmission path analysis was problematical and did not produce conclusive results due to limitations in the technique used. This arose because there was no clear single input and response on which to perform Coherence analysis and resolution problems using correlation techniques proved difficult.

Of the various Airline proposals one was found to be helpful namely that of incorporating a shortened rack which increased its first cantilever frequency at cruise above the HP shaft order excitation frequency.

In conjunction with this modification improved standards of balance in the gearbox drive system reduced the input forcing. This resulted in such a change to the vibration inputs that the alternative control box was not required .

The introduction of these modifications into Service is such that the in-flight shut down rate has reduced from 0.008 in 1977 to a current rate of less than 0.001.

2.3 Summary

Testing the lower Teleflex Control Box on Service engines which have exhibited severe wear to rack and quadrant teeth have shown differences to 'captive' Development engines. This testing has revealed that problems appear to be associated with the presence of several excitation sources which occur simultaneously at a critical operating speed. These excitations results in a three-dimensional response of the accessory and it is apparent this can result in a resultant response which is the vector addition of the measurement directions. This could result in vibration amplitudes considerably greater than those measured in the three chosen planes.

As a result of this testing modifications to the Control Box have been introduced which have increased their life from the point where they had to be inspected every 350 hours to an average life in excess of 3000 hours. The worst Service engine resulting in rejections after 84 hours, has recently achieved 3381 hours satisfactory running and is still in Service use. References 7.2.25 - 27 show that engines which initially incorporated the balanced drive shafts have achieved Box lives of over 5000 hours and those with the modified rack over 3000 hours.

As a result of the Service experience outlined in 2.0 and the results of 2.1 a detailed review of accessory vibration testing procedures has been undertaken. The results of this review are the subject of subsequent chapters.

3.0 ACCESSORY TEST REVISIONS

In the previous chapter it was shown that accessory reliability on in-service RB 211 engines was worse than that predicted from the development test programme. On the basis of lessons learnt from the case history of the lower Teleflex control box, the arguments for a proposed revision to the test procedure will be set out which better simulates the particular vibration environment generated by the aero gas turbine engine.

In section 1.5 the objectives, and methods of achieving them, used in vibration testing were outlined. These procedures were based on such standards as BS 36100 (part 2, section 3, sub-section 3 - Vibration) which in this instance refers to aircraft rather than engine mounted equipment. Other standards which have been followed are embodied in such documents as reference 7.1.5.

3.1 The Spoke Diagram

A study of engine test results from vibration testing on accessories has shown that the typical accessory is subject to various forcing functions associated with shaft out of balance, blade passing orders, pump pulsing or ripple rates and gear meshing. All these excitations occur at integer or non-integer harmonics of the appropriate drive shaft fundamental frequency and hence vary with shaft speed at a known rate. These harmonics are commonly referred to as engine orders relative to the appropriate engine shaft.

It has also been noted that several of the above excitations can occur simultaneously and usually result in a large response, i.e. resonance if coincident with a natural mode of the accessory. It is also the case that some of these 'orders' merely result in increasing response as engine speed increases, for example, an out of balance shaft order with no coincident fundamental modes in the engine running range. This excitation source can result in a significant forcing input into an accessory.

These various 'orders' can cause significant accessory response in three dimensions at differing regions of engine operation.

With a knowledge of the accessory location and the surrounding structures, it is possible to predict which engine orders are likely to be seen by the particular accessory and with experience, their probable magnitude can be estimated in broad terms.

Hence it is possible at the design stage to develop a frequency v. speed diagram with the appropriate engine orders shown on it, i.e. a Campbell or Spoke Diagram. It is then a short step to experimentally generate this Spoke Diagram when it comes to rig testing the appropriate accessory.

While it is feasible to sweep each order in the correct ratios, the control problems are difficult and hence it is proposed that this technique of simulating the accessory environment only be used for endurance testing. In fact it is not necessary for resonance searches since it is the existence rather than the response of a resonance which is of initial interest.

It is therefore proposed that on accessory rig testing a resonance search be performed using a suitable technique from those described previously in section 1.5 or detailed in references 7.1.4 to 7.1.6.

This is to be followed by Endurance testing using a complex broad band signal generated in a similar fashion to that seen on the engine by using multiple sine waves set at frequencies and amplitudes in accordance with the procedures to be set out in section 3.2, based on a Spoke Diagram. It should be noted that this testing is still performed in a single plane at a time on the rig due to the complication and expense that multidirectional excitation would involve. It will subsequently be shown that this need not be too severe a limitation.

3.2 Derivation of Spoke Diagram

A typical flight operating regime is shown in Fig 3.1.A where for particular speed bands three major regimes exist; namely "idle", "cruise" and "take-off". The frequency variation of three engine speed related excitation or forcing functions A, B and C are superimposed showing linear variation with speed. These could typically be a pump ripple rate and drive shaft fundamental excitation.

This plot constitutes the Spoke Diagram.

For typical mid-regime speed points the response spectra shown in Fig 3.1.B might be obtained. These spectra levels should be expressed in terms of root mean square velocity (V_{rms}) for reasons which are detailed in Appendix F.

From these response levels and based on experience, it is possible to weight these forcing functions to give an accessory designer an indication of whether a system natural frequency can be tolerated at a point coincident with one of the forcing inputs and/or one of the flight regimes. The proposed weighting scale is as follows:-

Category 1 forcing - Capable of causing short or long term failure if coincident with accessory natural frequencies in any region of the Spoke Diagram.

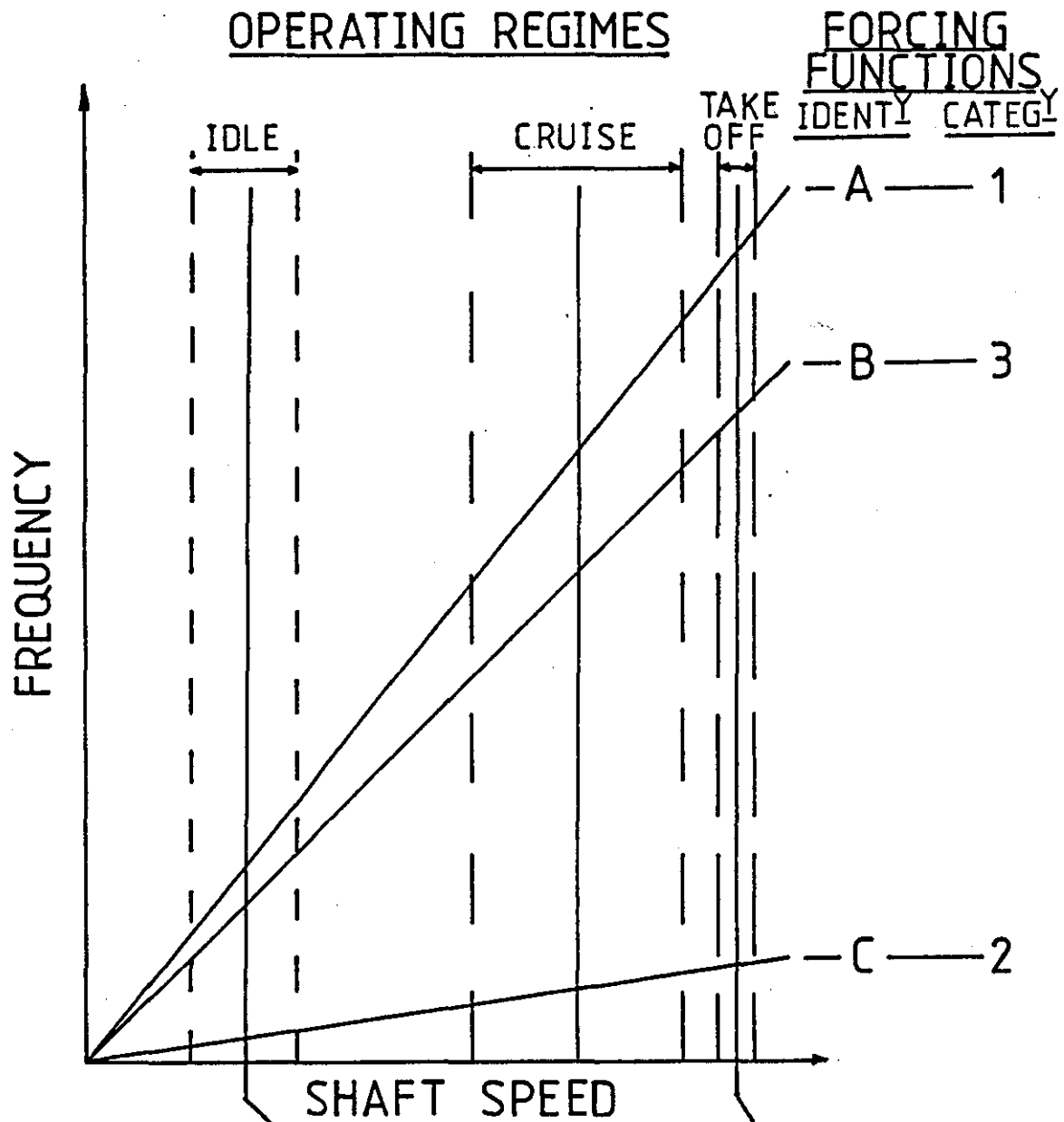
Category 2 forcing - Long term service problems probable if coincident with accessory natural frequencies in critical ranges of engine shaft speeds, i.e. flight regimes.

Category 3 forcing - Low input level which will only be significant if:-

- (a) Coincident with accessory high magnification natural frequency in critical ranges of engine shaft speeds.

Fig. 3.1

A. SPOKE DIAGRAM



B. RESPONSE DIAGRAM

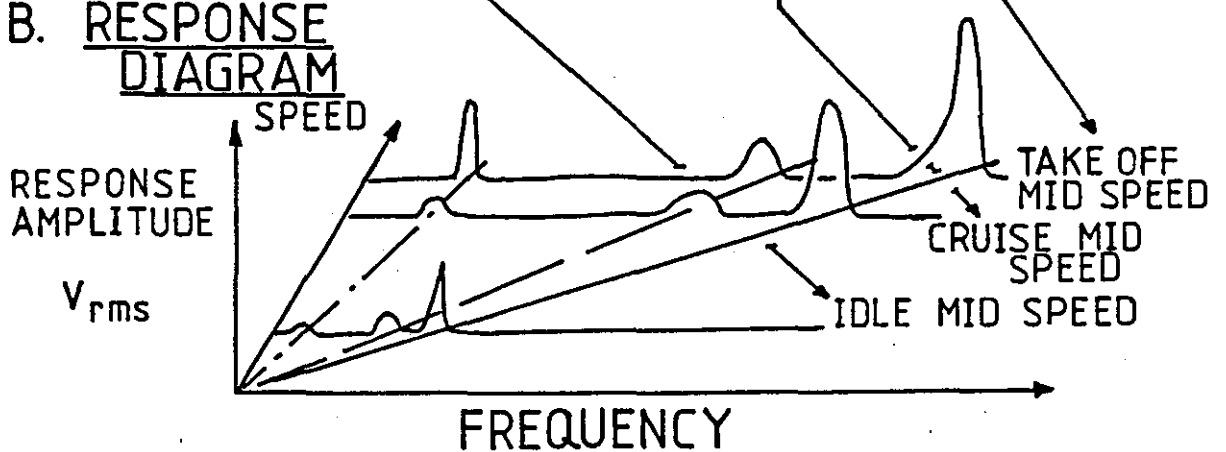


Fig. 3.1

- (b) Increased by known engine service problems.

With reference to fig 3.1, input A would be regarded as category 1 due to the general high response level over a wide speed range, B as category 3 due to its low amplitude over a wide speed range, and C as category 2 due to its high response in a limited speed range.

The above information contained in fig 3.1.A should be available early in the design programme and hence can be made available as a guide to the accessory designer. This should enable unacceptable resonant conditions to be avoided and designed out rather than developed out at a later stage of the programme.

From the above design considerations, probably backed by initial rig testing, the designer can enter the resonant frequencies found onto the Spoke Diagram as shown in fig 3.2.A. The component natural frequencies are represented by the constant frequency lines numbers 1 to 5, with number 4 being a high magnification mode. Typical points of coincidence between these natural frequencies and various engine order excitations are shown at points A through J.

On this Spoke Diagram only two flight regimes, Y and Z, are shown and it is only points of coincidence between engine order forcing and natural frequency within these regimes which are of interest or category 1 excitations within these speed bands. The former are illustrated by points B and D in range Y and A, G and C in range Z while the latter condition is shown by E and F.

3.3 Use of The Spoke Diagram in Endurance Testing

a) Endurance Period

The above points are verified by resonance sweep testing on a rig or development engine depending on timescales and degree of build. An accessory sub-assembly is more likely to have its natural frequencies investigated on

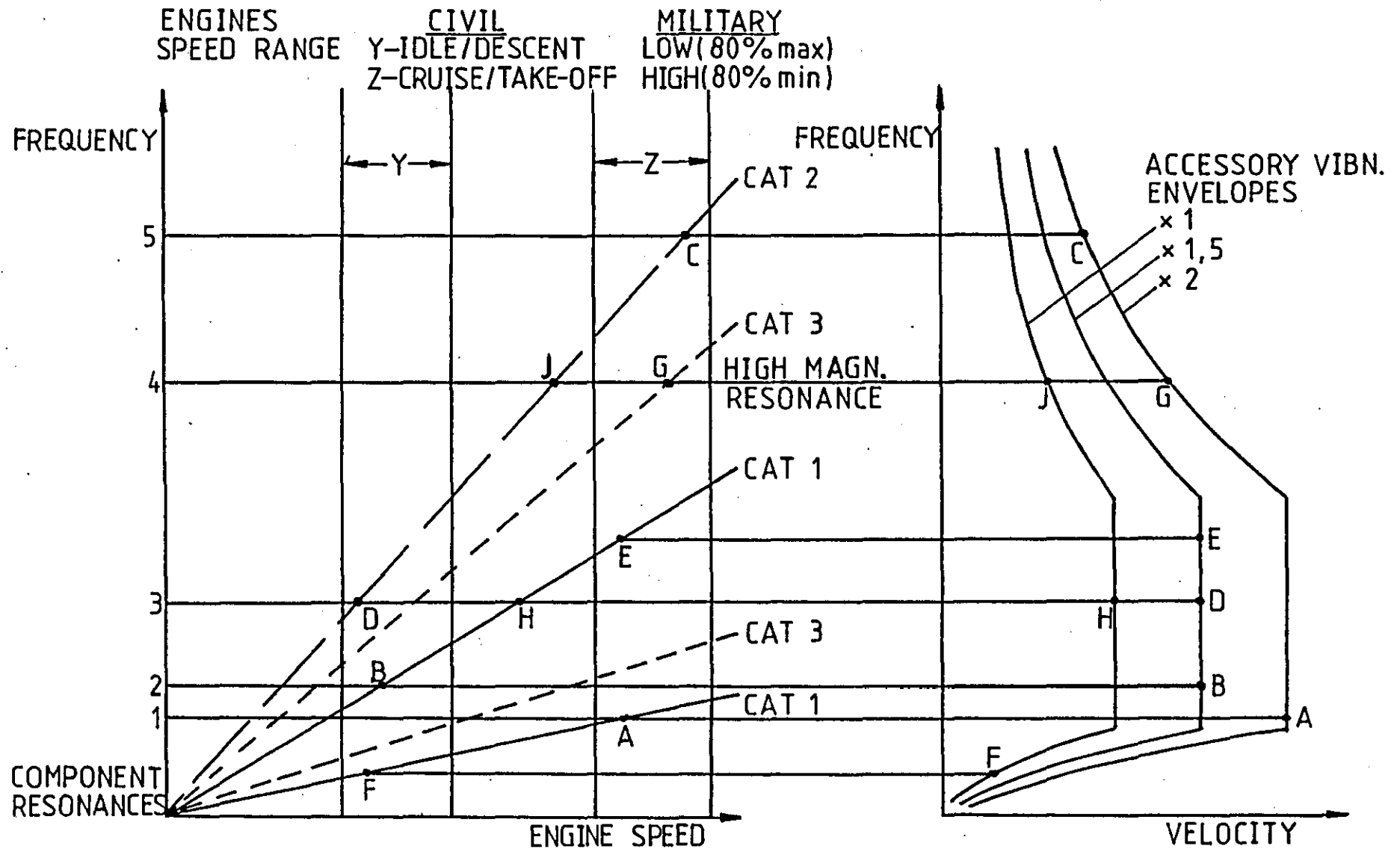


Fig. 3.2

A. SPOKE DIAGRAM WITH COMPONENT RESONANCES & SPEED BANDS ADDED

B. FACTORED VIBRATION ENVELOPES

a rig than as part of the whole assembly on the engine. However, the resonance search in conjunction with the Spoke Diagram only shows possible problem areas, it does not confirm the specification vibration test objectives stated in 1.5. This is attempted by rig endurance testing and hopefully verified by development engine endurance testing.

Historically endurance testing has been carried out at predetermined amplitudes and frequencies based on the resonance search results. The amplitude chosen by Rolls-Royce to ensure structural reliability based on Stress Office recommendations is 1.9 times the basic specification level at natural frequencies showing the highest response, e.g. component frequency number 4 in fig 3.1.A. Depending on the accessory this would either have been continued for 10^6 or 10^7 cycles assuming no prior failure occurred.

This could be very time consuming since at

100 Hz - 10^6 cycles takes 2.77 hours or 10^7 cycles takes 27.7 hours, while at

1000 Hz - 10^6 cycles takes 0.27 hours, 10^7 cycles takes 2.77 hours.

It also assumes that accessory functional failure would be due to a cyclic fatigue failure which obeys the classic steel S-N curve which has an endurance limit. Hence if the test amplitude was below the endurance limit and it survived 10^6 (or 10^7) cycles it would continue to operate satisfactorily for its guaranteed life. However, service experience has shown that the assumption of an endurance limit is invalid and problems have been occurring at a much lower level after 10^8 cycles say. This is illustrated by point B in fig 3.3.

In order to improve this aspect of the engine environmental simulation it is proposed that endurance testing should be based on the rig on a time rather than number of cycles.

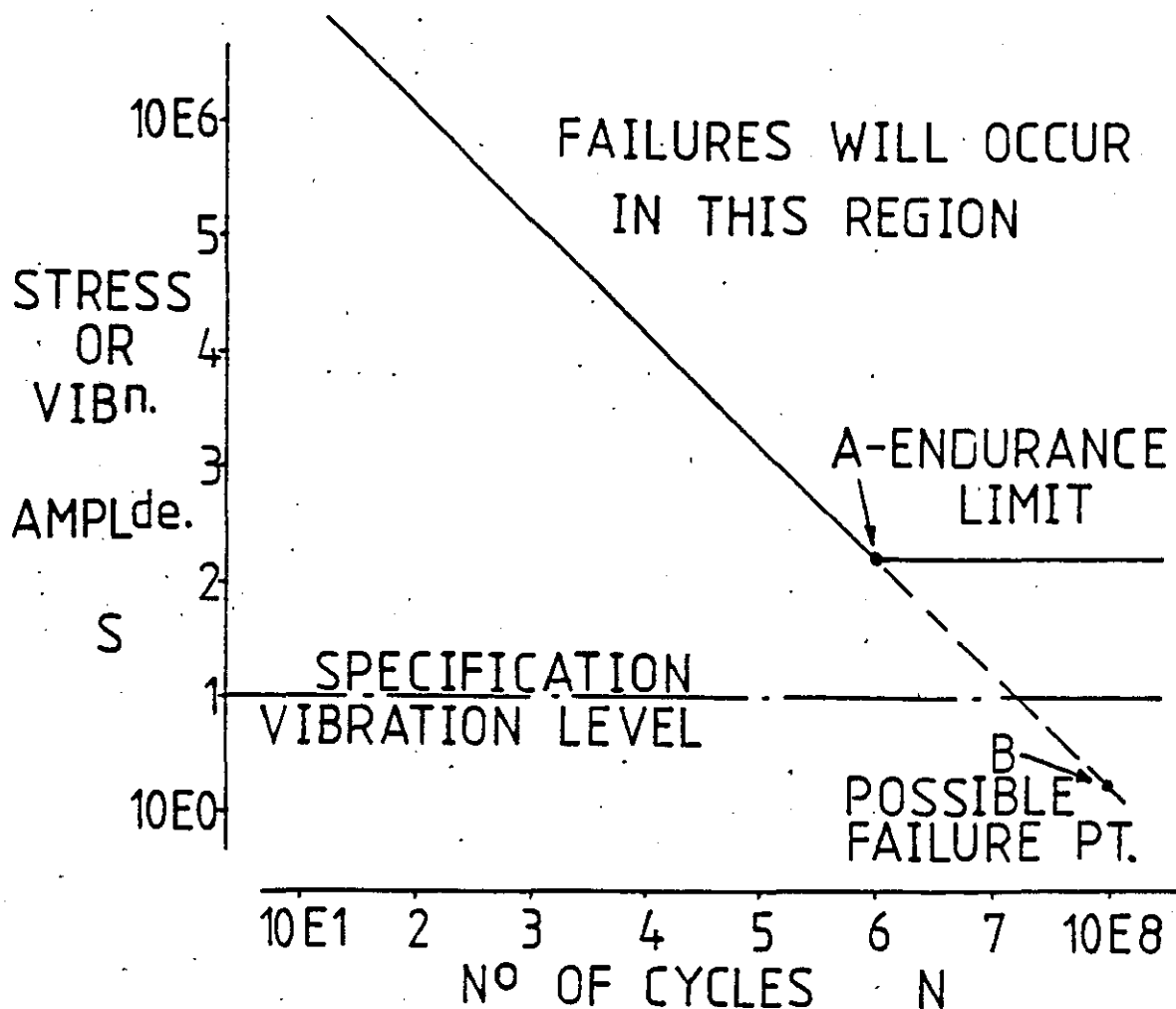


Fig.3.3

The endurance period proposed is 100 hours in each of three mutually perpendicular planes. As modification and type approval tests on engines are based on 150 hours of endurance running, and since this testing excites all three planes simultaneously a test which involves total testing to twice this period is arguably a reasonable compromise for ensuring that the desired degree of agreement with test objectives is achieved in terms of service reliability estimates. It is also reasonable in terms of cost and rig occupancy.

It is accepted that this time may not fully test any low frequency resonances but should give plenty of experience with the higher frequency spoke diagram test conditions, for example:-

10 Hz in 100 hours gives 3.6×10^6 cycles.

100 Hz in 100 hours gives 3.6×10^7 cycles.

1000 Hz in 100 hours gives 3.6×10^8 cycles.

However at the very low frequency end of the environment, the forcing functions are small and hence response of the typical aero-engine accessory is usually negligible. Possible problems occurring are with whole body resonances of units on anti-vibration mounts which have their first natural frequency in the 20-30 Hz region, and which due to the large displacements associated with low frequency might impact on adjacent fittings.

b) Mission Weighting

This 100 hours endurance would be split according to the mission profile to cover excitation sources in each speed band defined on the Spoke Diagram, e.g.

TABLE 3.1 Example of Possible Missions

Short-Haul Mission	Long-Haul Mission
Idle Speeds = 48% of mission	Idle Speeds = 18% of mission
Cruise Speeds = 50% of mission	Cruise Speeds = 80% of mission
Take-off Speeds = 2% of mission	Take-off Speeds = 2% of mission

Hence for testing on an accessory for use on a long-haul engine 80 hours in each plane would be performed with frequency points which occur in the cruise regime.

The exception to this would be where high magnification response occurs outside the critical speed range (e.g. point J on fig 3.2.a). Here a certain time should be allowed on endurance testing to include this resonance up to say 15 hours with appropriate adjustment to the flight regime times above.

c) Endurance Testing Levels

Having discussed the time in each plane, it is necessary to define levels at which to input the various forcing functions. With reference to fig 3.2.A it is proposed that categories 1 and 2 forcing functions coincident with a natural frequency in a critical high speed range (range Z in fig 3.2.A) should be endured at twice the specification vibration envelope appropriate to the particular coincident frequency (e.g. points A and C). This same criterion would be applied to any excitation due to a category 3 input which is coincident with a high magnitude natural frequency, i.e. lightly damped mode, e.g. point G in the high speed range.

For similar conditions in the low speed range it is proposed that 1.5 times the appropriate envelope level be adopted as the basic forcing function amplitudes are normally lower.

Cognisance should also be taken of any category 1 forcing functions which pass through a critical speed range but are not coincident with a natural frequency of the structure, since the response due to this forcing is still likely to be significant. In the high speed range a weighting of 1.5 is appropriate, while at the low speed a factor of 1 would apply (e.g. points E and F respectively).

Any endurance testing required at category 1 coincident conditions outside the critical speed bands (point H) or high magnification conditions (point J) should be at the basic vibration envelope level.

Having chosen the appropriate levels for each speed range the endurance testing should be carried out by setting those points to give a multi-sine input to the accessory concerned. For fig 3.2 endurance testing would comprise the amplitude factors and times for the component points shown in table 3.2.

These factors have been chosen with particular reference to the RB 211 family of engines and are based on experience which has been confirmed by a survey of production engine pass-off test vibration figures which indicate that the average engine is sent out at 50% of the pass-off test limit. Other factors could well be appropriate for other applications.

TABLE 3.2

Speed Regime	Ref Letter	Component Frequency Number	Spec Amplitude Factor	Endurance Period	
				Long-Haul Flight	Short-Haul Flight
Idle or low (Y-Fig 3.2)	F	6*	1.0	16 hrs/ plane	43 hrs/ plane
	B	2	1.5	16hrs/ plane	43 hrs/ plane
	D	3	1.5	16 hrs/ plane	16hrs/ plane
High or cruise/ take-off (Z-Fig 3.2)	A	1	2.0	74 hrs/ plane	47 hrs/ plane
	E	7*	1.5	74 hrs/ plane	47 hrs/ plane
	G	4	2.0	74 hrs/ plane	47 hrs/ plane
	C	5	2.0	74hrs/ plane	47 hrs/ plane
Non critical	J	4	1.0	10 hrs/ plane	10 hrs/ plane
	H	3	1.0	10 hrs/ plane	10 hrs/ plane

*Frequency at which peak amplitude of non-coincident category 1 forcing function occurs (Fig 3.2.A).

In practice the revision to the accessory specification for vibration (reference 7.1.6) has limited the speed ranges to two, grouping cruise and take-off conditions together as there is little practical difference in frequencies. Table 3.3 gives a listing of amplitude factors applicable in any instance for each speed regime.

The above describes the complete requirements for rig testing of accessories to ensure that they will meet their design environment. However, this does not negate the requirement for a check on the engine environment to which the accessory will be exposed. This is essential both to check the specification levels and inputs and also to verify the effect of three as opposed to single plane excitation.

TABLE 3.3 VIBRATION SPECIFICATION AMPLITUDE FACTORS

Speed	Forcing Category / Excitation Coincidence	With high magnification natural frequency	With any other natural frequency	With no natural frequency
Low	Category _____ 1	2.0	1.5	1.0
	_____ 2	2.0	1.5	0
	_____ 3	1.5	1.0	0
High	Category _____ 1	2.0	2.0	1.5
	_____ 2	2.0	2.0	1.0
	_____ 3	2.0	1.0	0
Non critical	Category _____ 1	1.5	0	0
	_____ 2	1.0	0	0
	_____ 3	0	0	0

NOTES.

1. '0' indicates no endurance testing for this condition unless there is a specific reason.
2. When choosing endurance conditions for each speed regime use highest value factor points first.

3.4 Use of the Spoke Diagram - Fuel Flow Regulator Case History

Having begun to appreciate the implications of several excitation sources acting simultaneously the opportunity was taken to use this knowledge and apply it to a problem occurring on another accessory.

In chapter 2 it was indicated that considerable service reliability problems had been experienced with the Fuel Flow Regulator (FFR) which meters the correct amount of fuel to the engine combustion chambers for each flight condition. A detailed description of this type of unit is given in 7.3.22. Part of the poor reliability was attributed to vibration. In this context the problem was initially observed as a reduction in starting fuel flow and hence difficulty in starting the engine.

The position of the variable metering orifice spool which schedules fuel to the burners in the combustion chamber is controlled by a set of bellows at the end of a pivoted stirrup assembly. The scheduling problem was attributed to gradual wear in the pivot bearings. Since this wear took up to 2000 hours to become apparent its simulation on the rig had proved elusive. As a result of measuring the engine environment and determining the various excitation sources it became possible to simulate the service environment and achieve representative wear within 300 hours running on the rig.

The proposed modification was then tested in a similar manner and found to be satisfactory.

Details of the above testing can be found in the references in 7.3.1 - 21 and are summarised in Appendix B.

3.5 Summary

This chapter has shown that using the lessons learnt from engine testing accessories have been used to develop an improved simulation of the aero-engine accessory vibration environment. That this is an improvement has been demonstrated by the FFR VMO Stirrup testing on which the service wear was simulated. Incorporation of this revised Stirrup assembly is partly the reason for a reduction of the in-flight shut down rate due to the FFR of 0.011 in 1979 to 0.007 to March this year. On the basis of experience and engine testing it

is possible to derive and verify a Spoke Diagram so that coincidence of natural modes and engine excitation can be avoided at an early stage.

However, while this reduces the probability of Service problems by improving the design information base it does not confirm that service performance will be acceptable. Methods of improving this assessment by direct engine measurement and by modal testing will now be discussed.

4.0 ASSESSING THE VIBRATION ENVIRONMENT

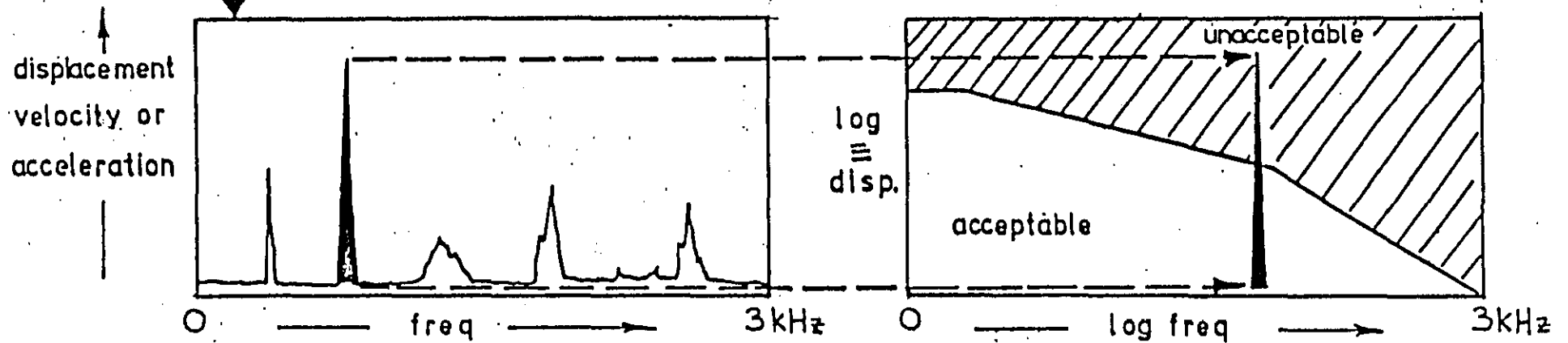
Most assessments of component reliability are based on testing sufficient samples to give confidence in applying the results to the whole component population. This work is well detailed by standard works on Statistics. In an aero-engine development programme the sample population is usually very small although it is hoped the final population will not be. In practice, reliability estimates are based on the results of the accessory's performance in a limited number of tests.

Historically, therefore, confirmation of probable service performance has been based on the results of endurance and cyclic testing combined with specific tests such as the measurement of the vibration environment. For accessories this form of engine testing together with the original type of rig testing had resulted in service problems which were not discovered during the development programme.

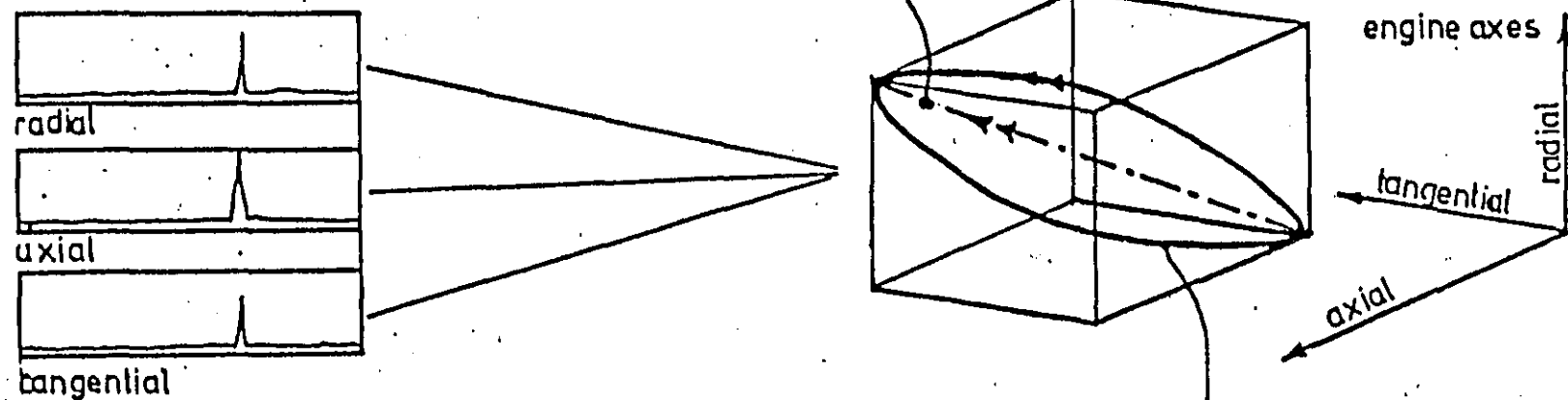
As far as vibration was concerned, the vibration response of the accessory and its mounting at some representative points was measured and then compared with the original design specification limits. If the accessory vibration exceeded this limit, appropriate action to rectify the point of exceedance would be undertaken. This could result in effort being expended on an exceedance that would not cause a Service problem as it did not occur in a significant part of the operating range. It could also be that the limit was exceeded at one point in one measurement plane only and that the resultant of all three planes was not excessive, or conversely a potential problem was missed because the resultant of all three planes was excessive while the individual directions were not.

In order to overcome these deficiencies summarised in Fig 4.1 an assessment of vibration severity based on the results of three dimensional accessory vibration testing will now be derived.

Current assessment method abstracts individual peaks in isolation from simultaneous constituents of total vibration.



Severity assessment via individual spectra as above neglects resolved amplitude of total vibration



Amplitude/phase or time domain data enables visual presentation of complex motion and hence correlation with problem symptoms.

Figure 4.1 ON SEVERITY ASSESSMENT

Fig 4.1

4.1 Severity Criterion

In order to obtain an estimate of probable service life from engine testing some form of acceptance criterion is required. These criteria have been developed particularly for process industry prime movers. Initial work was carried out by Rathbone (7.4.1) and other researchers have followed his lead (7.4.2 to 7.4.4). In the UK and Europe this has resulted in an industry standard (7.4.5) which develops a criterion based on the measurement of root-mean-square velocity (V_{rms}) for classes of machines within the frequency range 10 to 200 revolutions/sec.

A review of these criteria (7.4.6, 7.4.7) with particular reference to the accessory design specification and a survey of the available accessory measurements Fig 4.2 has suggested that an extension to 7.4.5 is appropriate for aero-engine accessories.

In this new standard the value of V_{rms} is found for the frequency band of interest for each point in the engine speed range. This can be done by using an RMS voltmeter, suitably scaled, or in the case of aero-engine accessories by looking at the peak levels in the spectrum at each speed since

$$V_{rms} = \left[\frac{1}{2} (\hat{V}_1^2 + \hat{V}_2^2 + \hat{V}_3^2 + \dots + \hat{V}_N^2) \right]^{1/2} \quad \text{-----} \quad 4.1$$

where \hat{V}_N^2 is the velocity amplitude peak of the Nth speed point.

This value of V_{rms} is obtained for each engine related plane i.e. axial, radial and tangential and the nominal resultant found

$$V_{RES} = \left[V_{ax_rms}^2 + V_{rad_rms}^2 + V_{tan_rms}^2 \right]^{1/2} \quad \text{-----} \quad 4.2$$

ACCESSORY VIBRATION PEAKS SEEN ON ENGINE TESTING

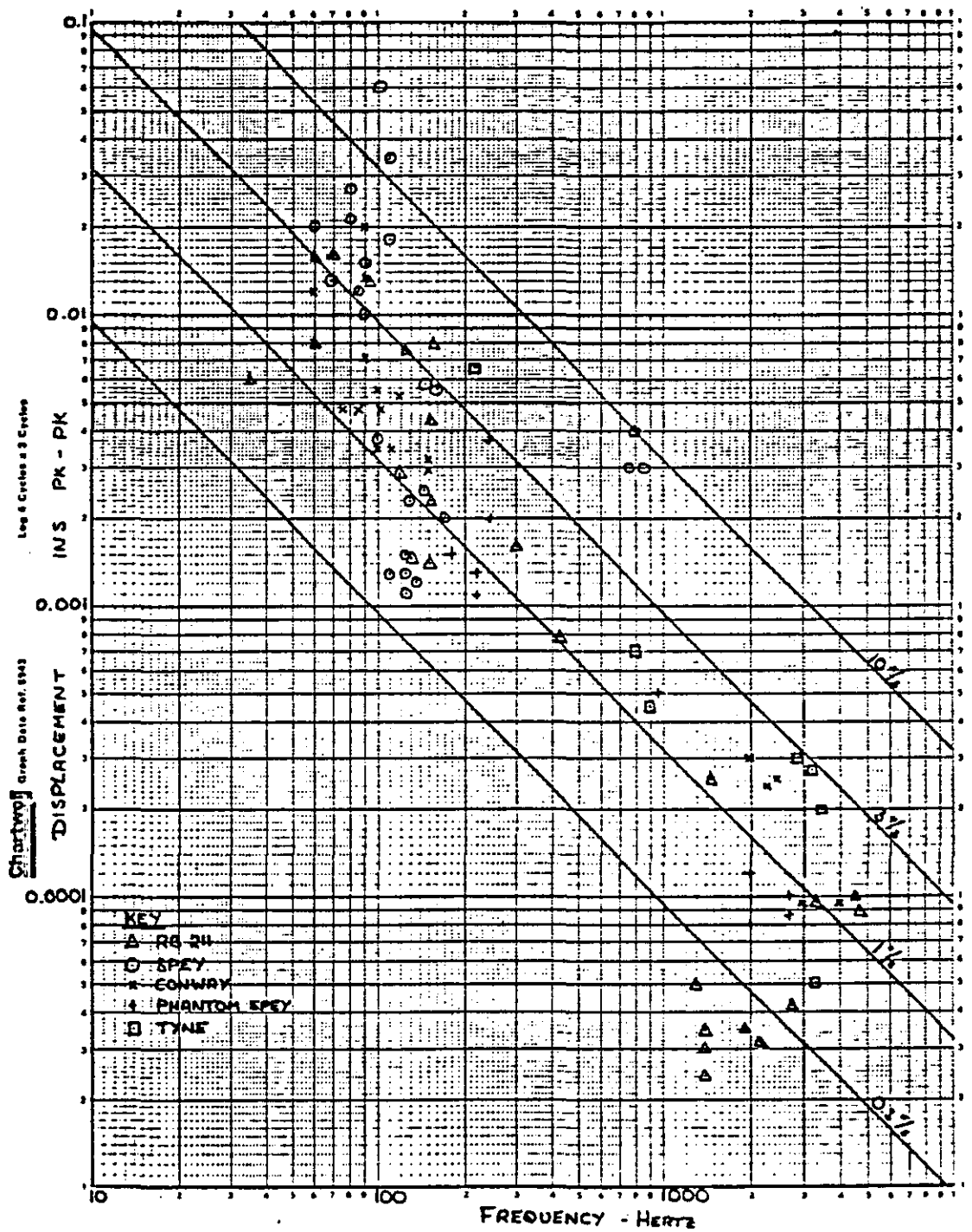


Fig. 4.2

This resultant value (V_{RES}) is then compared with the levels shown in table 4.1 and a classification obtained. This table is purely empirical and is based on accumulated test evidence from several Rolls-Royce aero engine types, the summary of the evidence for it being given in Fig 4.2 which shows some peak vibration levels measured on various gearbox and casing mounted accessories.

It is apparent that there is a large range of scatter in the results especially at the higher frequencies. This scatter is in part due to the measurement techniques employed but this is now impossible to verify without repeating all the tests to a common instrumentation standard and technique.

TABLE 4.1 SEVERITY CLASSIFICATION FOR AERO-ENGINE ACCESSORIES

Resultant Velocity V_{RES} ins/sec rms (mm/sec)	Classification	Predicted Service Life
10 or above (254)	Extremely rough	Probable immediate failure
3---10 (76 - 254)	Very rough	Short-term failure, especially if peak occurs in critical speed range.
1---3 (25 - 76)	Rough	Long term failure, especially if peak occurs in critical speed range.
0.3---1 (7.6 - 25)	Fair	No service problems expected within guaranteed life.
0.1---0.3 (2.5 - 7.6)	Smooth	No failures expected within guaranteed life.
Less than 0.1 (2.5)	Very smooth	No failures expected.

The levels seen are considerably higher than those set out in references 7.4.1 to 7.4.4 and attributed originally to empirical levels determined by Rathbone in 1939. The reason for this is due to the differences in measurement location. The work in other industries is based on the measurement of vibration at bearings or "solid" parts of the structure and is more comparable with the standard engine vibration monitoring pick-up location than to measurements on accessories. In fact taking into account the increase in flexibility inherent in the design of an aero-engine structure when compared to a ground based prime mover, the differences are not that different between the aero-engine vibration levels and the published standards. A summary of the appropriate levels from BS 4675 is given in table 4.2 for comparative purposes.

TABLE 4.2 SEVERITY CLASSIFICATION FOR TURBO MACHINERY (BS 4675 Pt1 :1976)

rms - Velocity at Range Limits ins/sec (mm/sec)	Classification	Possible Description*
0.71 and above (18)	D	Inadmissable
0.28 - 0.71 (7 - 18)	C	Improvement Desirable
0.11 - 0.28 (2.8 - 7)	B	Admissable
Less than 0.11 (2.8)	A	Good

*BS 4675 does not give a description for the classification, or quality, letters A through D. The descriptions appended are taken from the German standard VDI 2056. The levels refer to single axis measurements taken at the machinery bearings. If it is assumed that the same amplitude exists in all three planes, a V_{RES} covering the rough to smooth regions in table 4.1 is obtained at the range limits quoted above.

Recent testing at Rolls-Royce has not found any accessory vibration which falls within the "extremely rough" classification so the choice of $10''/\text{sec}$ rms remains to be validated. The occasional accessory in the "very rough" classification has been found and action taken to reduce the response to acceptable levels.

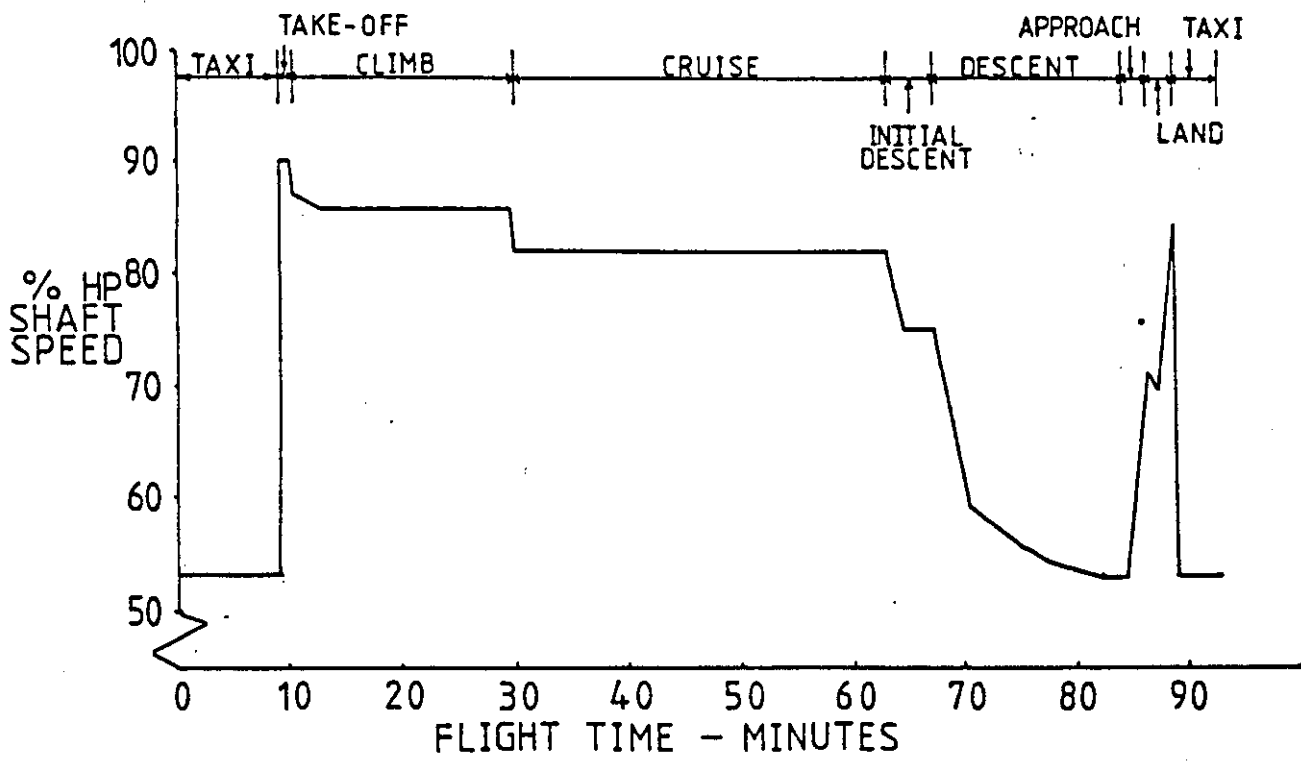
Experience would indicate that the levels originally proposed are reasonable and that the split between acceptable and not acceptable at $1''/\text{sec}$ rms is correct for this large aero-engine over the mid frequency ranges. At lower frequencies ($< 100 \text{ Hz}$) this level could probably be increased without detriment to the accessory and similarly at higher frequencies ($> 2000 \text{ Hz}$) vibration levels above this level are commonly seen with no known hazard to accessory reliability. However, the objective must obviously be to expose any accessory to the lowest practical vibration environment and hence the level chosen appears to be an acceptable compromise.

4.2 Mission Weightings

Having obtained severity classification for various parts of the operating range as indicated in the previous section, it may in some instances not be clear which of several problem areas is the greatest potential reliability hazard. An estimate of this can be obtained by consideration of the mission (or flight) profile. This profile gives the typical flight times spent at various engine speeds and hence a factor expressed as a percentage of the total time can be obtained for each operating condition or speed band. A typical mission profile is shown in Fig 4.3.A. The percentage of the overall flight time at each condition is then shown in Fig 4.3.B.

Simple multiplication of the various V_{RES} peak values can then be made and the necessary comparisons made. It is quite clear from the factors of Fig 4.3.B that a relatively low

A-TYPICAL MISSION PROFILE FOR NOMINAL 500 NAUTICAL MILE FLIGHT



B- MISSION WEIGHTING ENVELOPE FOR 500Nm FLIGHT

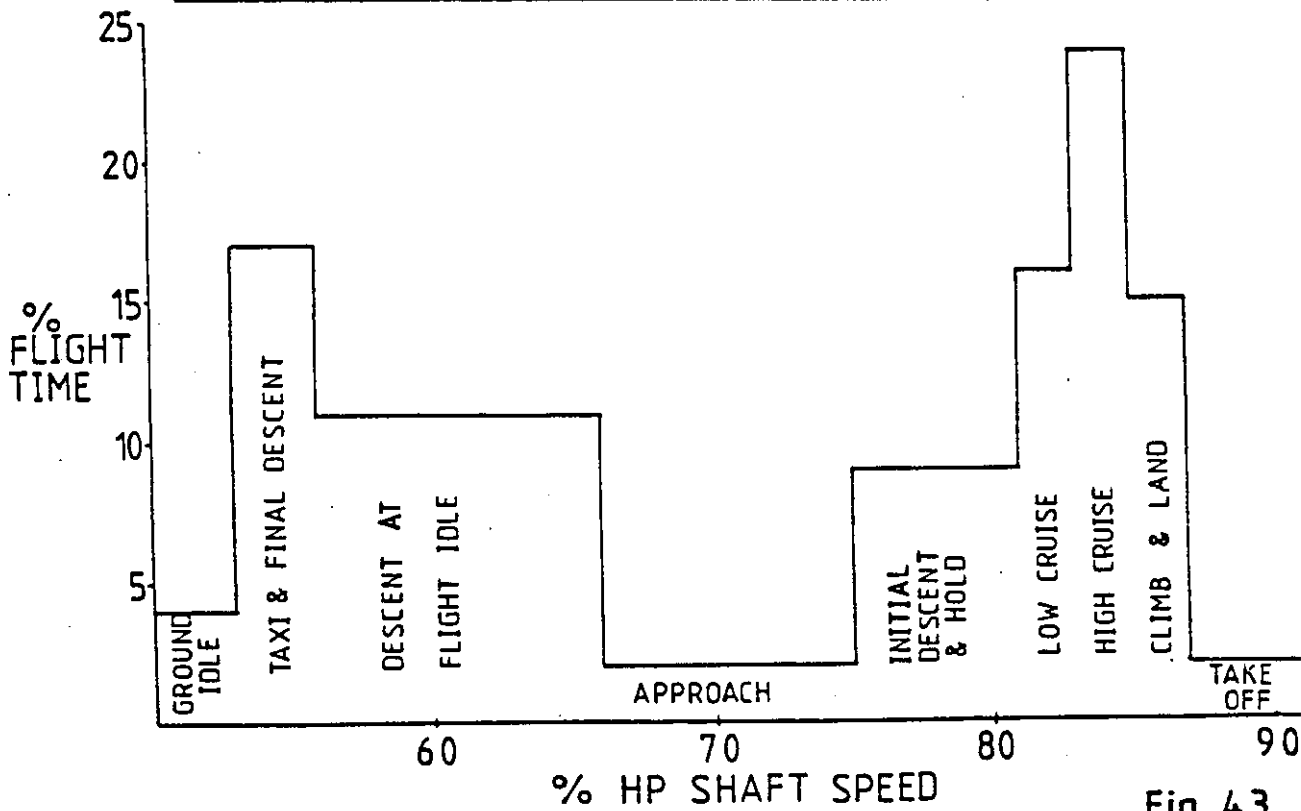


Fig. 4.3

level in the cruise regime can result in greater unreliability than a higher level at take-off. A simple example of this is shown in the case histories in the next section.

It is not necessary to apply this final weighting in every instance as it usually is quite clear what is causing a particular problem. However, where this is not so, application of this weighting can prove useful.

4.3 Testing the Severity Criterion

Having developed a Severity Criterion to give an assessment of potential engine service life it was necessary to apply it to a new engine. The only suitable vehicle for this was a new derivative RB 211 engine type the 535C, which was shortly to commence development testing.

Unfortunately the accessories had been designed to the pre-SpokeDiagram specifications but the opportunity was taken prior to engine testing to draw Spoke Diagrams for the major accessory locations (7.4.8).

When engine testing had occurred some minor revisions to the Diagrams were found necessary.

The peak vibration levels seen on these tests were used to manually estimate the Rms Velocity level for each axis in accordance with equation 4.1. These values were then applied to equation 4.2 to derive V_{RES} . The appropriate Severity Classification from Table 4.1 was obtained for particular speeds and the worst classifications highlighted. Subsequently the mini-computer described in Appendix D was modified to perform the V_{rms} calculation (7.4.28).

Table 4.3 summarises and references 7.4.9 - 27 give the details of this testing. Any accessory with a 'rough' or worse classification was retested and if the classification was confirmed appropriate remedial action taken.

It should be noted that the Severity Criterion is derived from Standards with an upper frequency limit of 1000 Hz. Figure 1.2 has already shown that significant excitation sources exist above this frequency, in particular LP fan blade passing and external gearbox gear mesh excitation. A rider is therefore added in the reported classification where this depended primarily on any excitation up to 5000 Hz and above 1000 Hz. Accumulating Development experience has not given rise to any events to cause revision to this extension.

An example of typical V_{rms} plots for a gearbox and a fancase mounted accessory are shown in figures 4.4, 4.5. These also show an estimate for V_{RES} for the various peaks and the corresponding Severity Classification. In fig 4.4 a 'rough' classification is only obtained in the high speed region while in 4.5 a 'rough' classification is obtained at both low and high speeds. In the latter case it is appropriate therefore to apply the mission weightings of fig 4.3 to decide which peak is potentially more hazardous. In this example it is the high speed peak which is more likely to cause problems although it does not result in the greatest amplitude. In practice this particular vibration level was reduced to acceptable levels by attending to a balance problem in a shaft.

4.4 Summary

In this chapter a Severity Criterion has been developed from existing Standards to provide an assessment of the three dimensional vibration environment experienced by the installed accessory. The levels chosen are based on surveys of past and present vibration levels measured on Rolls-Royce aero-engine accessories and are weighted in a similar manner to the existing standards.

Where it is not clear which of several excitations may prove most troublesome factoring V_{RES} at particular engine conditions with a mission weighting can be used to clarify the situation.

Application of these procedures is straightforward and has been tested on an engine which is on the point of entering airline service. Data is now awaited to confirm the predictions of satisfactory service life which are indicated by Development experience.

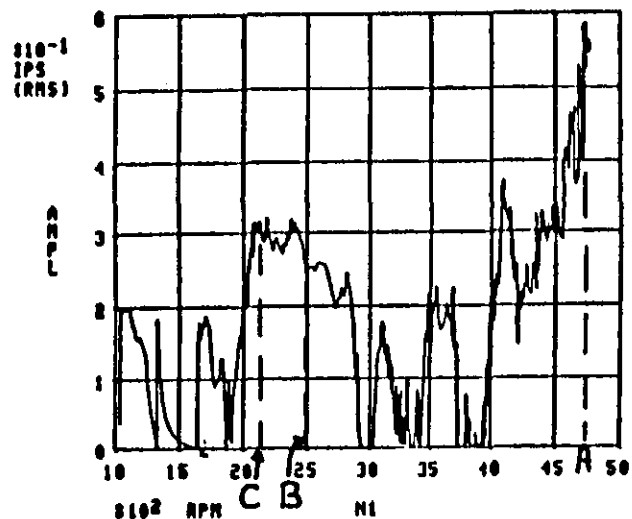
TABLE 4.3 SUMMARY OF RB 211-535C ACCESSORY VIBRATION CLASSIFICATIONS ON INITIAL TESTING

LOCATION	ACCESSORY	SEVERITY CLASSIFICATION	REMARKS
External High Speed Gearbox	Woodward Fuel Flow Governor	Fair	'Rough' with poor LP Fan Balance 'Very rough' during start
	HP Fuel Pump	Fair	
	LP Fuel Pump	Fair	
	Hydraulic Pump	Fair	
	Starter Motor	Fair	
	Oil Pump	Fair	
	HP Tachometer	Fair	
	Integrated Drive Generator Simulator	Fair	
LP Compressor (or Fan) Case	HP3 Handling Bleed Solenoid Valve	Rough	
	HP3 Starting Bleed Solenoid Valve	Fair	
	Integrated Engine Pressure Ratio Transmitter	Rough	
	Electric Engine Supervisory Controller	Fair	
	High Energy Igniter Boxes	Rough	
	Fuel Cooled Oil Cooler	Rough	
	Bleed Valve Control Unit	Smooth	
	P1 Altitude Pressure Switch	Rough	
LP Compressor Casing	Deceleration Detector Unit	Smooth	
	T ₁ Sensor	Fair	
	Top Temperature Limiter	Fair	
IP Compressor Casing	IP Bleed Valve Solenoid Valves	Rough	
	T ₂ Sonic Thermocouple	Very Rough	

NB: If confirmed 'rough' or worse on retest modification to the mounting or unit was undertaken as appropriate.

PROBLEM TITLE: HP3 HANDLING BLEED SOLENOID VALVE VIBRATION.
 CONFIGURATION: 4 MIN ACCEL.
 TRANSDUCER: SOLENOID RADIAL

THRESHOLDS: 0.20 IPS

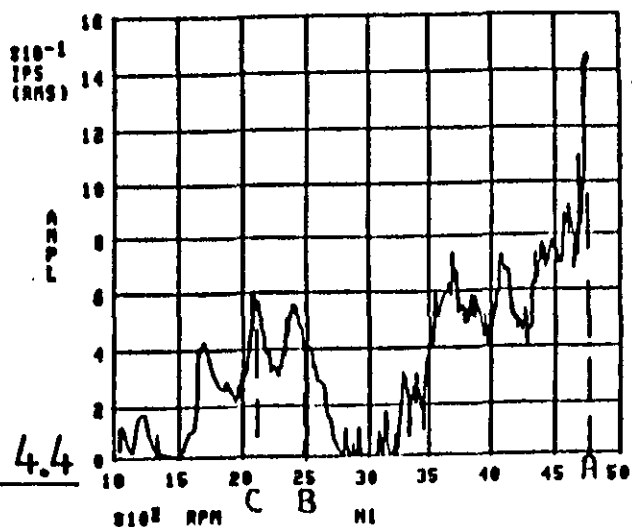


NET NO: 58202
 RD211-535
 ENG NO: 17/2
 DATE: 12-7-80
 PLOT NO: 1

BR 20-500
 AR 500
 AA -20
 CA 8
 TT 3
 TI 63

PROBLEM TITLE: HP3 HANDLING BLEED SOLENOID VALVE VIBRATION.
 CONFIGURATION: 4 MIN ACCEL.
 TRANSDUCER: SOLENOID AXIAL

THRESHOLDS: 0.20 IPS

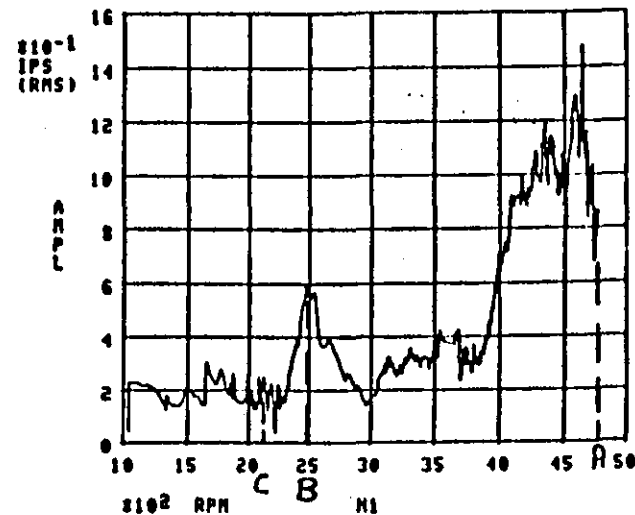


NET NO: 58202
 RD211-535
 ENG NO: 17/2
 DATE: 12-7-80
 PLOT NO: 1

BR 20-500
 AR 500
 AA -20
 CA 8
 TT 2
 TI 63

PROBLEM TITLE: HP3 HANDLING BLEED SOLENOID VALVE VIBRATION.
 CONFIGURATION: 4 MIN ACCEL.
 TRANSDUCER: SOLENOID TAN.

THRESHOLDS: 0.20 IPS



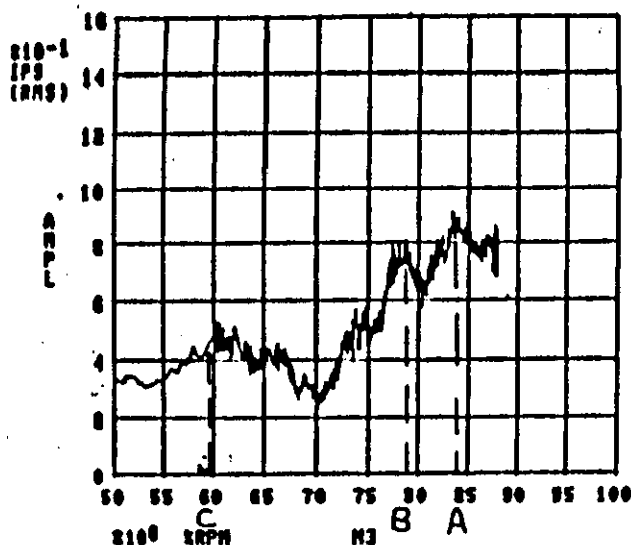
NET NO: 58202
 RD211-535
 ENG NO: 17/2
 DATE: 12-7-80
 PLOT NO: 1

BR 20-500
 AR 500
 AA -20
 CA 8
 TT 1
 TI 63

REF	RADIAL	V RMS		AXIAL	V RES	SEVERITY CLASSIFICATION
		Tang ¹				
A	0.58	0.85		1.45	1.78	ROUGH
B	0.25	0.6		0.4	0.76	FAIR
C	0.31	0.25		0.6	0.72	FAIR

Fig. 4.4

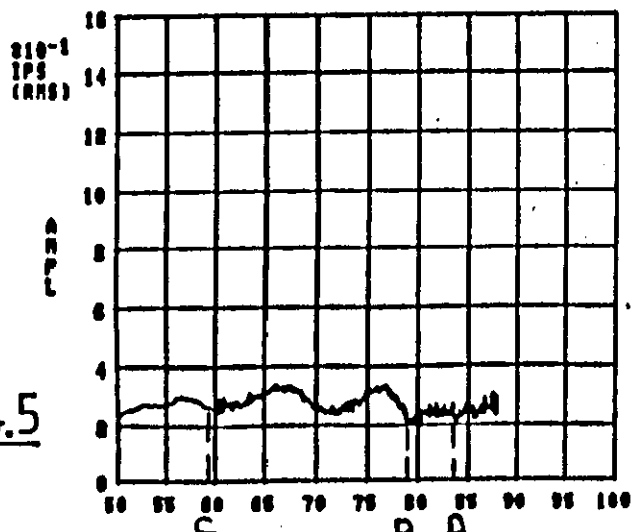
PROBLEM TITLE: FUEL FLOW GOVERNOR VIBRATION
 CONFIGURATION: 4 MIN ACCEL TO MAX - HI HYD LOAD
 TRANSDUCER: FFR END RAD THRESHOLDS 10.10 IPS



NET NO: 581300
 R0211-535C
 ENG NO: 17-1
 DATE: 20-4-80
 PLOT NO: 1

BR 10-5000
 AR 5000
 AA -30
 CA 4
 TT 5
 TI 32

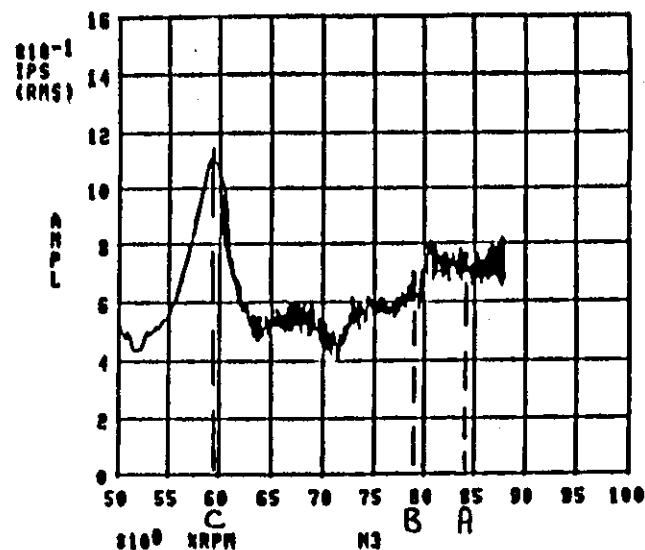
PROBLEM TITLE: FUEL FLOW GOVERNOR VIBRATION
 CONFIGURATION: 4 MIN ACCEL - HI HYD LOAD
 TRANSDUCER: FFR END AX THRESHOLDS 10.10 IPS



NET NO: 581300
 R0211-535C
 ENG NO: 17-1
 DATE: 20-4-80
 PLOT NO: 1-1

BR 10-5000
 AR 5000
 AA -30
 CA 4
 TT 6
 TI 32

PROBLEM TITLE: FUEL FLOW GOVERNOR VIBRATION
 CONFIGURATION: 4 MIN ACCEL HI HYD LOAD
 TRANSDUCER: FFR END TAN THRESHOLDS 10.10 IPS



NET NO: 581300
 R0211-535C
 ENG NO: 17-1
 DATE: 20-4-80
 PLOT NO: 1

BR 10-5000
 AR 5000
 AA -30
 CA 4
 TT 4
 TI 32

REF	RADIAL	V RMS TANGL	AXIAL	V RES	SEVERITY CLASSIFICATION
A	0.9	0.75	0.25	1.20	ROUGH
B	0.8	0.7	0.2	1.08	ROUGH
C	0.45	1.1	0.25	1.21	ROUGH

REF	V RES	SPEED	FLIGHT TIME WEIGHTING	FACTORED V RES
A	1.20	84%	24	28.8
B	1.08	79%	9	9.7
C	1.21	59%	11	13.3

RESPONSE AT A PROBABLE MAJOR SOURCE OF PROBLEMS

Fig. 4.5

5.0 MODELLING THE ACCESSORY

As part of the engine design process finite element models are used to predict probable engine dynamic behaviour and structural loadings. This is essential if costly mistakes are to be avoided. These models are correlated with rig and engine testing and modified as necessary. Recent work on this is cited in 7.5.1.

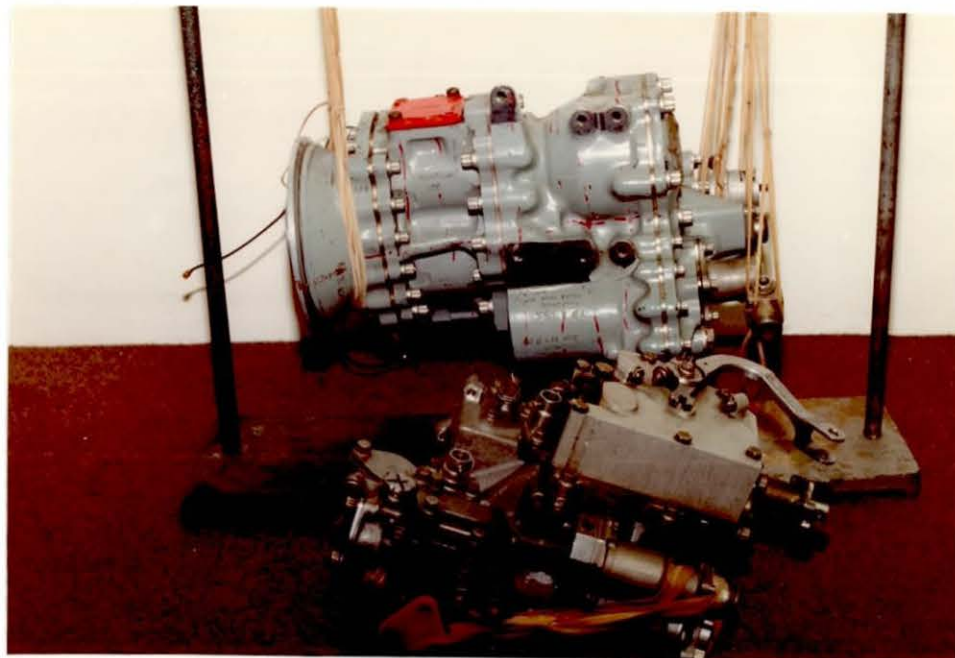
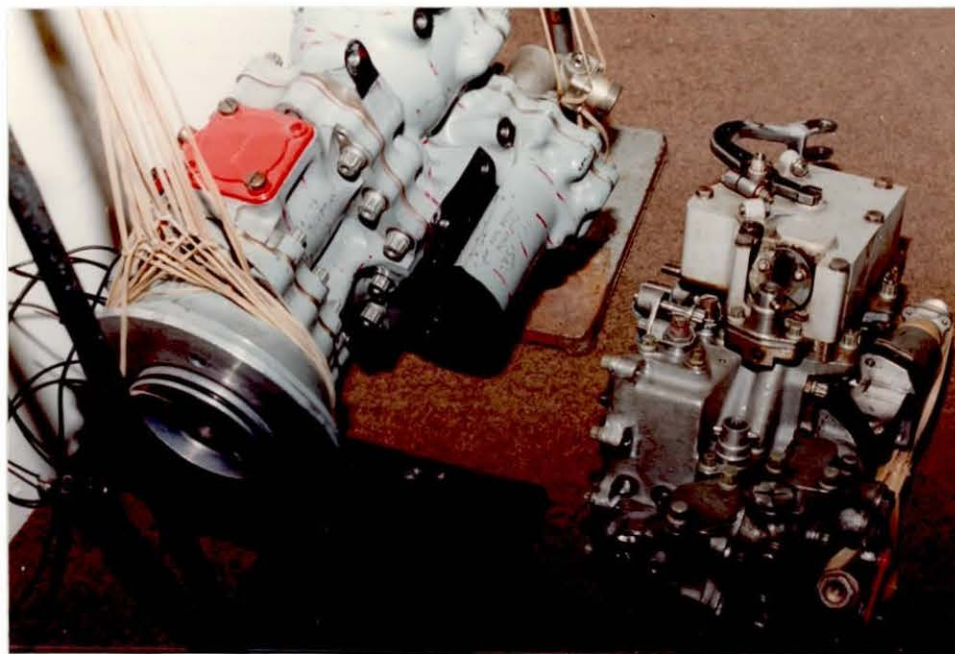
In order to achieve accurate predictions of the engine dynamics the approach has been to model the low frequency whole engine modes separately from those which occur at higher frequencies. At low frequencies the effects of shaft and rotor dynamics can be neglected and these structures represented by appropriate mass and stiffness at the various bearing surfaces. In a similar way the presence of accessories can be catered for. As the frequencies of interest increase the effects of shaft and rotor dynamics must be included in the response calculations as the engine no longer exhibits whole body modes and localised response begins to occur. At these higher frequencies, from 20 Hertz upwards approximately, it may still be appropriate to represent accessories as masses and stiffnesses acting at their mounting features but at some frequency even accessory structures will begin to have their own localised modes. These modes in turn will be modified by the response of the various internal components.

As already indicated simply designing and testing an accessory to a simple vibration envelope does not necessarily result in an acceptable service unit. The existing vibration testing and the improvements called for still only give an indication of the response to the estimated Service vibration environment when hardware in the form of accessory and engine exist. There is no fundamental reason why modelling of accessories should not take place in the early design and development programme as occurs on the complete engine. However this would result in increased cost in both manpower and computing facilities which may not be readily available to an accessory supplier. Further, the complexity in shape and construction of many accessories makes finite element modelling of the accessory difficult.

Therefore it is suggested that once the basic design has been finalised and some development units are available an experimental approach using modal testing be used to obtain a basic spring-mass subsystem model of the accessory based on techniques given in such works as 7.5.2 - 7.5.6. From this testing it is possible to experimentally obtain the modal properties of the accessory which could then be combined with existing engine models to predict overall response.

In order to investigate this approach transfer function testing has been performed on a Fuel Flow Regulator (FFR) using the free-free mounting arrangement and rig set-up shown in figures 5.1 and 5.2. Details of this set-up are given in Appendix C and of the analyser in 7.5.7.

This unit was chosen for both its convenient size and because it had been exhibiting vibration problems in Service as described previously. It was possible therefore, that this testing might have thrown further light on the problem. However the testing summarised in 3.4 was successfully completed before this work.



FUEL FLOW REGULATOR - FUEL SIDE BODY FREE - FREE MOUNTED
WITH AIR SIDE SEPARATED

DETAIL OF SD1002E ANALYSER



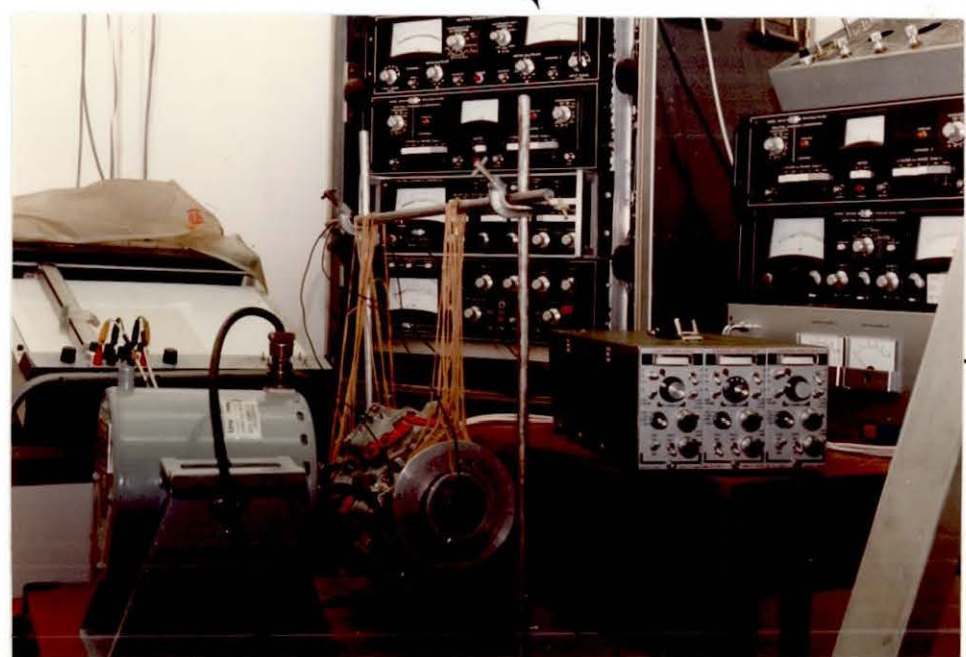
TWO CHANNEL LOG CONVERTOR

TWO CHANNEL TRACKING FILTER

TRANSFER FUNCTION ANALYSER

SWEEP OSCILLATOR

SD 1002E TRANSFER FUNCTION ANALYSER.



PLOTTER CONTROLLER

TRACKING FILTER

CO-QUAD ANALYSER

POWER AMP

CHARGE AMPLIFIERS

SHAKER

TEST RIG ARRANGEMENT



FIG. 5.2

5.1 Modal Test Results

A fully assembled FFR mounted as shown in figure 5.1 was excited by a sine wave sweeping from 10 - 3000 Hz. The input force and response were measured and the transfer function plotted as Mobility (velocity/force) is shown in figure 5.3.

After an initial rigid body mode of shaker and FFR at 10 - 12 Hz the Mobility plot shows a basically linear response with gradient of -1 to 70 Hz. Since it can be shown (7.5.5) that Mobility, M , is given by

$$|M| = -1/\omega m \quad \text{-----} \quad 5.1$$

where ω is the exciting frequency and m is the dynamic mass of the accessory this response shape is mass-like in that the structures driving-point stiffness and damping have little effect, the motion being that of the mass alone. Hence up to 70 Hz the assumption used in the engine model, that the accessory represents added mass is true for the FFR. In practice this frequency will be modified by it being clamped to the gearbox and further restrained by the connecting pipework.

Using equation 5.1 it can be shown that for this test the dynamic mass varies with frequency between 16.5 lbs (7.5 kg) and 18.7 lbs (8.5 kg), compared with an actual mass of 53.5 lbs (24.3 kg), nominal. Since for convenience the exciting force was adjacent to the mounting flange rotational effects have apparently reduced the mass by the amount shown. A simplified calculation shown in Appendix C gives a value of 19.9 lbs (9.05 kg) for the dynamic mass as measured at the flange. For a free-free beam reference 7.5.8 shows that the dynamic mass measured at the end of the beam can be a quarter of the mass acting through the centre of gravity of the beam.

As the mobility plot of fig 5.3 is traced above 70 Hz the effect of initially damping and then stiffness begin to predominate until the response from 115 Hz to 250 Hz is essentially entirely spring-like.

Since it can be shown (7.5.5) that

$$|M| = w/k \quad \text{-----} \quad 5.2$$

where k is the dynamic stiffness, it is found that the FFR has a stiffness varying between 16.9 to 13.9×10^3 lbf/ins (2.9 and 2.4×10^6 N/m) over this frequency. It should be noted that the response anti-resonance shown here is typical of an over-damped system since the intersection of the mass and stiffness lines is below the mobility curve. This is explained in 7.5.2. This level of damping also explains the continual change in phase of slightly over 180° in this region. If the structure was lightly damped a localised change of 180° would be observed.

Between 220 and 230 Hz the perturbation in the plot is due to a drive rod resonance.

An over-damped resonance at 240 Hz is followed by a mass-line to 300 Hz. This leads to a strong anti-resonance, resonance pair at 330 and 445 Hz respectively with little evidence of a stiffness line between the two. A discrete 180° , nearly, phase change is associated with these conditions. Based on half-power point theory damping estimates have Q values of 33 and 18 for the anti-resonance and resonance.

The signal glitch in the anti-resonance signal is the result of the lack of servo control in the test rig. At an anti-resonance the increasing force is 'soaked up' by the structure and no response is obtained resulting in very low signals from the measuring accelerometer. Under manual control it was found difficult to keep the force and response signals matched within the dynamic range of the analyser.

Above 445 Hz the mobility changes to a shape indicating increasing modal density and coupling between modes. This is probably the result of local resonances both of the FFR body and its internal members.

Further testing to investigate the effects of various internal and structural components was carried out and is summarised in Appendix C. The structures tested were the FFR with the fuel side internals removed and the FFR fuel side body on its own. The air side of the FFR shown in fig 5.1 was assumed to add mass and stiffness to the fuel structure.

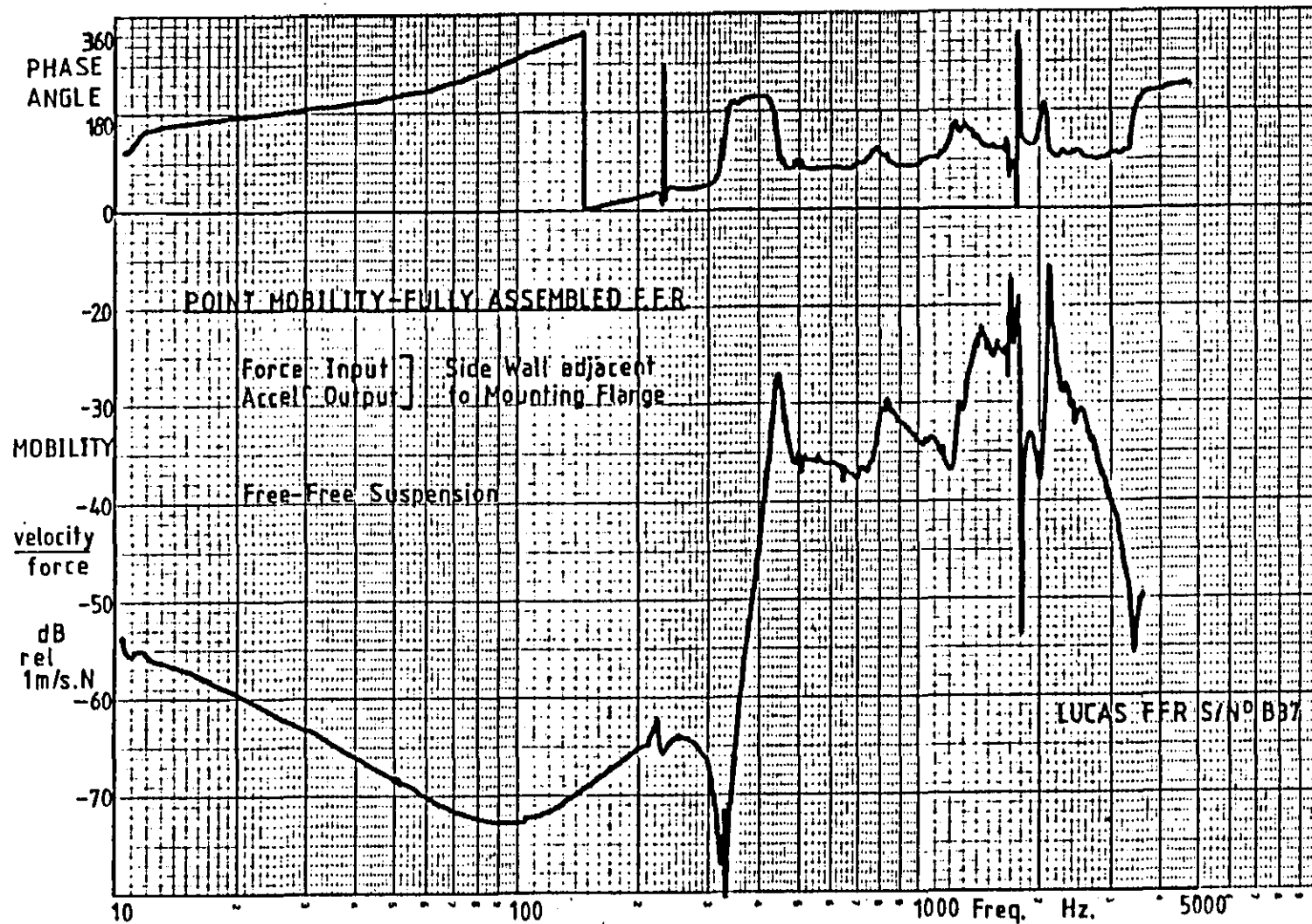


Fig. 5.3

5.2 Spring - Mass Subsystem Representation

It has been shown by Salter in 7.5.2 that it is possible to graphically derive the dynamic properties of a structure from its Mobility Plot. This technique is based on drawing the 'skeleton' of the plot. This skeleton is then used to deduce the mass and stiffness values of the structure which can then be represented by an arrangement of simple masses and springs. It should be noted that the springs might be termed 'real' rather than 'idealised' springs as they include the effect of damping, since damping is more closely associated with relative motion than inertia.

For simplicity the mobility plot of the FFR fuel side body with its internal components removed will be used to demonstrate this technique. The mobility plot obtained from testing in a similar manner to that described in 5.1 and detailed in Appendix C.1 is shown in fig 5.4. Superimposed on this plot is its skeleton, although again for clarity of illustration a mode around 2000 Hz has been ignored.

The skeleton illustrated has two mass and two stiffness lines and hence can be represented by a mass-spring system comprising two masses and two springs.

If the force applied at the driving point is represented by F and suffixes 1,2 refer to the two subsystems comprising M_1 , K_1 , and M_2 , K_2 the complete system can be represented by the model shown in figure 5.5.

At frequencies below 474 Hz ($= 1500 / \sqrt{10}$) the response follows a mass line M_1' which is given by

$$M_1' = M_1 + M_2 = 7.9 \text{ lbs (3.6 kg)} \quad \text{--- 5.3}$$

At frequencies above 9961 Hz ($= 3150 \times \sqrt{10}$) the system follows a spring line K_2' which is given by

$$K_2' = K_1 + K_2 = 365 \times 10^3 \text{ lbf/ins (62.83} \times 10^6 \text{ N/m)} \quad \text{--- 5.4}$$

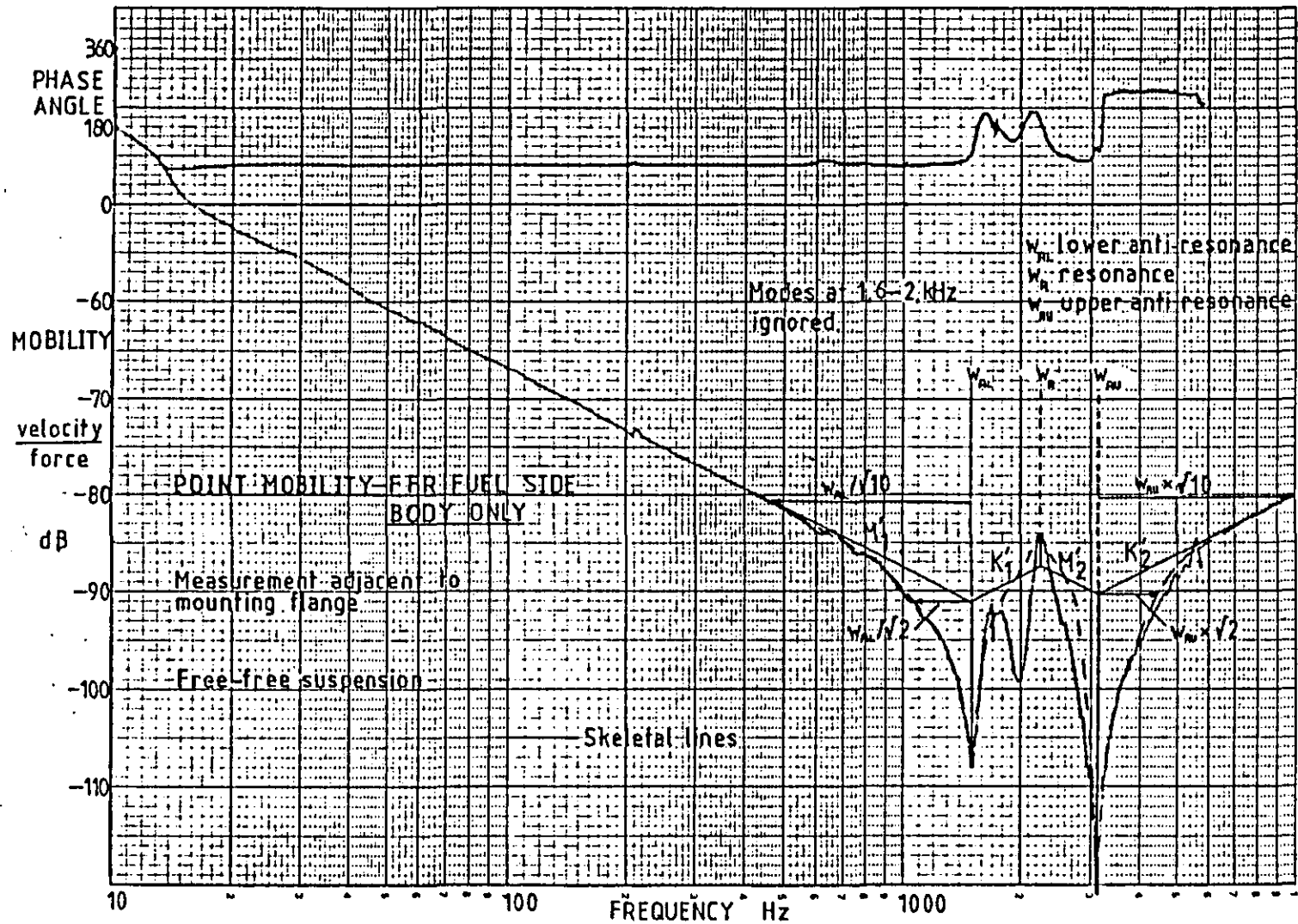
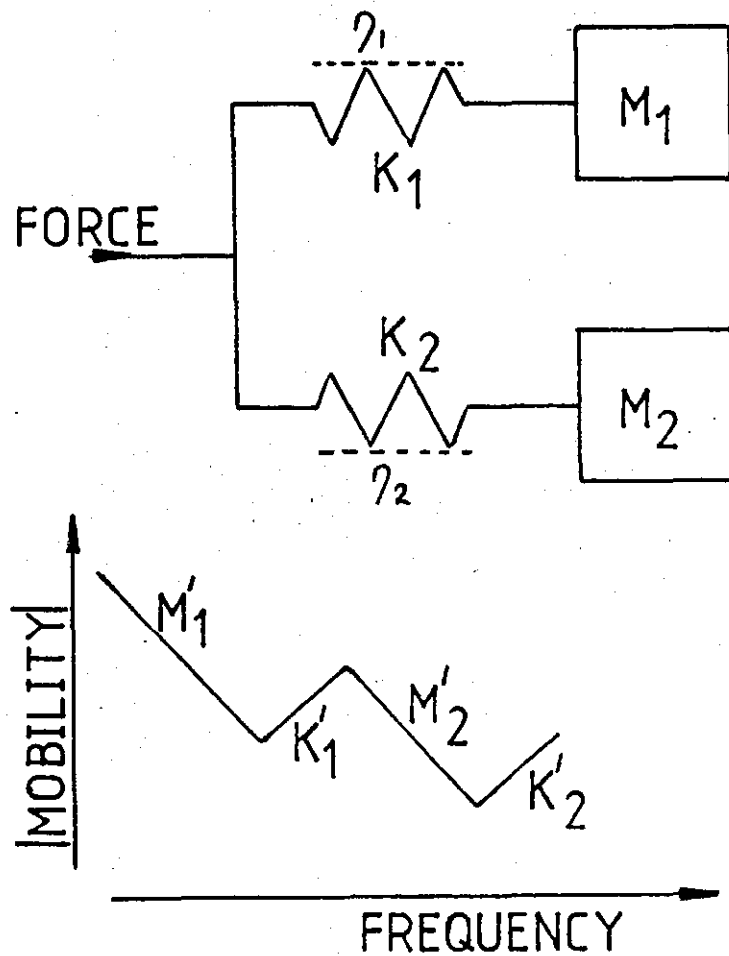


Fig. 5.4



PARALLEL MASS-SPRING SUB-SYSTEM MODEL
OF FFR FUEL SIDE BODY

At low frequencies, response is Mass-like

$$M'_1 = M_1 + M_2$$

At high frequencies, response is Spring-like

$$K'_2 = K_1 + K_2$$

Fig. 5.5

The frequencies cited above are the values $\sqrt{10}$ below and $\sqrt{10}$ above the appropriate anti-resonance frequency at which points for a lightly damped structure it can be shown (7.5.2) that the error in measuring a mass or spring-like response is small ($<10\%$).

At the resonant point (2273 Hz) all the elements are active with the system comprising two masses joined by a spring and we have the resonant frequency W_R given by

$$W_R^2 = \frac{K_1 K_2}{K_1 + K_2} \left(\frac{1}{M_1} + \frac{1}{M_2} \right) \quad \text{-----} \quad 5.5$$

Whilst at the two anti-resonances all the elements are active and we have the lower and upper anti-resonant frequencies W_{AL} , W_{AU} given by

$$W_{AL}^2 + W_{AU}^2 = \frac{K_1}{M_1} + \frac{K_2}{M_2} \quad \text{-----} \quad 5.6$$

Hence from a knowledge of W_R , W_{AL} , W_{AU} and M_1 , K_1 the sub system mass and spring stiffness values can be determined, giving

$$M_1 = 6.0 \text{ lbs (2.7 Kg)}$$

$$M_2 = 2.2 \text{ lbs (1.0 kg)}$$

$$K_1 = 138 \times 10^3 \text{ lbf/ins (23.8} \times 10^6 \text{ N/m)}$$

$$K_2 = 227 \times 10^3 \text{ lbf/ins (39.1} \times 10^6 \text{ N/m)}$$

It is apparent that the rotational effects described in 5.1 are reducing the apparent mass below that of the actual weight of 19.3 lbs (8.75 kg).

It is not clear from comparing the above simplified model which parts of the structure are acting as masses and springs. However if the small resonances and anti-resonances which were originally ignored are included they would change the model to a four mass system. The fuel side body comprises four sections bolted together and it is not unreasonable to hypothesise that these sections represent the masses with the

springs acting through the flanged joints.

The final requirement to fully define the FFR body using this spring-mass subsystem representation is to obtain an estimate of the damping at resonance and anti-resonance. This is simply done from consideration of the interpretation of the mobility plot. For a structure with critical damping the mobility plot would consist solely of mass and stiffness lines, i.e. the basic skeleton. However, with zero damping the mobility plot would tend to infinity in either a positive direction at resonance or a negative at anti-resonance. Hence the difference between the intersection of the mass and stiffness and the appropriate point on the mobility plot gives the damping or Q value directly.

In this example at	1500 Hz	Q =	17
	2273 Hz	Q =	3.5
	3150 Hz	Q =	30

These values can be confirmed using the half power point formula for Q given in reference 7.5.5 for example. It should be noted however that as the damping increases, i.e. Q gets smaller, the errors inherent in the assumption on which this technique is based increase (see 7.5.2). It should not be applied for Q less than 3, which implies the damping estimate at resonance is in error in the above example.

This technique can therefore be used to obtain a simple but accurate model of the accessory simply from the mobility plot results.

5.3 Modal Property Estimate using Vector Techniques

The previous section outlined a simple graphical approach to the interpretation of the driving point mobility plot of the test structure. With the availability of mini-computer based analysis equipment it is becoming easier to determine the modal properties of a structure based on the solution of eigen vectors and eigen value equations.

The derivation of these matrix equations while being based on classical theory allows much to the vector analysis techniques first reported by Kennedy and Pancu (7.5.3) and their interpretation by other researchers such as the works cited in 7.5.4 to 7.5.9.

Any vibrating structure, such as an aero engine accessory, can, in general, be represented as a multi-degree of freedom system having a number of modes of vibration. Each of these modes will have an eigen value and an eigen vector associated with it as well as a modal mass, M_r , and damping loss factor η_r . The eigen value gives the natural frequency, W_r , and the eigen vector the mode shape.

In general terms this may be expressed as:-

$$\alpha_{pq}(w) = \sum_{r=1}^n \frac{\psi'_{rp} \cdot \psi'_{rq}}{(1 - (w/W_r)^2 + i\eta_r)} \quad \text{-----} 5.7$$

where α_{pq} is the receptance (displacement/force) measured at a point p due to an exciting force of frequency w applied at point q. For each of the r modes of the structure there exists a modal flexibility coefficient ψ'_{rp} . The flexibility being given by

$$\psi'_{rp} = \frac{[\psi]_r}{M_r \cdot W_r} \quad \text{-----} 5.8$$

where $[\psi]_r$ is the mode shape vector.

Equation 5.7 can be expressed in complex notation in the form

$$\alpha(w) = \sum_{r=1}^n \frac{C_r \cdot e^{i\theta_r}}{(1 - (w/W_r)^2 + i\eta_r)} \quad \text{-----} 5.9$$

and at frequencies close to W_r this can be written as

$$\alpha(\omega) = \frac{C_r e^{i\theta_r}}{(1 - (\omega/\omega_r) + i\eta_r)} + D_r \dots 5.10$$

where D_r is a complex residual representing the effective contribution of all other modes to the resonance.

If the receptance is plotted on a Nyquist Diagram it can be shown that the resonant frequency occurs at that point where the spacing of equal frequency increments is greatest i.e. at the point of maximum rate of change of frequency. A diameter drawn through this point of the arc can be shown to represent the value C_r/η_r , as indicated in figure 5.7. With reference to this figure η_r can be found using the relationship.

$$\eta_r = \frac{(\omega_2'^2 - \omega_1'^2)}{\omega_r^2} \times \frac{1}{(\tan \theta_1/2 + \tan \theta_2/2)} \dots 5.11$$

The displacement of the end of the diameter opposite ω_r to the origin of the Nyquist axes gives the value of D_r and the angle of D_r to the imaginary axis gives θ_r .

The derivation of the above relationships is given in such works as 7.5.5.

Hence by measuring the transfer function at the driving point and at a number of other locations on the structure the modal properties of the test structure may be determined. It does not matter which form of transfer function is measured as receptance, mobility and inertance are related by frequency.

Using the same FFR fuel side structure as in 5.2 and the rig shown in figure 5.2 with the SD 109B Co/Quad analyser the real and imaginary mode response vectors (or coincident and quadrature vectors) were found. Applying the excitation at the centre of the FFR body the Nyquist plots of figure 5.6 were obtained. (It should be noted that these plots are inertance plots, mobility circles would be rotated 90° clockwise.)

It should be observed from figure 5.6 that due to coupling between the modes complete circles are not obtained and each mode is determined from the characteristic loops in the plot.

Using the least-squares technique (7.5.9) a computer programme was developed, Appendix C.5 which plotted a best fit circle through the experimental data points for each mode and derived the natural frequency, damping, flexibility, and residual terms for each mode as summarised in figure 5.7.

Having obtained the modal parameter values the final piece of information for complete determination of the mode is its shape. Since for a pure mode the real term tends to zero and the imaginary to a maximum, measurement of the normalised imaginary term at different parts of the structure give the mode shape directly for a particular value of W_r .

Using the measurement locations shown in figure 5.8 the mode shapes at the two different frequencies of figure 5.8 are obtained. These show simple bending of the FFR fuel side body.

Hence, although simplified it has been shown in this section that it is feasible to obtain the dynamic properties of an accessory from a measurement of its transfer function.

NYQUIST PLOT 1400-2120.Hz

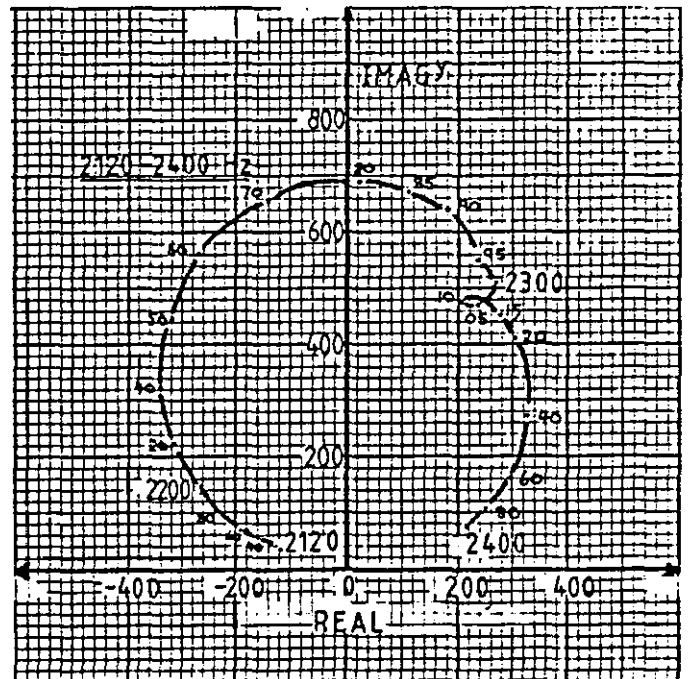
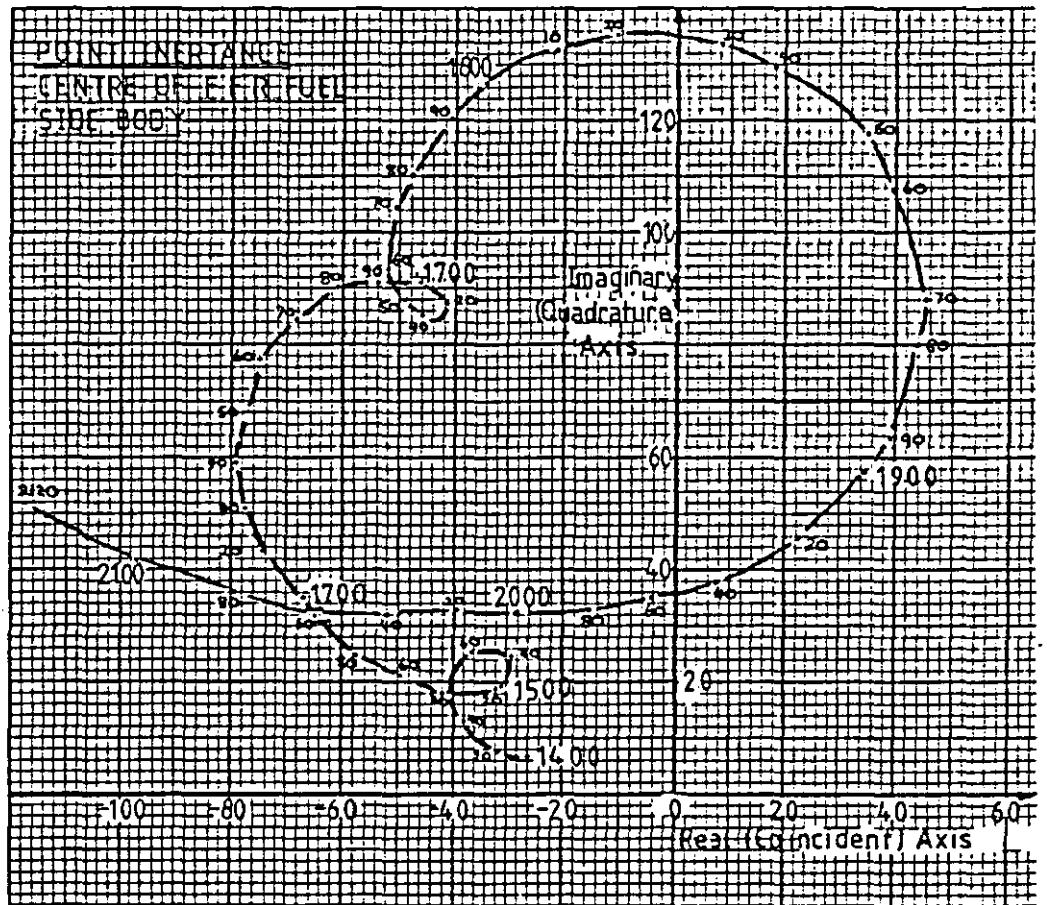
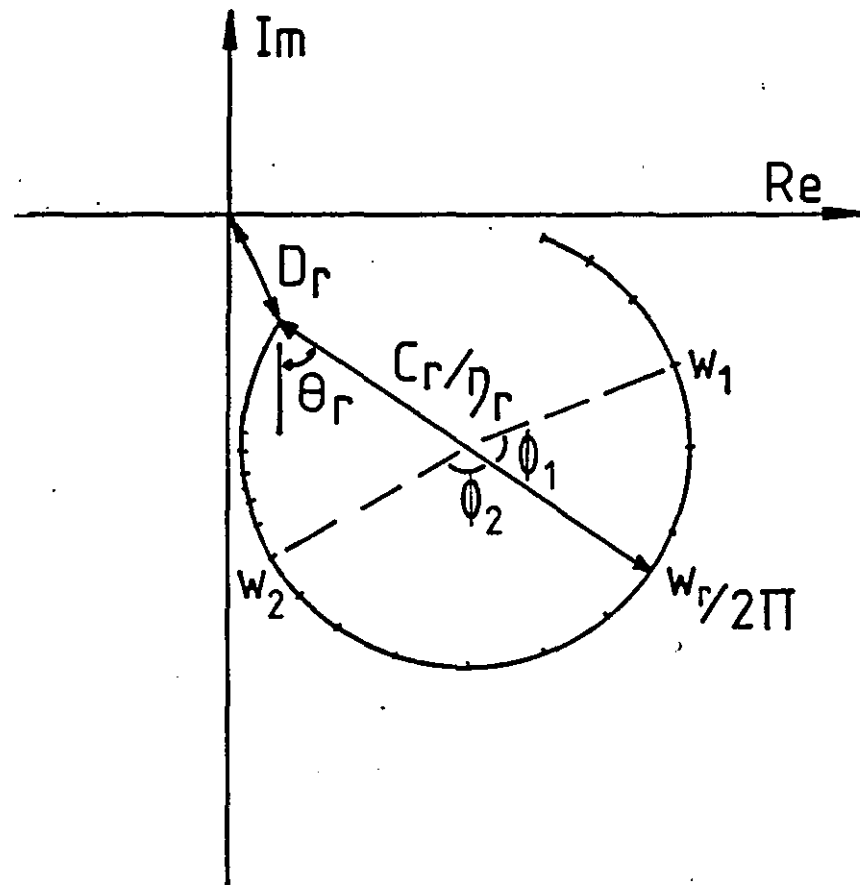


Fig. 5.6

NYQUIST PLOT OF MODAL CIRCLE



Now

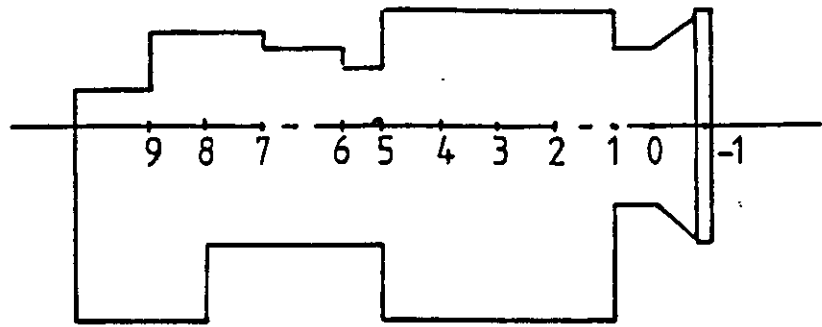
$$\eta_r = \frac{w_2^2 - w_1^2}{w_r^2} \times \frac{1}{\tan \phi_2 + \tan \phi_1}$$

Hence we can solve the Receptance Eqn.

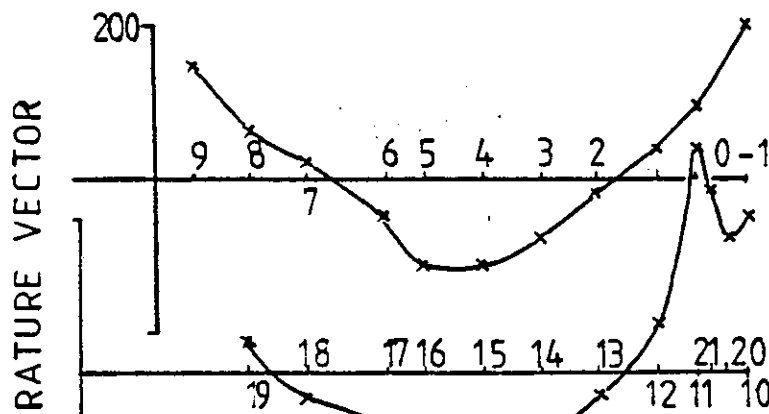
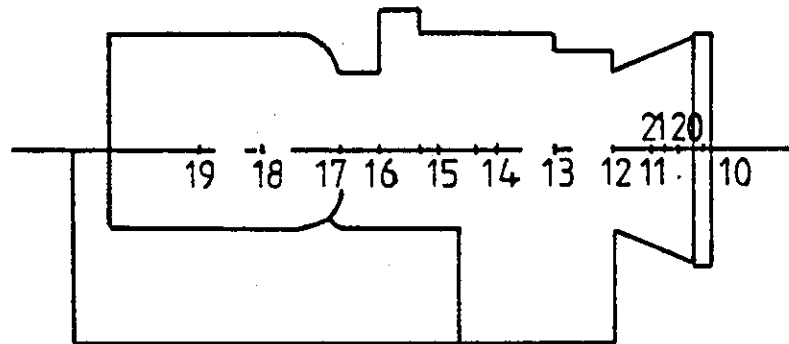
$$\underline{\underline{\alpha(w) = \frac{C_r \times e^{i\theta_r}}{1 - (w/w_r)^2 + i\eta_r} + D_r}}$$

Fig. 5.7

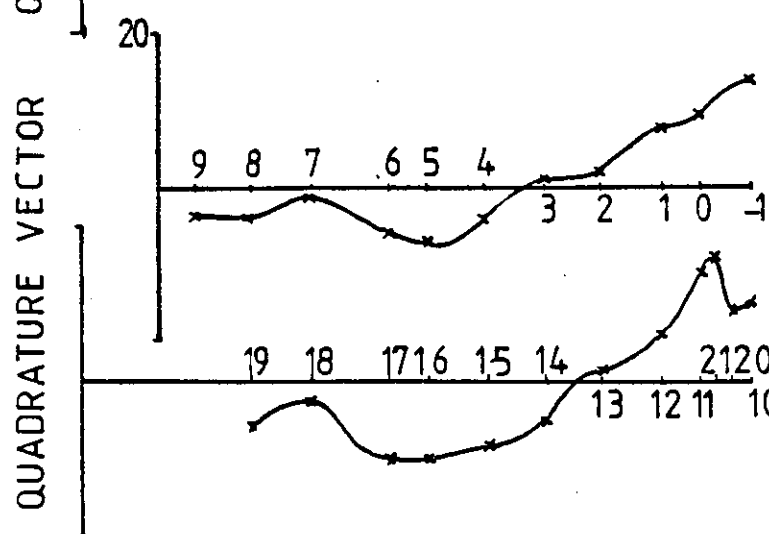
SCHEMATIC OF F.F.R.



MEASUREMENT REFERENCE LOCATIONS SHOWN



MODE AT
2282 Hz



MODE AT
1665 Hz

Fig. 5.8

5.4 Summary

In this chapter it has been argued that further insight into accessory dynamic behaviour can be achieved by incorporation of the accessory response in an engine model. The assumption that the accessory can be modelled basically as an additional mass element has been validated although the frequency range over which this assumption can be made will depend on the accessory and its attachments to the engine.

Further it has been demonstrated using the FFR that existing graphical or modal techniques can be used to obtain an adequate representation of the structure which could be used in the engine models. The development of mini-computer systems favour the modal testing vector approach with systems now being available which directly obtain the modal parameters found in section 5.3.

This increased understanding of accessory dynamics can only help in the goal of achieving acceptable service reliability.

6.0 CONCLUSIONS

Since the reliability of an aero-engine depends in part on the reliability of its accessories, accessory dynamic behaviour has become of increasing interest. Problems highlighted in chapter 2 have shown that the initial testing described in chapter 1 had proved inadequate, especially in terms of vibration simulation. A careful study of both rig and engine testing showed where improvements in this simulation of the engine environment could be achieved.

This thesis has detailed this work and the improvements which have recently emerged as a revision to the basic Accessory Vibration Specification used at Rolls-Royce, Derby.

The major revision has been the provision of a Spoke Diagram, both as a design aid for the Accessory Manufacturer and as a development aid for rig endurance testing. The use of this diagram should help to significantly reduce vibration problems occurring during all phases of the accessory and associated engine development programme. This will assist the achievement of these programmes within the desired project costings and timescales.

The use of multi-sine testing has been shown by the FFR Pivot Arm example to better represent the engine environment on the rig than previous techniques. With the increased endurance period associated with this form of testing improved service reliability is expected, since a better indication of functional problems associated with accessory operation in service use has been demonstrated.

These improved vibration endurance tests will result in increased testing costs. One supplier has estimated that his basic testing costs will rise from £5000 to £14,500, almost a three-fold increase. This neglects the costs of any additional equipment needed to meet the test requirements. However these costs are minimal when compared to the costs incurred by poor reliability, whether this be judged as the costs involved in an engine repair or even loss of further orders.

Some recent accessory testing has further indicated that for many fancase mounted electronic accessories coincidence between natural frequencies and engine spokes have only occurred on one or at the most two major conditions. This has meant that if this new vibration specification had been applied to these accessories apart from the endurance period the testing would have reduced to the existing methods i.e. existing endurance methods could be considered to be a particular application of a more generalised technique suggested in this thesis.

Having shown how better simulation of the engine vibration environment on the rig can be achieved improved reliability assessment techniques on the engine were developed. This involved the use of a Severity Criterion based on the evidence from three dimensional measurements on the accessory. The resultant level seen at a speed was obtained and compared with a classification table derived from experimental evidence. Where several unacceptable classifications resulted in the operating ranges their relative significance could be estimated by applying a Mission Weighting Factor. This would enable decisions to be made on which areas would best warrant further investigations in order to improve the vibration environment of the accessory and hence its performance on the engine.

The forgoing has shown how improved simulation of the engine environment can be achieved on the rig and probable service reliability predicted from engine test, this being summarised in figure 6.1. One further approach to assessment of behaviour in the service environment was shown in chapter 5 where the extension of existing engine structural dynamic modelling to the accessory was made. Although at an elementary level it was shown that an adequate model of the accessory could be achieved from modal testing techniques.

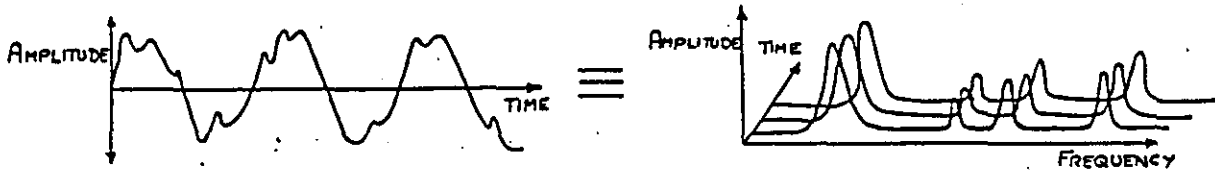
This thesis has been based on the lessons learnt from vibration problems with accessories containing mechanical components which have exhibited some form of wear. With the increasing use of electronics to perform control functions it is probable that other types of problem manifestation will occur. In this case it may well be appropriate to modify the testing detailed in this work

although the principles used will be the same. Hence this work could be regarded as a statement of the general case for accessory testing.

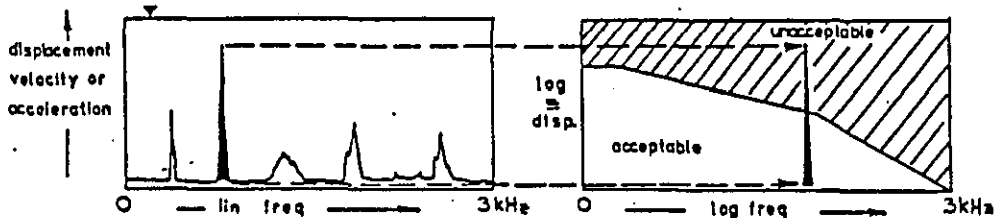
Why existing rig and engine testing have not always revealed all the potential vibration problems that could occur on an accessory has been shown in this work. Having revealed these failings appropriate revisions to improve this have been developed to the point where confidence in their validity exists. This has resulted in a revised Accessory Vibration Specification, successful solution of vibration problems, and predictions of probable service experience on accessories fitted to a major new derivative engine. In addition the development of a route towards better prediction of vibration behaviour has been outlined and should be the subject of further research.

VIBRATION SEVERITY CRITERION FOR ACCESSORIES

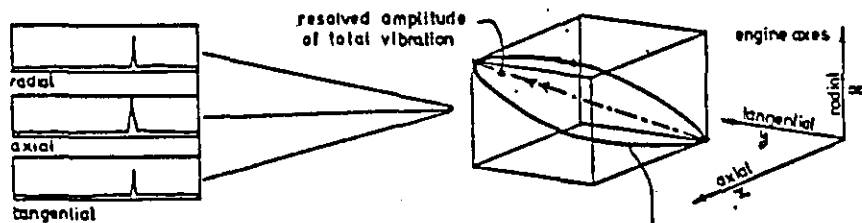
1.0 Transducer signals of time (or speed) varying waveforms from 3 perpendicular directions may be broken into instantaneous amplitude components at a frequency.



2.0 To decide whether any vibration is likely to cause a problem current Rolls-Royce assessment methods abstract individual spectral peaks for each direction in turn and apply a simple severity envelope.



3.0 This neglects the fact that the damage caused by real life motion is the result of all simultaneous spectral peaks in 3 directions.



Amplitude/phase or time domain data enables visual presentation of complex motion

4.0 To improve the current severity assessment the following two steps are taken:-

4.1 Incorporate all spectral peaks for a speed and direction (B.S. 4675 refers). The vibration amplitude of the peaks should be expressed in velocity r.m.s. as this has the advantage over displacement or acceleration that upto 1000 Hz similar amplitudes can be considered as equally severe.

At a speed, we have $V(x)_{rms} = \sqrt{\frac{1}{2} (\hat{V}_1^2 + \hat{V}_2^2 + \dots + \hat{V}_n^2)}$ Where \hat{V}_n is the peak amplitude of nth peak in the particular direction.

4.2 Obtain the Resultant Amplitude. Whenever possible resolve rms velocity values obtained from the 3 directions above as follows:-

$$V_{RES} = \sqrt{(V_x^2_{rms} + V_y^2_{rms} + V_z^2_{rms})}$$

If only 2 directions are measured assume third is equal to the resultant of the other two.

$$V_{RES} = \sqrt{(2[V_x^2_{rms} + V_y^2_{rms}])}$$

If only 1 direction is measured assume the remaining two are equal to the measured one:-

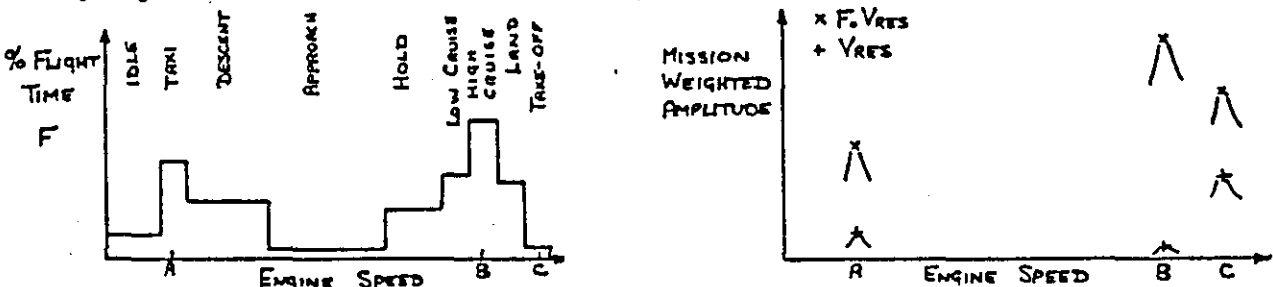
$$V_{RES} = \sqrt{3 V_x^2_{rms}}$$

unless there is a strong reason otherwise

5.0 The value so obtained is then compared to the empirical table opposite to obtain a severity classification for the unit in that environment. The effect of vibration defined by the severity classification must be assessed bearing in mind the structural properties and functional complexity of the accessory, and weighted for the 'worst engine' case.

V_{RES} ins/sec	Classification
> 10	Extremely Rough
3 - 10	Very Rough
1 - 3	Rough
0.3 - 1	Fair
0.1 - 0.3	Smooth
< 0.1	Very Smooth

6.0 The classifications obtained at various speeds should then be multiplied by the appropriate flight time factor to obtain a mission weighted estimate of the relative severities, e.g. a "rough" classification at take-off could have a lower weighting than a "smooth" classification at cruise.



7.0 REFERENCES

7.1 Introductory References

- 7.1.1 Gas Turbine Carcase and Accessory Vibration - Problems of Measurement and Analysis - D S Pearson, A H E Holme, P R Watts, Proc, Sym Soc Environmental Engineers.
- 7.1.2 Considerations in Vibration Testing on Gas Turbine Aero-engines - A H E Holme. Paper presented at I Mech E, Derby Branch, March 1979.
- 7.1.3 The Testing and Approval of Aircraft Engine Mounted Accessories - D S Pearson, Proc I Mech E Vol 196 No 5 1982.
- 7.1.4 British Standard Specification for General Requirements for Equipment in Aircraft - BS 3G 100 1969 (in particular Pt 2, Section 3 Sub-section 3.1: Vibration).
- 7.1.5 Military Standard Environmental Test methods for Aerospace and Ground Equipment: MIL - STD - 810C (in particular Method 514:2 - Vibration).
- 7.1.6 Accessory Control Specification (ACS) 1014 - Accessory Vibration Testing, Issue 1, 26-9-69; Issue 3, 8-8-77; Issue 4, 24.6.82 Rolls Royce Ltd.
- 7.1.7 The Mechanics of Vibration - R E D Bishop, D C Johnson, C U P 1960.
- 7.1.8 Vibration Problems in Engineering - S Timoshenko, D H Young, W Weaver 4th Edition, Wiley 1974.
- 7.1.9 Shock and Vibration Engineering - C T Morrow Vol 1, Wiley, 1963.
- 7.1.10 The Dynamical Behaviour of Structures - G B Warburton 2nd Edition, Pergamon 1976.

- 7.1.11 Selection and Performance of Vibration Tests -
A J Curtis, N G Tinling, H I Abstein - SVM 8
Shock and Vibration Information Centre 1971.

7.2 References on Vibration Experience

- 7.2.1 RB 211 - Summary of Operations: Rolls-Royce Ltd
(Bi-monthly).
- 7.2.2 RB 211 - Operators Conference Proceedings: Rolls-
Royce Ltd (Annual).
- 7.2.3 RB 211-22 Teleflex Box Problems - Static Test Results
prior to Cathay Engine Test - MEM 62619 D S Pearson
25-5-77, Addendum 1, 2 J C Maguire 25-5-77 Rolls-
Royce Ltd.
- 7.2.4 Cathay Teleflex Failure Investigation, RB 211-22
Engine 10518, 10529 MER 62619, D S Pearson 15-6-77.
Rolls-Royce Ltd.
- 7.2.5 Random Data: Analysis and Measurement Procedures -
J S Bendat, A G Piersol, Wiley - Interscience 1971.
- 7.2.6 The Technique of Correlation, Selection of Correlation
Parameters and Applications to Noise and Vibration
Analysis - V Marples, A Ryde-Weller, Applied Acoustics
Vol 12 1979.
- 7.2.7 RB 211 Fancase Rig Vibration, comparison of Standard
Rubber Mounted and Bowstring Lower Teleflex Boxes.
MER 63043 C D Lee 4-6-79, Rolls-Royce Ltd.
- 7.2.8 RB 211-22B Lower Teleflex Box, Comparison of Standard
and Modified Racks. VLR 083 T Martin 3-6-80 Rolls
Royce Ltd.
- 7.2.9 Initial investigation of the vibration on the external
wheelcase due to out of balance of the Radial Drive
System. MER 62853A P R Watts 20-7-78 Rolls Royce Ltd.

- 7.2.10 Radial Drive Shaft Balancing, Interim Report.
MDR 61370 J D Towler 6-6-78 Rolls Royce Ltd.

- 7.2.11 Vibration Testing of Bow String Type Lower Box
Assembly TR 2106-2319 E A Jelesiewicz August 1979
Teleflex Incorporated.

- 7.2.12 RB 211 - Teleflex 'Bowstring' Throttle Control -
Vibration Test, Report of Lab. Testing conducted
at AEL Philadelphia, 2-10th April 1979. MER 63055
D S Parson 18-4-79 Rolls-Royce Ltd.

- 7.2.13 Comparison between Derby Test Bed and Flight Vibration
Levels - Teleflex Box MER 62736A N L Gibson 17-5-78
Rolls Royce Ltd.

- 7.2.14 Addendum to MER 62736A. MER 62736B N L Gibson
P R Watts 9-6-78 Rolls Royce Ltd.

- 7.2.15 Rig Evaluation of RTS 62040 - Modification to Teleflex
System ESL 10123 D Kemp, D M Blomley 18-7-78 Rolls
Royce Ltd.

- 7.2.16 A comparison of Vibrations in the Region of the
Lower Teleflex Box with Standard and Modified mount-
ing configurations. MER 62715 P R Watts, N L Gibson
5-10-78 Rolls-Royce Ltd.

- 7.2.17 Influence of Out-of-Balance of Input Drive Systems
to the External Gearbox on vibration in the region
of the lower Teleflex Box MER 62882 P R Watts 6-10-78
Rolls-Royce Ltd.

- 7.2.18 Fancase Rig: Influence of Out-of-balance of Input
Drive System to the External Gearbox on Vibration in
the Region of the Lower Teleflex Box. MER 62871A
P R Watts 10-10-78 Rolls-Royce Ltd.

- 7.2.19 A comparison between Vibration in the region of the
lower Teleflex Box etc. MER 62736E P R Watts 30-10-78
Rolls-Royce Ltd.

- 7.2.20 Teleflex "Bowstring" Box - Investigation Report -
J C Vaughan 11.12.78 ADR 60238 Rolls Royce Ltd.
- 7.2.21 RB 211 Teleflex System: Conclusions from Examination
of Specification of TWA Isolating Bushes - D Kemp
Rolls Royce Ltd ESL 10163 18.1.79.
- 7.2.22 Teleflex Lower Box - Tuned Rack Modification -
Vibration Survey J C Vaughan Rolls Royce Ltd ADR 60260
11.10.79.
- 7.2.23 Comparison of Vibration characteristics between
Standard and Anti-Vibration Mounted Lower Teleflex
Box - C Wright Rolls Royce Ltd MER 63037B 18.3.80.
- 7.2.24 Effect of Out Of Balance on the Input Drive Shafts
to the Vibration in the Region of the Lower Teleflex
Box - C D Lee Rolls Royce Ltd MER 62871C 2.4.80.
- 7.2.25 Anti-Vibration Mounted lower Teleflex Box - Summary
of Experience to Date - J C Vaughan - Rolls Royce
Ltd ADR 60273 24.4.80.
- 7.2.26 RB 211-22B and -524 Lower Teleflex Box Wear SPA 60285
C J Waltho 9.7.81 Rolls Royce Ltd.
- 7.2.27 RB 211-535 E4 Teleflex Cable Installation/Design
L Millington 26.2.82 Rolls Royce Ltd (Internal
Memorandum).

7.3 Accessory Revision References

- 7.3.1 RB 211 FFR: Summary of Capsule Pivot Vibration
Testing prior to Report J.52752/FY AA Crawley
Lucas Aerospace Ltd Report J.52752/FF 22.4.75.
- 7.3.2 RB 211-22 FFR Vibration Testing of Capsule Pivot
Assembly. Scheme 52752/1206 A A Crawley Lucas
Aerospace Ltd Report J.52752/FY 6.12.74

- 7.3.3 Vibration Surveys Conducted on Schemes 52752/1206 and 52752/1207 B J Baker Lucas Aerospace Ltd Report J 52752/GN 29.7.75
- 7.3.4 RB 211 FFR Interim Report on Development Testing to reduce Fretage Wear of Capsule Lever Trunnions D P Whatley Lucas Aerospace Ltd Report J 52752/HP 11.2.77.
- 7.3.5 Investigation of 211 VMO Lever/Capsule Ball Race Failures from a Vibration Standpoint T Roberts Lucas Aerospace Ltd Report E and DD 7791 29.11.77
- 7.3.6 RB 211 Fuel Flow Regulator 2nd interim Report on Rocker Lever Improvements V M Lucas Lucas Aerospace Ltd Report J52752/JD 13.12.77
- 7.3.7 Further investigation into RB 211 VMO Lever Ball Race Failures T Roberts Lucas Aerospace Ltd Report E and DD 7795 4.1.78.
- 7.3.8 Simulation of Vibration Spectrum on RB 211 FFR to conform with results taken on an engine at Rolls-Royce Derby. T Roberts Lucas Aerospace Ltd Report E and DD 7814 11.8.78.
- 7.3.9 RB 211 FFR, 1000 hours Endurance with Modified Rocker Lever (SCH 52752/1231) BG Jeffries Lucas Aerospace Ltd Report J 52752/JQ 19.9.78
- 7.3.10 RB 211 FFR interim report on vibration endurances to induce Capsule Lever Wear D P Whatley Lucas Aerospace Ltd Report J52752/KD 1.2.79
- 7.3.11 RB 211, FFR Serial No B4, Condition of CP 5009 Components after Vibration testing B G Jeffries Lucas Aerospace Ltd Report J52752/KF 24.5.79

- 7.3.12 RB 211/22 Comparison of Capsule Lever Standards
CP 5009 and CP 5620 under Vibration Endurance
Conditions. D P Whatley Lucas Aerospace Ltd
Report J 52752/KI 12.6.79.

- 7.3.13 RB 211 Fuel Flow Regulator, Vibration Testing of
Rocker Lever to CP 5620 Standard V M Lucas
Lucas Aerospace Ltd Report J 52752/KJ 5.7.79.

- 7.3.14 Comparison of Vibration Levels inside and out-
side the RB 211 Fuel Flow Regulator R I Hay
Rolls Royce Ltd Report FDR 60217 17.4.74

- 7.3.15 Vibration Survey of VMO Stirrup (Lockheed Standard)
RB 211-524 38/8, G H Busby, P R Watts Rolls Royce
Ltd Report MER 62720 7.6.78

- 7.3.16 Fuel Flow Regulator, Capsule Stirrup Assembly with
Carbon Trunnion Bearings and Spring Loaded Thrust
Bearing and Articulation J Whitmarsh Rolls Royce
Ltd Report FJR 60086 7.9.78

- 7.3.17 Vibration Survey of VMO Stirrup (Tolerance limit)
RB 211-22 1012/12 P R Watts Rolls Royce Ltd
Report MER 62781 18.9.78.

- 7.3.18 Vibration Survey on VMO Stirrup (Worn unit) RB 211
-22B 10462/8 P R Watts Rolls Royce Ltd Report
MER 62939 16.10.78

- 7.3.19 Vibration Survey of VMO Stirrup (Boeing Std -524)
RB 211-524 38/8 P R Watts Rolls Royce Ltd Report
MER 62737 30.10.78.

- 7.3.20 RB 211 -524 36/7C Summary of FFR Vibration Investigation
in flight and on the Derby Test Bed P R Watts
Rolls Royce Ltd Report MER 62736I 14.11.78.

- 7.3.21 RB 211-22B Fuel Flow Regulator, Status of Lucas
Vibration Test etc J Whitmarsh Rolls Royce Ltd
Report FDR 60516 6.3.79.
- 7.3.22 The Jet Engine - Rolls Royce Ltd 3rd Edition
1969.

7.4 Environment Assessment References

- 7.4.1 Vibration Tolerance - T C Rathbone Power Plant Engineering Vol 43 1939.
- 7.4.2 The Rationale of Monitoring Vibration on Rotating Machinery in Continuously Operating Process Plant - E Downham, R Woods ASME 71-Vibr-96 1971.
- 7.4.3 Velocity Criteria for Machine Vibration - S Maten Hydrocarbon Processing 1967 (Reprint Vibration and Acoustic Meas Handbook edited by Blake and Mitchell, Spartan Books 1972).
- 7.4.4 The Practical Vibration Primer - C Jackson Chap 8 Gulf Pub Co. 1979.
- 7.4.5 Mechanical Vibration in Rotating and Reciprocating Machinery: Pt 1 British Standard BS 4675 1976 (I.S.O. 2372 - 1974)
- 7.4.6 On the Severity of External Gearbox Vibration: etc. MER 62736 F P R Watts 25.7.78 Rolls Royce Ltd.
- 7.4.7 The Severity of Vibration on the External Wheelcase on the RB 211 Engine MER 00434 P R Watts 17.5.78 Rolls-Royce Ltd.
- 7.4.8 Prediction of Engine Vibration orders which may be expected on Fan Case, Compressor and Gear box Mounted Accessories. A H E Holme RB 211-535 Rolls Royce Ltd Report MER 58026 4.6.79.
- 7.4.9 Vibration Survey on Gearbox Mounted Accessories RB 211-535 Eng 1 Bld 1 A H E Holme Rolls Royce Ltd Report No. (See over).

Lucas Fuel Flow Regulator	MER 58010A	21.6.79
HP Fuel Pump	B	28.6.79
LP Fuel Pump	C	11.7.79
IDG Mass Simulator	D	12.7.79
Hydraulic Pump	E	17.7.79
Starter Motor	F	18.7.79
Oil Pump	G	20.7.79
HP Tacho Generator	H	23.7.79

7.4.10 Vibration Survey on IP Bleed Valve Solenoid Valve
RB 211-535 Eng 1 Bld 1 A H E Holme Rolls Royce
Ltd Report MER 58008 5.7.79.

7.4.11 Vibration Survey on Gearbox Mounted Accessories
RB 211-535 Eng 1 Bld 1 A H E Holme, A J Liles,
Rolls Royce Ltd Report No:-

Woodward Governor Fuel Flow Regulator	MER 58027	4.9.79
Repeat on Bld 1A	MER 58027A	5.10.79

7.4.12 Vibration Survey on IP Bleed Valve Solenoid Valve
RB 211-535 Eng 3 Bld 1 A H E Holme Rolls Royce
Ltd Report MER 58044 24.10.79.

7.4.13 Vibration Survey on Woodward Governor Fuel Flow
Regulator RB 211-535 Eng 3 Bld 1 A H E Holme
Rolls Royce Ltd Report MER 58046 30.10.79.

7.4.14 Investigation into the effect of LP out of balance
on FFR Vibration -535 Eng 3 Bld 1 A H E Holme
Rolls Royce Ltd Report MER 58076 21.12.79.

7.4.15 Comparison of 'Definitive' and 'Lash Up' Woodward
FFR Vibration. RB 211-535 Eng 1 Bld 2 A H E Holme
Rolls Royce Ltd Report MER 58087A 14.3.80.

- 7.4.16 Vibration Survey on HP Tacho Generator - RB 211-535 Eng 1 Bld 2 A H E Holme Rolls Royce Ltd Report MER 58087B 19.3.80.
- 7.4.17 Vibration Survey on Pancake Mounted Accessories - RB 211-535 Eng 7 Bld 1 A H E Holme Rolls Royce Ltd Report Nos:-
- HP3 Handling Bleed Solenoid Valve MER 58139A 18.6.80
HP3 Starting Bleed Solenoid Valve MER 58139B 14.7.80
DEPR and EEC Units MER 58139C 23.7.80
- 7.4.18 Fuel Cooled Oil Cooler Vibration Survey RB 211-535 Eng 2 Bld 4 A H E Holme Rolls Royce Ltd Report MER 58223A 28.10.80
- 7.4.19 Vibration Survey on High Energy (HE) Igniter Box RB 211-535 Eng 2 Bld 4 A H E Holme Rolls Royce Ltd Report MER 58223B 5.11.80
- 7.4.20 Vibration Analysis of Fuel Cooled Oil Cooler RB 211-535 Eng 9 Bld 1 D J Forbes, A H E Holme Rolls Royce Ltd Report MER 58288 22.9.80.
- 7.4.21 HP3 Handling Bleed Solenoid Valve - Further Vibration Survey RB 211-535 Eng 7 Bld 2 A H E Holme Rolls Royce Ltd Report MER 58202 12.1.81.
- 7.4.22 RB 211-535 T2 Sonic Thermocouple Vibration Measurements Eng 2 Bld 5A R A Clough Rolls-Royce Ltd Report MER 58382 18.5.81.
- 7.4.23 Accessory Vibration Testing of Production Standard Bleed Valve Control Unit RB 211-535C Eng 30003 Bld 1 G R Moore Rolls Royce Ltd Report MER 58476 9.12.81.
- 7.4.24 P1 Pressure Switch Vibration Survey RB 211-535C Eng 9 Bld 2 C D Lee Rolls Royce Ltd Report MER 58367 8.12.81.

- 7.4.25 Vibration Investigation on Deceleration Decay Unit
RB 211-535C Eng 30003 Bld 1C C R Daniels Rolls
Royce Ltd Report MER 58471 13.1.82.
- 7.4.26 TF Sensor Vibration Investigation RB 211-535C
Eng 9 Bld 1 C R Daniels Rolls Royce Ltd Report
MER 58226 20.1.82.
- 7.4.27 Vibration of Top Temperature Limiter RB 211-535C
Eng 9 Bld 2B C R Daniels Rolls Royce Ltd Report
MER 58559 9.2.82.
- 7.4.28 Computation of the RMS of a signal using the
Measurement Engineering Campbell Diagram System -
P R Watts Rolls Royce Ltd Report MER 08019 10.12.80.

7.5 Modelling References

- 7.5.1 Development of a Correlated Finite Element Model
 of a Complete Aero-Engine R A Bellamy, J C Bennett,
 S T Elston ASME 81-DT-74 1981

- 7.5.2 Steady State Vibration - J P Salter Publ K Mason
 1969.

- 7.5.3 Use of vectors in Vibration Measurement and Analysis
 - C C Kennedy, C D P Pancu, Jnl Aero Sci Vol 14
 No 11 1947

- 7.5.4 A Critical Introduction to some Industrial Resonance
 Testing Techniques - J W Pendered, R E D Bishop,
 Jnl Mech Eng Sci Vol 5 No 4 1963.

- 7.5.5 Measurement and Application of Mechanical Mobility
 Data - D J Ewins Pts 1, 2 and 3 Jnl Soc Env Engrs
 Dec 1975, March, June 1976.

- 7.5.6 The Whys and Wherefores of Modal Testing - D J Ewins,
 Dynamics Section, Mech Eng Report No 78005 Imperial
 College, London Univ.

- 7.5.7 The Measurement of Structural Transfer Functions
 and Mechanical Impedance Spectral Dynamics Corporation
 Tech Publ M-3 1974.

- 7.5.8 Receptance Series for Systems Possessing "Rigid Body"
 Modes - G M L Gladwell, R E D Bishop, D C Johnson
 Tech Notes Jnl Roy Aero Soc Vol 66 1962.

- 7.5.9 Modelling of Structural Behaviour from Frequency
 Response Data - A P Lincoln Inst Sound Vibn Res Tech
 Report 83 1977 Southampton Univ.

7.6 References in Appendices

- 7.6.1 The Campbell Diagram System Instruction Manual,
Jan 1981 Rolls Royce Ltd.
- 7.6.2 Signal Processing Methods enabling rapid appreciation
of Gas Turbine Vibration Problems. D S Pearson, R Wood,
Proc Soc Envr Engrs Conf 1977.
- 7.6.3 Dynamic Data Analysis D S Pearson Proc 'Transducer
'78' Conf. Publ by Trident Exhibitions Ltd.
- 7.6.4 A Code of Practice for Accelerometer Measurements
A H E Holme 19.9.80 MER 00643 Rolls Royce Ltd.
- 7.6.5 Frequency Response Methods - J Trampe Broch Tech
Review No 4 1975 Bruel and Kjaer.
- 7.6.6 Random Vibration - Vol 2 S H Crandall ed MIT Press 1963.
- 7.6.7 The Development of Vibration Test Specifications for
Spacecraft Applications G H Klein, A G Piersol NASA
CR-234 May 1965.
- 7.6.8 Random Noise and Vibration in Space Vehicles - Lyon
SVM-1 Shock and Vibn Info Centre, Naval Res Lab,
Washington D C.
- 7.6.9 Random Vibration and Spectral Analysis - D E Newlands
Longmans 1975.
- 7.6.10 Random Vibration in Mechanical Systems - S H Crandall,
W D Mark Acad Press 1963.
- 7.6.11 The Fast Fourier Transform - E Oran Brigham Prentice
Hall 1974.
- 7.6.12 Frequency Analysis (a collection of reports/trade
literature) - R Winstone, MER 00592 1980 Rolls
Royce Ltd.

- 7.6.13 Evaluation of the Dynamic Characteristics of Structures by Transient Testing R G White
Symposium of Structural Dynamics, Loughborough Univ
1970.
- 7.6.14 Spectrally Shaped Transient Forcing Functions for Frequency Response Testing R G White Jnl of
Sound and Vibn Vol 23(3) 1972.
- 7.6.15 Data Analysis Criteria and Instrumentation Requirements for the Transient Measurement of Mechanical Impedance
P J Holmes and R G White Jnl S and V 25(2) 1972
- 7.6.16 Effective Measurements for Structural Dynamics Testing - K A Ramsey Pts 1, 2 Sound and Vibn.
Nov 1975, April 1976.
- 7.6.17 Shake, Rattle or Rap? - G F Lang App Note No 10
Nicolet Sci Corp 1975.
- 7.6.18 Mechanical Vibration and Shock Measurement - J Trampe
Broch 2nd Edition 1980 Bruel and Kjaer.
- 7.6.19 Practical Application of the Rapid Frequency Sweep Technique for Structural Frequency Response
Measurement - R G White, R J Pinnington Aeronautical
Jnl Vol 86 p 179-199 May 1982.

APPENDIX A Lower Teleflex Control Box-Problem Solutions Testing

As a result of the vibration problems seen in Service and the lessons learnt from testing engines installed in the aircraft the following investigative programme was undertaken:-

a) Investigation of possible forcing function transmission paths

With the Teleflex control box mounted on the end of the gearbox input drive tower there were three possible transmission paths into the control box rack and quadrant. These were via the gearbox casing, from the FFR via the throttle rod, or from the fan casing via the throttle cable and conduit.

Initially coherence measurement comparisons were made between Teleflex box response and various other appropriate locations. In this measurement the recorded data is transformed into the frequency domain and the product of the auto-spectra at each measurement location is divided by the square of the cross-spectra between measurement locations. For locations A and B coherence function γ_{AB}^2 it is expressed mathematically as:

$$\gamma_{AB}^2 = H_{AA} \cdot H_{BB} / |H_{AB}|^2$$

where H_{AA} , H_{BB} represent the auto-spectra of A and B and H_{AB} the cross-spectrum between them.

Where A is an input and B is an output to a linear system the coherence value tends to unity if B is completely the result of A. In the test it was found that at the relevant frequencies this condition was met within experimental accuracy but for all three possible paths. It was realised therefore that A and B could well be responding to an unmeasured source C giving rise to the type of problem indicated by figure A1 and described in greater detail in 7.1.1, 7.2.5.

This investigation then attempted to make use of correlation techniques in order to try and resolve this matter further.

However this met with only limited success due to the time scales involved. The frequencies seen experimentally resulted in periods varying between 2 and 7 milliseconds but assuming that the vibration travelling between transducer locations travelled at the speed of sound in the structure required a resolution in the order of nano seconds as summarised in figure A1. Again resolution problems proved intractable.

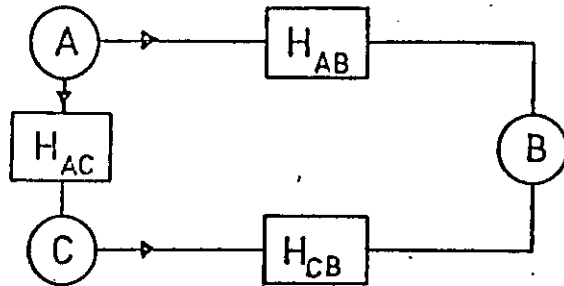
Subsequent work detailed in reference 7.2.6 confirms from another source that this technique was of limited use in this situation and it was eventually abandoned being superseded by the results of other actions.

b) Investigate the various solutions proposed by Customer Airlines Service Departments

The proposals were to isolate the control box from the gearbox vibration by fitting anti-vibration mounts, and to change the rack response characteristics by removing some of the over-hung teeth on the end of the rack.

The former modification could present fuel scheduling problems since the anti-vibration mounts might result in increased motion of control box and by implication the scheduling controls. In practice this was not found to be the case but the claimed improvements could not be verified because rig simulation of the engine environment was poor (7.2.7).

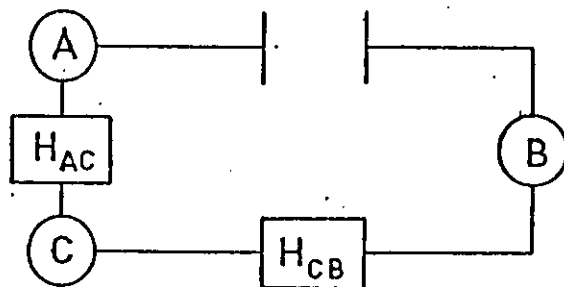
Testing the shortened rack was shown to reduce the vibration problems in that the rack natural frequency for correctly adjusted tensioning rollers was further increased above the operating range of 1st HP shaft order excitation i.e. from around 170 Hz to 185 Hz (fig A2). Further 'tuning' could be achieved by varying the load applied via the tensioning rollers which hold the rack against the quadrant (7.2.8). This modification has subsequently been incorporated into the Service fleet.



The Signal at B has a content from A direct and via C.

$$B = [H_{AB} + H_{AC} \cdot H_{CB}] \cdot A + H_{CB} \cdot C$$

Fig 27b

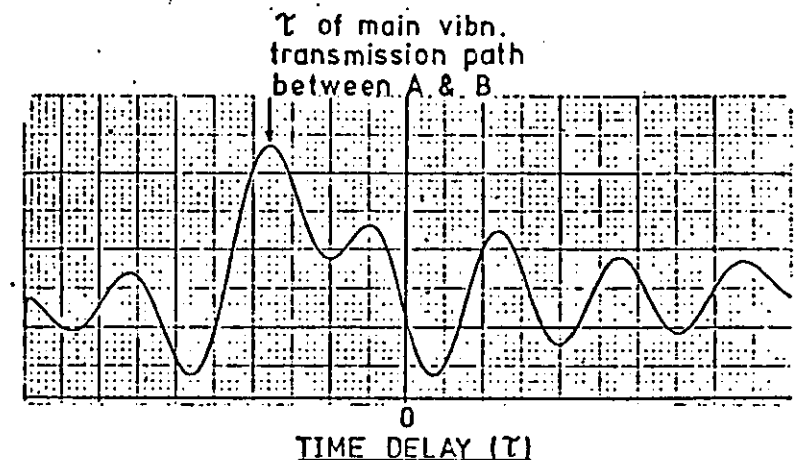


The Signal at B has a content from A via C when $\gamma_{AC}^2 \rightarrow 1$ although no link exists from A to B

$$B = H_{AC} \cdot H_{CB} \cdot A + H_{CB} \cdot C$$

FIGURE A.1A

CORRELOGRAM OF ACCELEROMETER OUTPUTS AT POSITIONS 'A' & 'B'



A(t) lags B(t)

A(t) leads B(t)

SAMPLE CALCULATION OF PATH DELAY

Velocity of Sound in Metal = 6 km/s

Path distances between A & B = 0.5, 0.6m

Time taken for wave to travel from A—B

0.5m path = 83.3 μs

0.6m path = 100.0 μs

In order to resolve between peaks analyser resolution has to be better than 16.7 μs. Typical analysis range would be at least 50,000 Hz.

Figure A.1B

c) Investigate possible improvements to the vibration environment

From the testing detailed above it was apparent that the Teleflex control box was being excited by the HP shaft and the drive train to the external gearbox shown in figure 2.3. Work therefore concentrated on looking at the balance standard of the various shafts and gears concerned. It was found that although basically balanced to normally acceptable standards, the high rotational speeds of the shafts (10,000 rpm HP shaft, 14,500 rpm inclined drive shaft and 25600 rpm radial quillshaft) meant that unacceptable out of balance forces could exist. This situation was further aggravated by one of the gears having an offset oil distributor hole which gave large out of balance forces. Rig and engine testing showed that improved balancing of the radial drive quillshaft halved the vibration levels measured at the teleflex box and that better balancing throughout the system further improved the vibration environment, figure A3 (7.2.9 - 7.2.10).

Improved balance shafts and gears have been introduced into Service engines.

d) Control Box Alteration

In conjunction with the above testing and as a back-up in case modifications to the vibration environment were unsuccessful a design change to the control box was proposed. This eliminated the troublesome rack and quadrant and replaced it with a cable system (fig A4). This was fully tested (7.2.11 - 12) and would have been put forward, in spite of some problems (fig A5) as an alternative solution if the other modifications indicated above had not been successful. The rig testing of this Box was used to partially investigate the effects of some of the revisions to test procedure to be proposed in chapter 3 (7.2.12 refers).

Other testing on the Lower Teleflex Control Box is detailed in references 7.2.13 - 24.

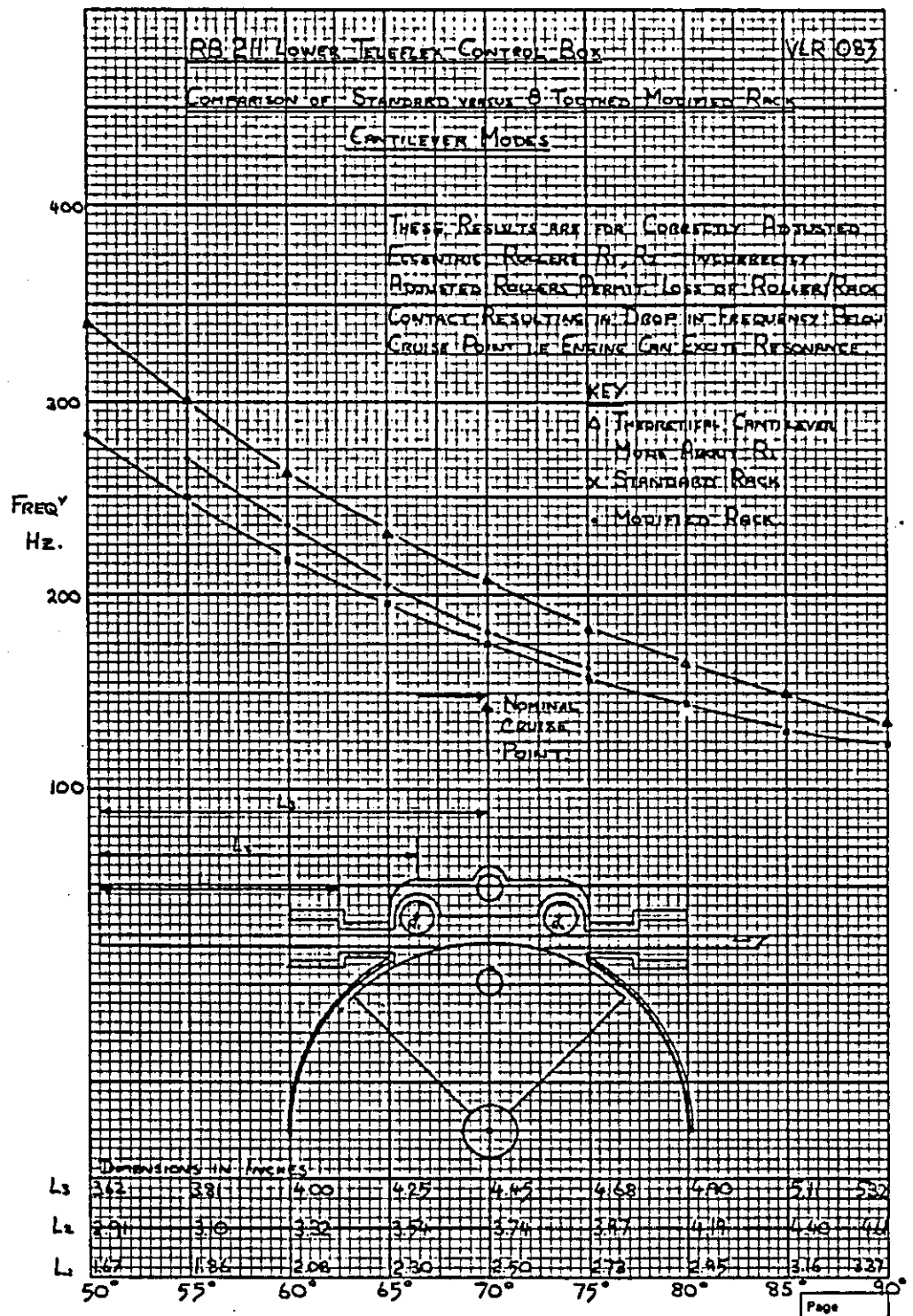


Fig. A.2



RB211 GEARBOX VIBRATION
EFFECT OF BALANCE ON RADIAL DRIVE SYSTEM (2.56 N3)

27 NOV 78
Chart No.
VML 82474/

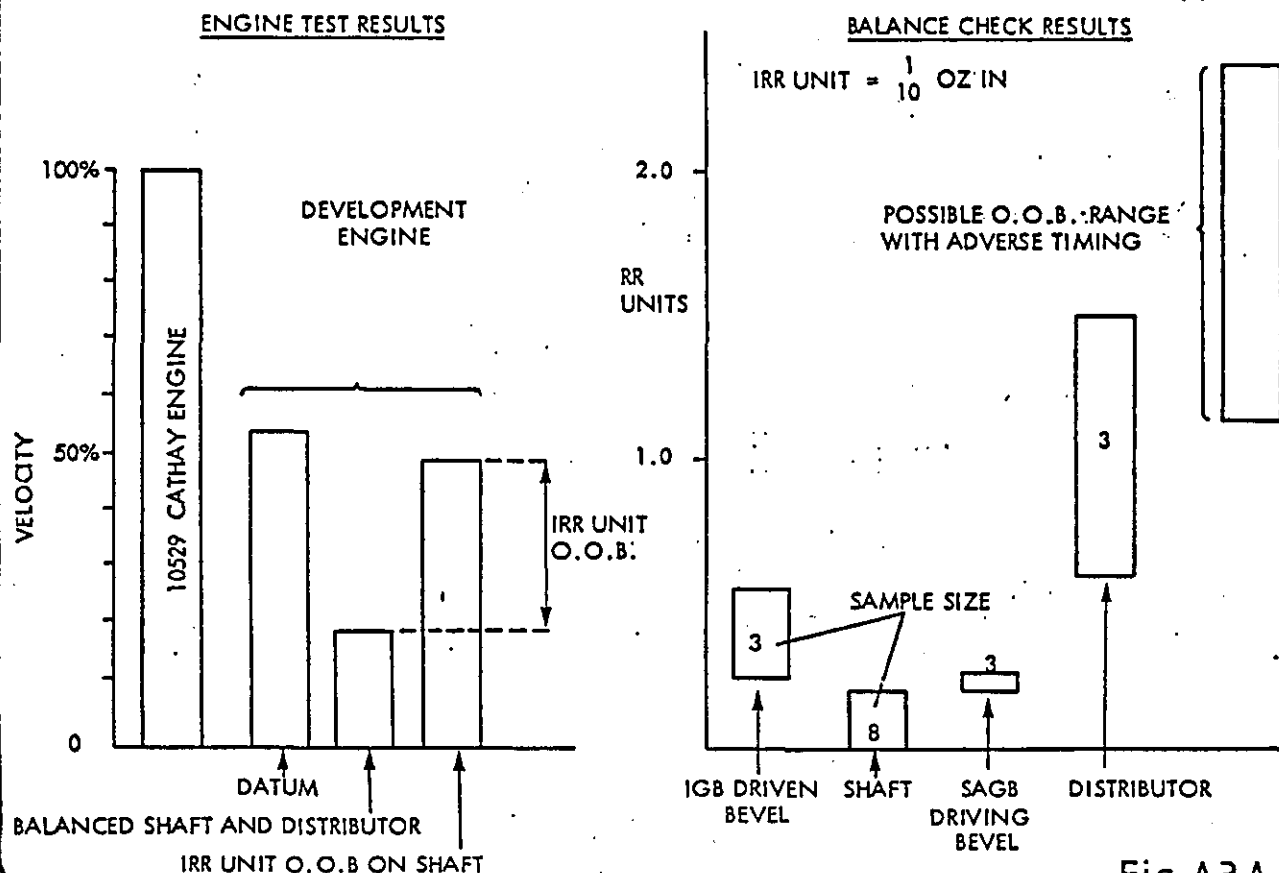


Fig. A3.A



RB211 GEARBOX VIBRATION
EFFECT OF BALANCE ON INCLINED DRIVE SYSTEM (1.46 N3)

Date
25 AUG 78
Chart No.
VML 83022

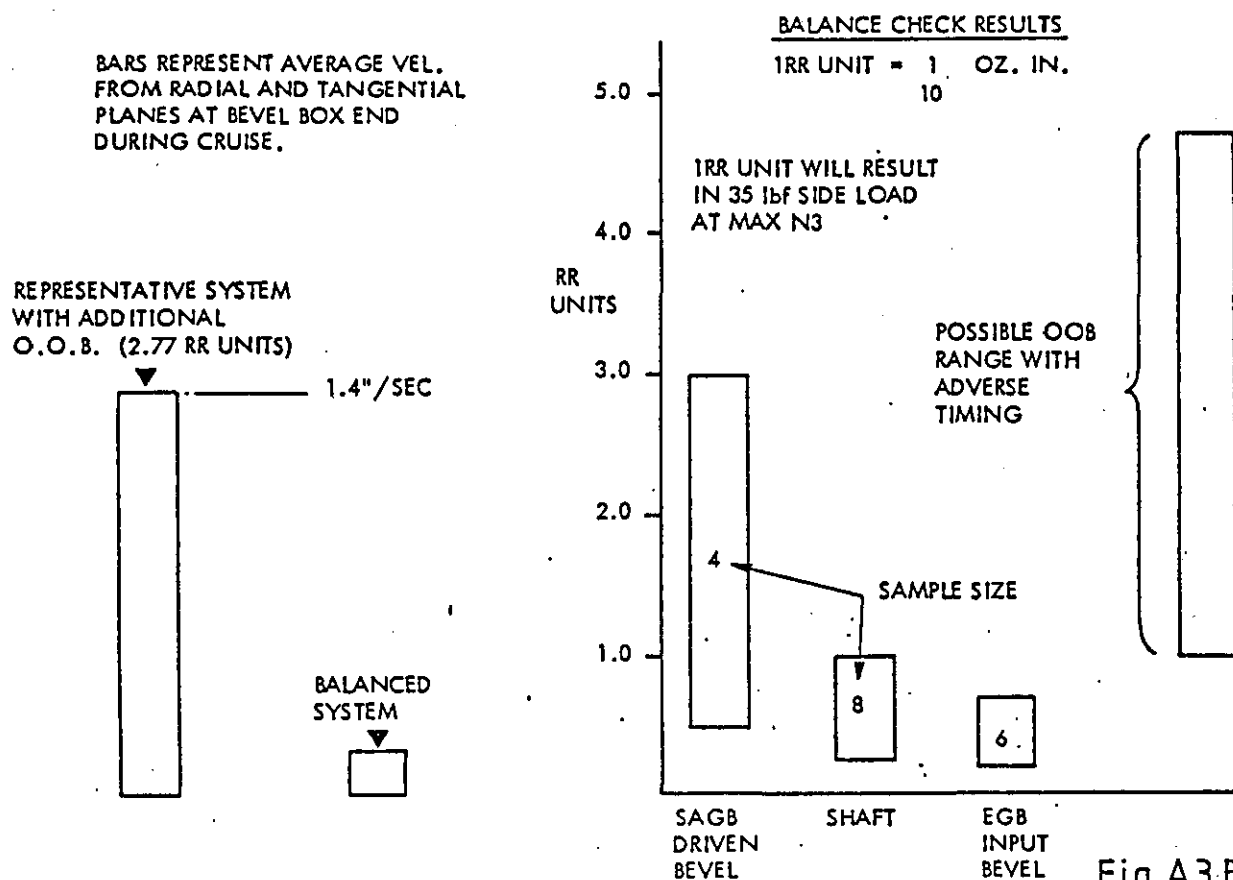
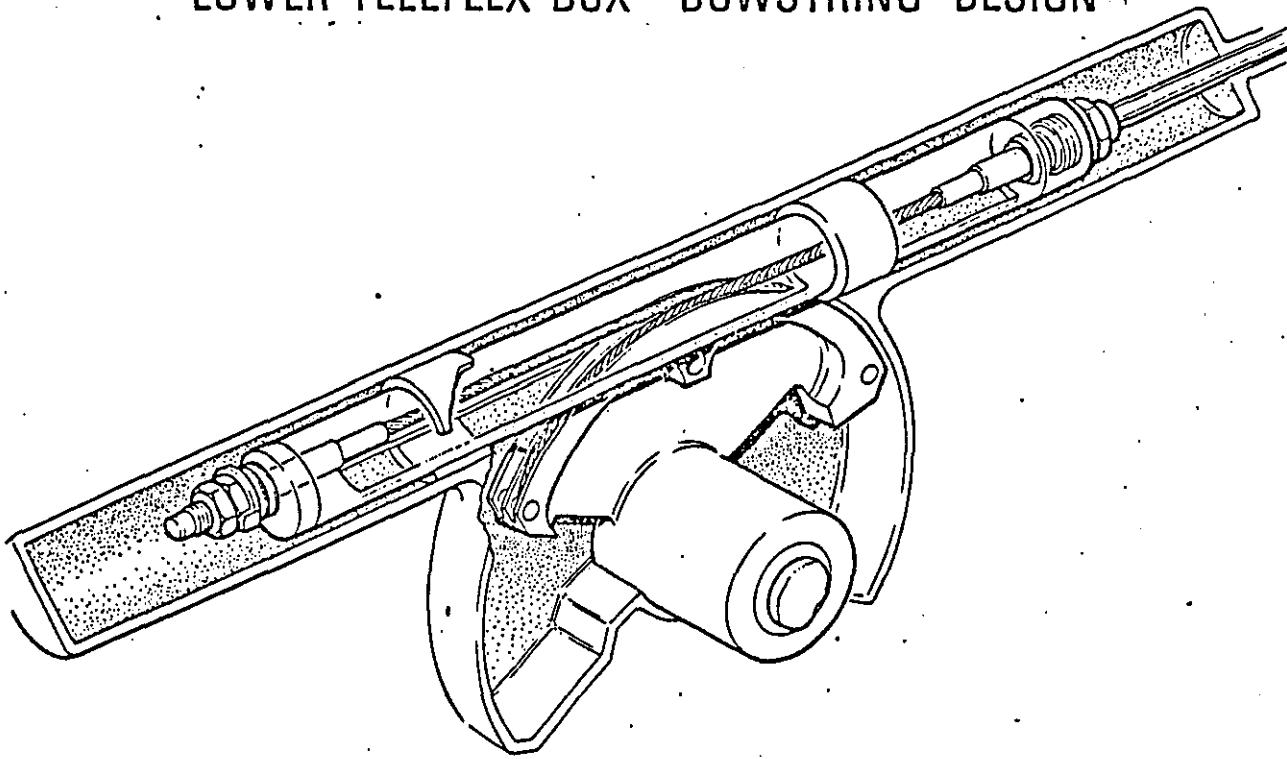


Fig. A3.B

Fig. A3

LOWER TELEFLEX BOX 'BOWSTRING' DESIGN



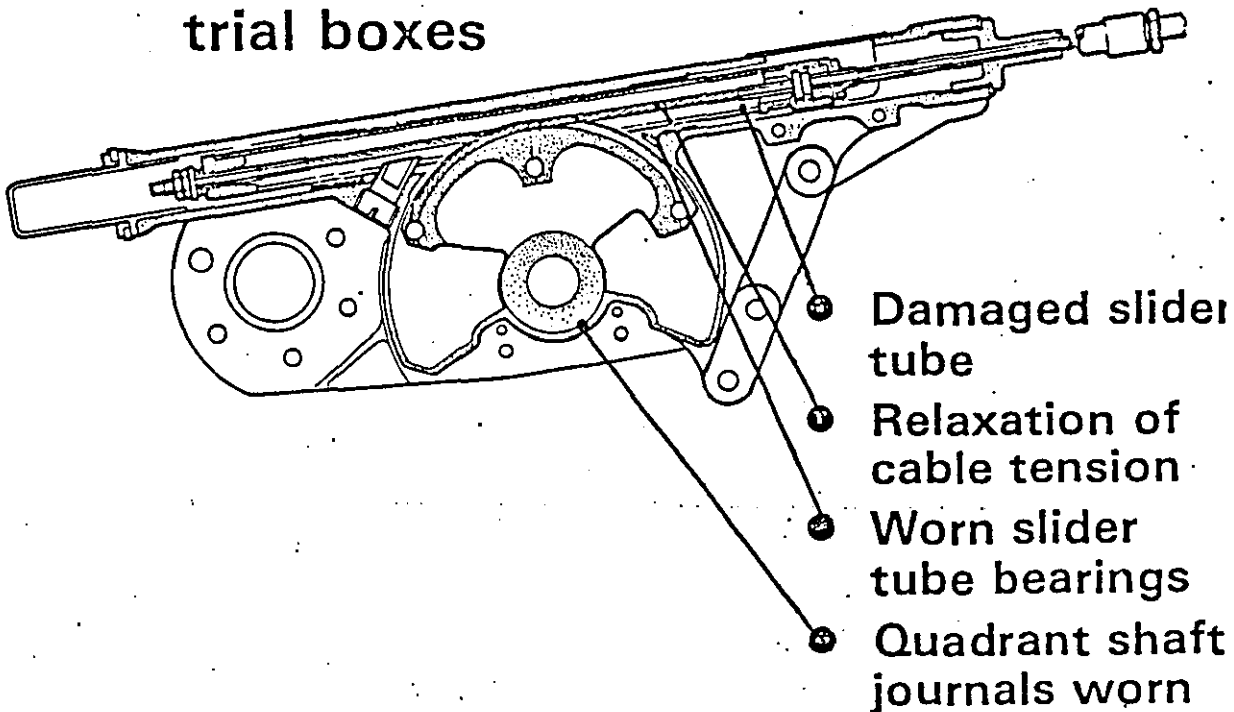
ETG 24380



RB211 THROTTLE CONTROL SYSTEM

Bowstring box (SB75-5245)

- Problems seen on strip of trial boxes



ETG 24382/1

Fig A4

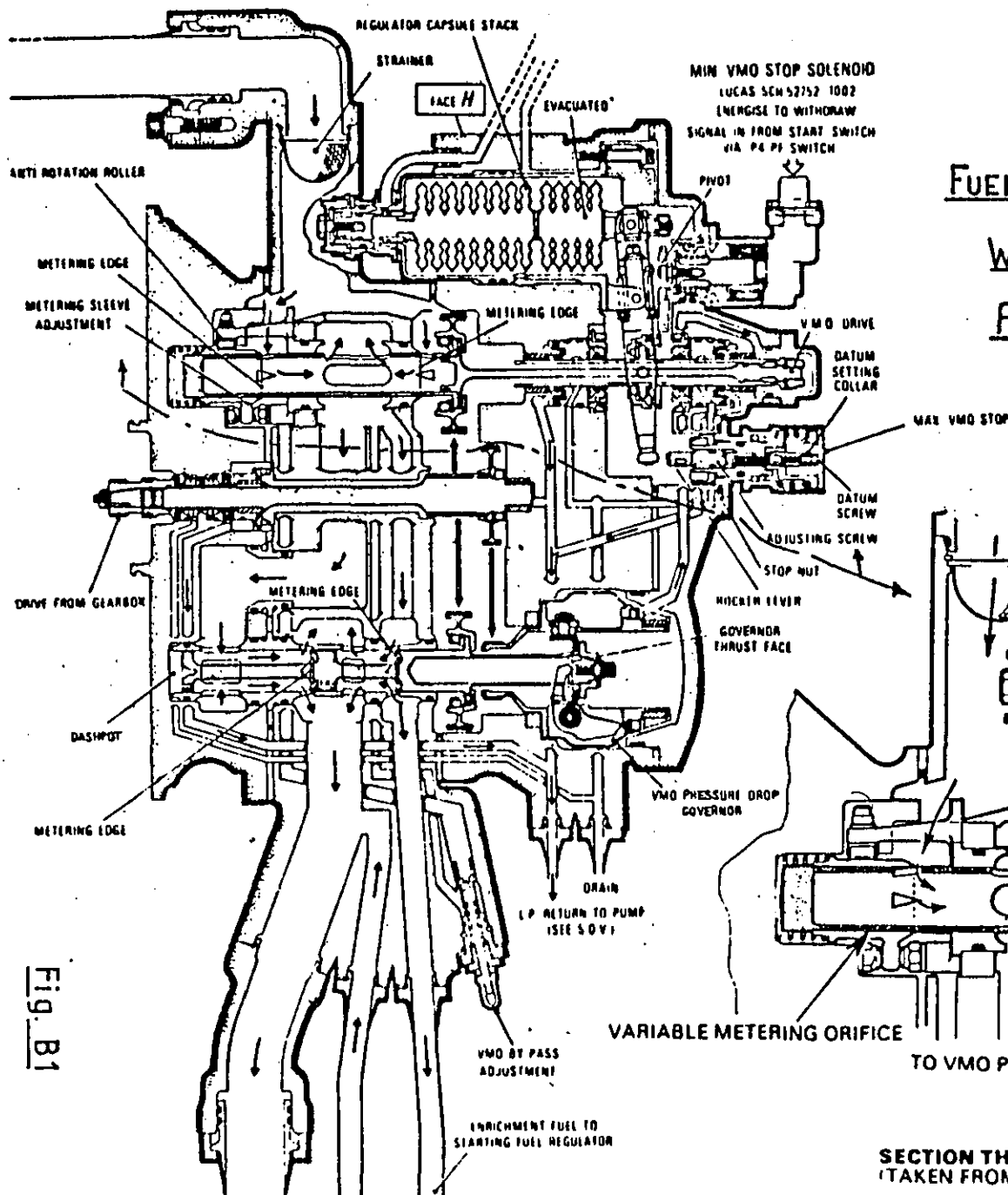
APPENDIX B - Fuel Flow Regulator - Testing the new technique

A reduction in starting fuel flow and hence difficulty in starting the engine had been attributed to vibration induced problems with the Fuel Flow Regulator (FFR). The FFR operates as follows:-

The Variable Metering Orifice (VMO) in the FFR controls the amount of fuel passed to the fuel burners in the combustion cans. This orifice is basically a triangular hole in a spool which is positioned relative to a fixed opening in the duct wall in which the VMO spool is located. The VMO spool rotates and is moved axially by means of a complex pivot mechanism and bellows system (Fig B.1). At the pivot point there are some small ball bearings. As these balls were not rotating it was found that in service they were wearing resulting in increased end-float of the VMO spool which was experienced as low fuel flow. Due to the lever arm effect of the pivot, wear of only 0.001" would result in an end float of 0.005" which lead to a reduction in fuel flow of 25 gph approximately, a critical amount on start-up.

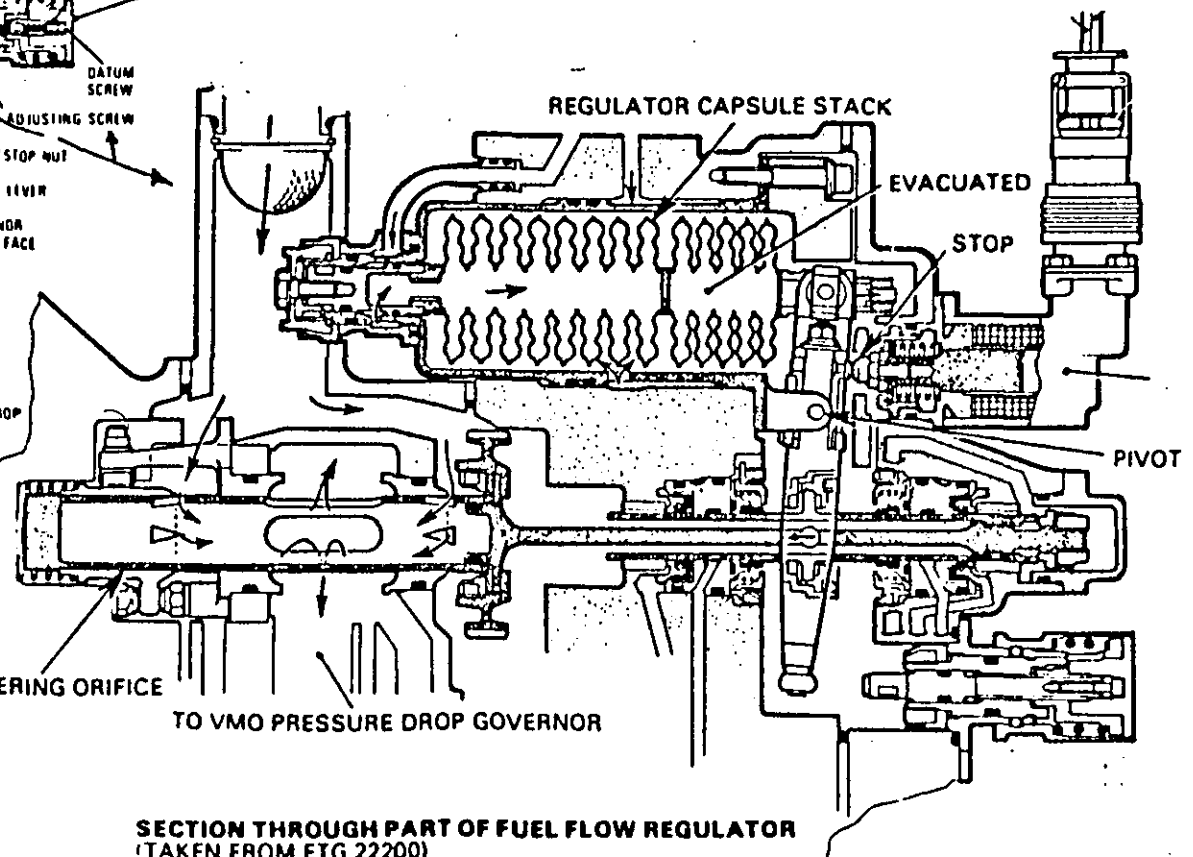
The FFR manufactures, Lucas Aerospace Ltd, put forward and tested various proposals, 7.3.1 to 7.3.9, but were in difficulty in reproducing the Service wear problem on their test rigs. Analysis of engine and rig work showed several resonant conditions of the pivot assembly (Fig B.2). Some of these resonances were coincident with engine shaft orders seen on the external gearbox at certain flight conditions, in particular an excitation due to the HP Fuel Pump Ripple Rate (number of teeth on gear pump x rotational speed of pump) was observed (Fig B.2).

Initial rig work had shown that the use of carbon bushes in place of the roller bearings gave a much improved result in terms of wear, therefore it was decided to compare the existing standard of assembly with the proposed modification by endurance testing using engine excitation levels and frequencies. It was realised that as existing standards of units were achieving lives of 2000 hours on the engine considerable rig test hours would have to be built up to detect any significant wear. Hence it was proposed that the standard FFR should be endurance tested for at least 100 hours.



FUEL FLOW REGULATOR - FUEL SIDE

WITH DETAIL OF CAPSULE STACK AND PIVOT ARM ASSEMBLY



SECTION THROUGH PART OF FUEL FLOW REGULATOR
(TAKEN FROM ETG 22200)

RB 211-22B AND -524 SPECTRUM ANALYSIS OF CAPSULE
STIRRUP (Y ACCELEROMETER) ENGINE VIBRATION ENVELOPE

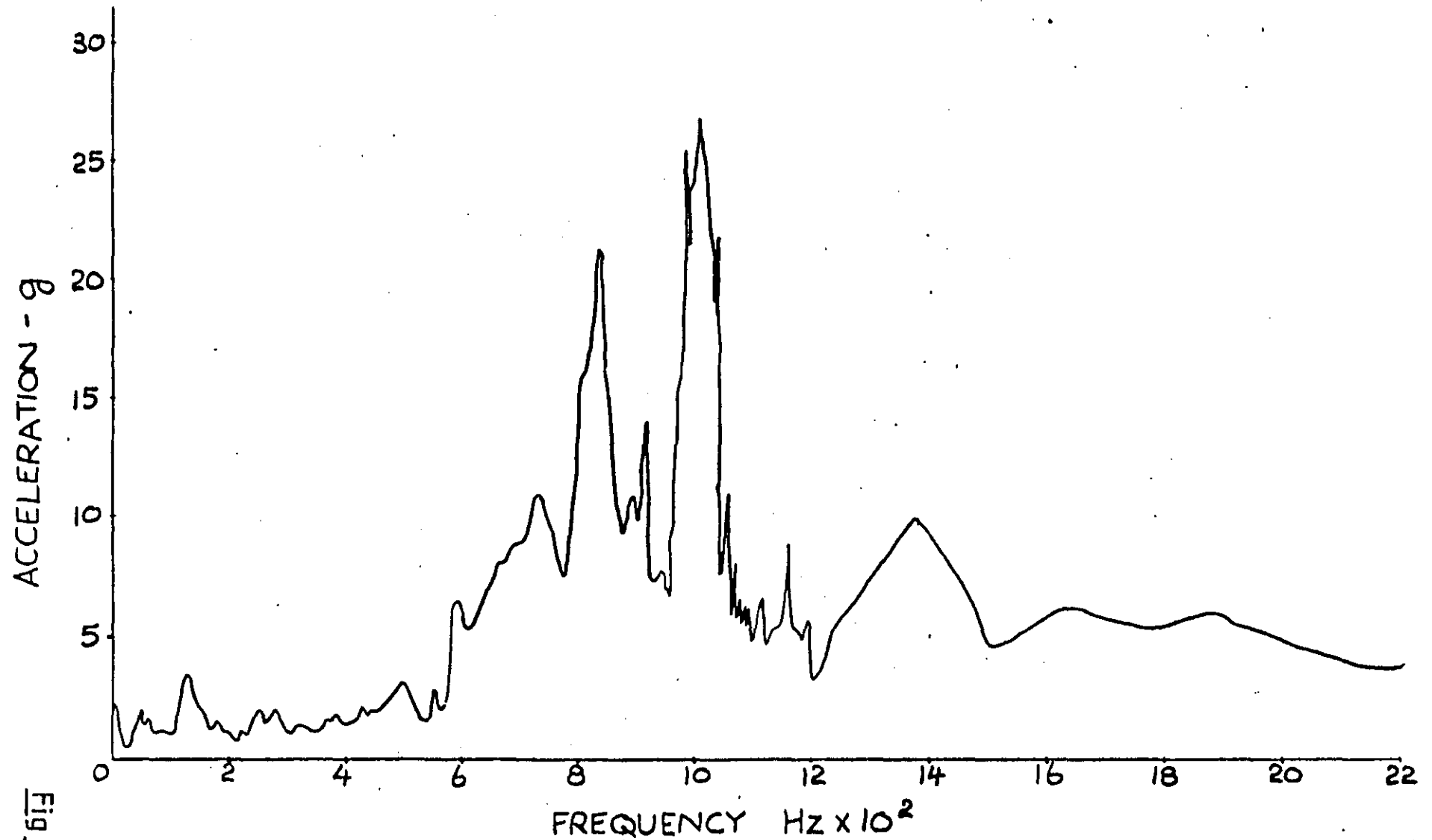


Fig B2

From engine testing the vibration spectrum was obtained for a reference point on the pivot arm (Fig B.3) and in order to simulate the worst possible service environment the spectrum was scaled for a 'rough' engine case based on the vibration levels measured at the standard engine vibration monitoring points.

Hence scale factor 'X' is given by

$$X = \frac{\text{Service Vibration Limit (1.0"/sec)}}{\text{Test Engine Vibration Level}}$$

This gave a factor value for frequencies up to 200 Hz approximately, covering the basic shaft orders. For frequencies above this an arbitrary value of 2 was chosen for the scale factor.

On the engine the FFR is subject to excitation in more than one plane and normally directions radial, tangential and axial to the engine centre line are taken as reference directions. However rig endurance testing could only be carried out in one plane. This was initially chosen as the vertical plane (FFR Y Fig B.3) for convenience on the rig set-up. A detail of the measurement set up on the pivot arm is shown in fig B.3. Some testing was also performed at the $Y + 45^\circ$ plane in order to combine the trunnion axial movement with a known in service side load on the trunnion bearings, as well as to more nearly represent the true Engine radial direction of the installed unit.

As rig testing to existing techniques had failed to produce the wear problem outlined above initial simulation of the engine vibration using four sine wave inputs to a 3kw shaker was attempted and shown to be feasible (7.3.8) although no service type wear had been found after extending the test to 323 hours. It was decided that this was the result of using input levels below those seen on engine test. Testing was then transferred to the 10 kw shaker system shown in figure B.4 and increased testing at cruise conditions performed. This resulted in an increase in the V_{rms} level based on the endurance frequencies from 0.8 ins/sec to 2.1"/sec ($20.3 - 53.3 \times 10^{-3}$ m/s). With some change to the test conditions this was continued for a further 214 hours with no apparent change to calibration settings or wear in the pivot system. A change to the engine radial direction for a further 38 hours produced the same result.

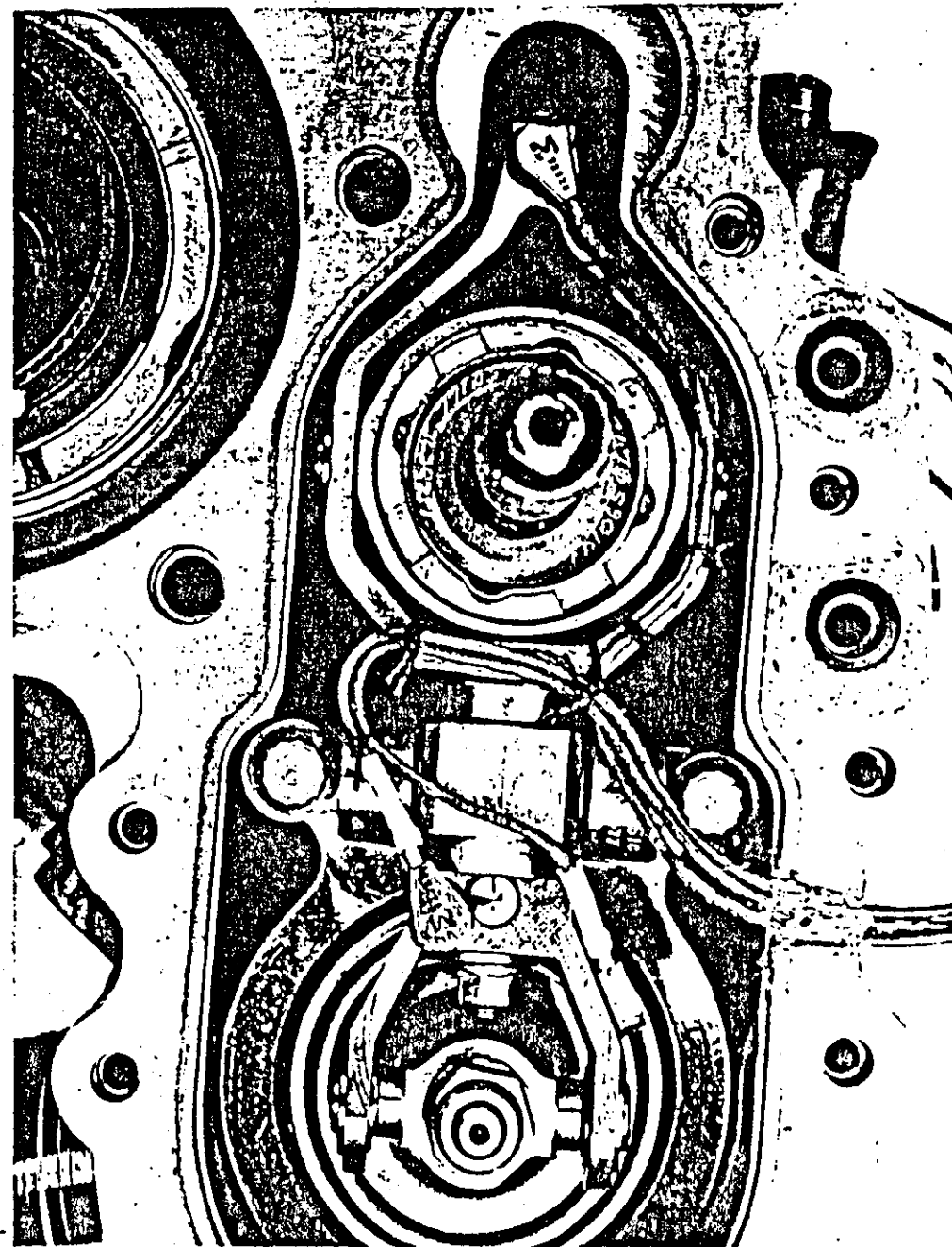
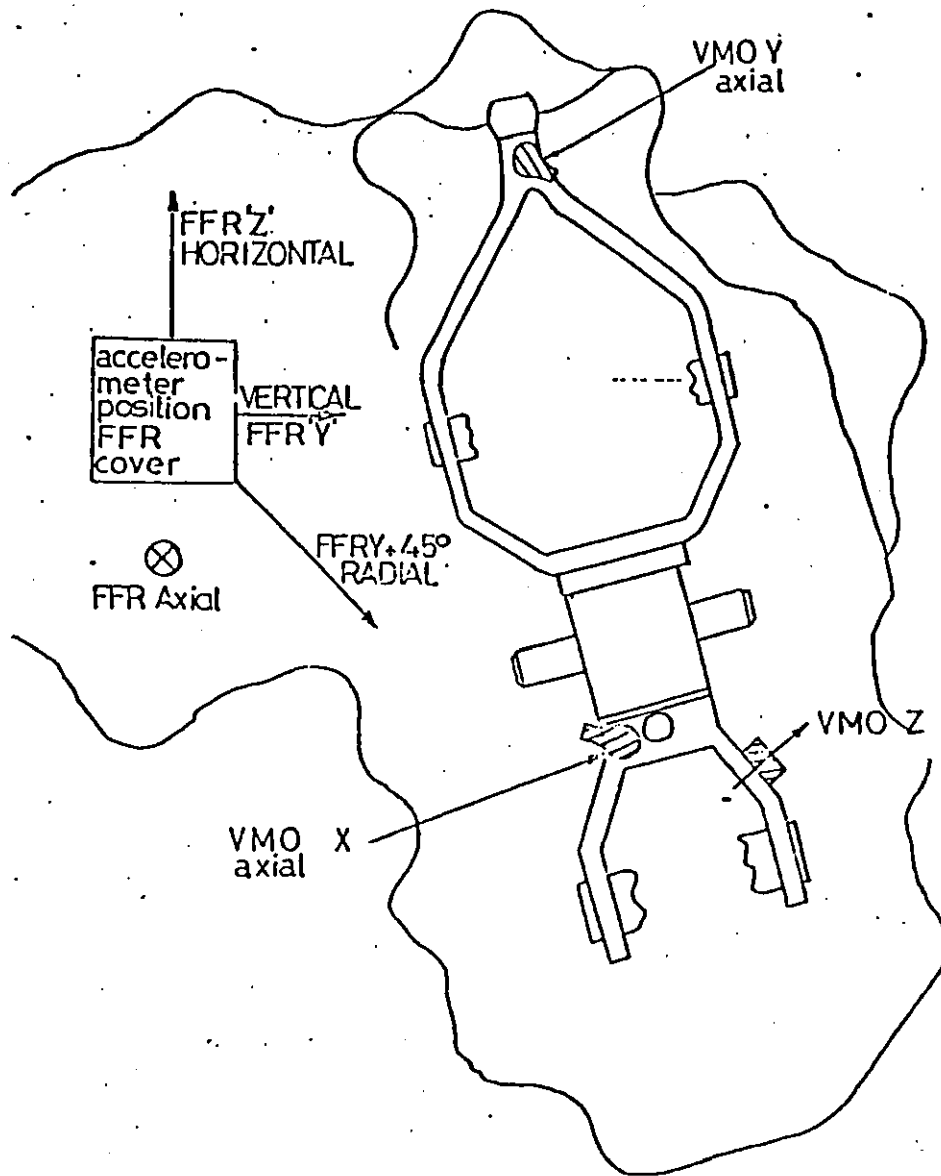


Fig B3

LUCAS AEROSPACE LIMITED

ACCELEROMETER POSITIONS & ENGINE
PLANES IN RELATION TO FFR J52752/K1

DRAWN BY: D P W DATE: 5/1/70 LOG NO: 40 696

By this time further engine results from worn units (7.3.17 - 19) indicated that the vibration levels could be increased further and that the effects of HP Fuel pump ripple rate at 800 - 1200 Hz approximately (fig B.2) were not being simulated correctly due to too long a length of connecting pipework on the rig (over 40 feet from pump to FFR instead of the 2-3 feet on the engine).

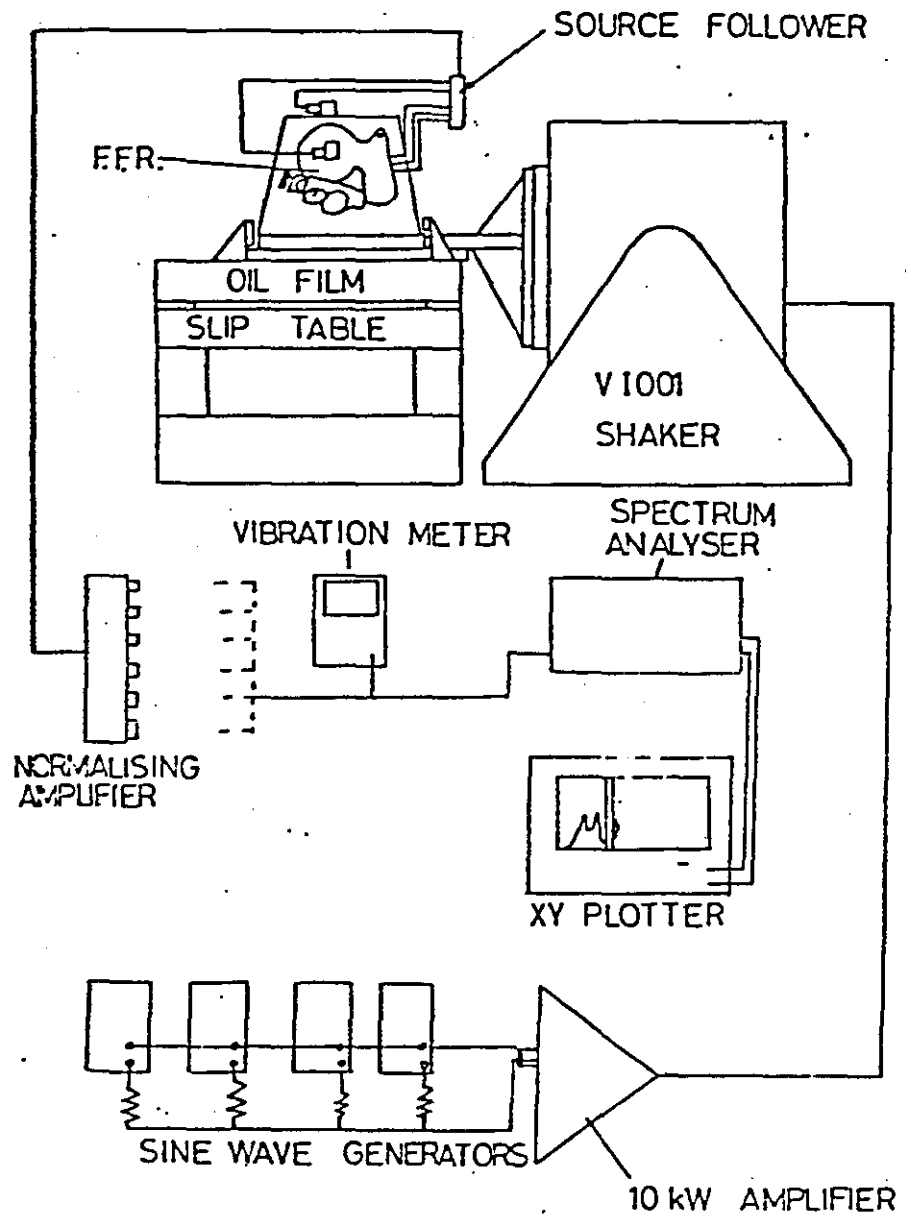
This necessitated a change to the 20 kw shaker rig shown in figure B.5. After some initial problems with setting realistic levels which did not result in failures that were not seen on the engine it was found that a small increase to 2.4"/sec (61.0×10^{-3} m/s) Vrms produced service type wear and fuel flow calibration drift within 100 hours of resuming the test.

The test was then repeated with the modified FFR to approximately the same input levels, the Vrms level having reduced to 2.3"/sec (58.4×10^{-3} m/s) due to small changes in the test frequencies. The frequencies were changed to tune in resonances of various parts of the pivot assembly. After 303 hours testing no wear or calibration drift was found. These results are summarised both in fig B.6 which shows the change in calibration over the final 100 hours with the original unit and the lack of change with the modified unit; and in fig B.7 which summarises the test excitations and their effects.

Details of the above testing are given in 7.3.10 - 13 and 7.3.21 from which a set of typical vibration plots are taken, figures B.8 and B.9.

It was concluded from this that the rig testing now simulated the engine environment with sufficient accuracy to indicate that it would be satisfactory in Service. Statistics from Service operation unfortunately do not confirm this directly since other faults have now been shown up which were masked by the problem with the stirrup assembly.

LUCAS AEROSPACE LIMITED



10kW VIBRATION RIG

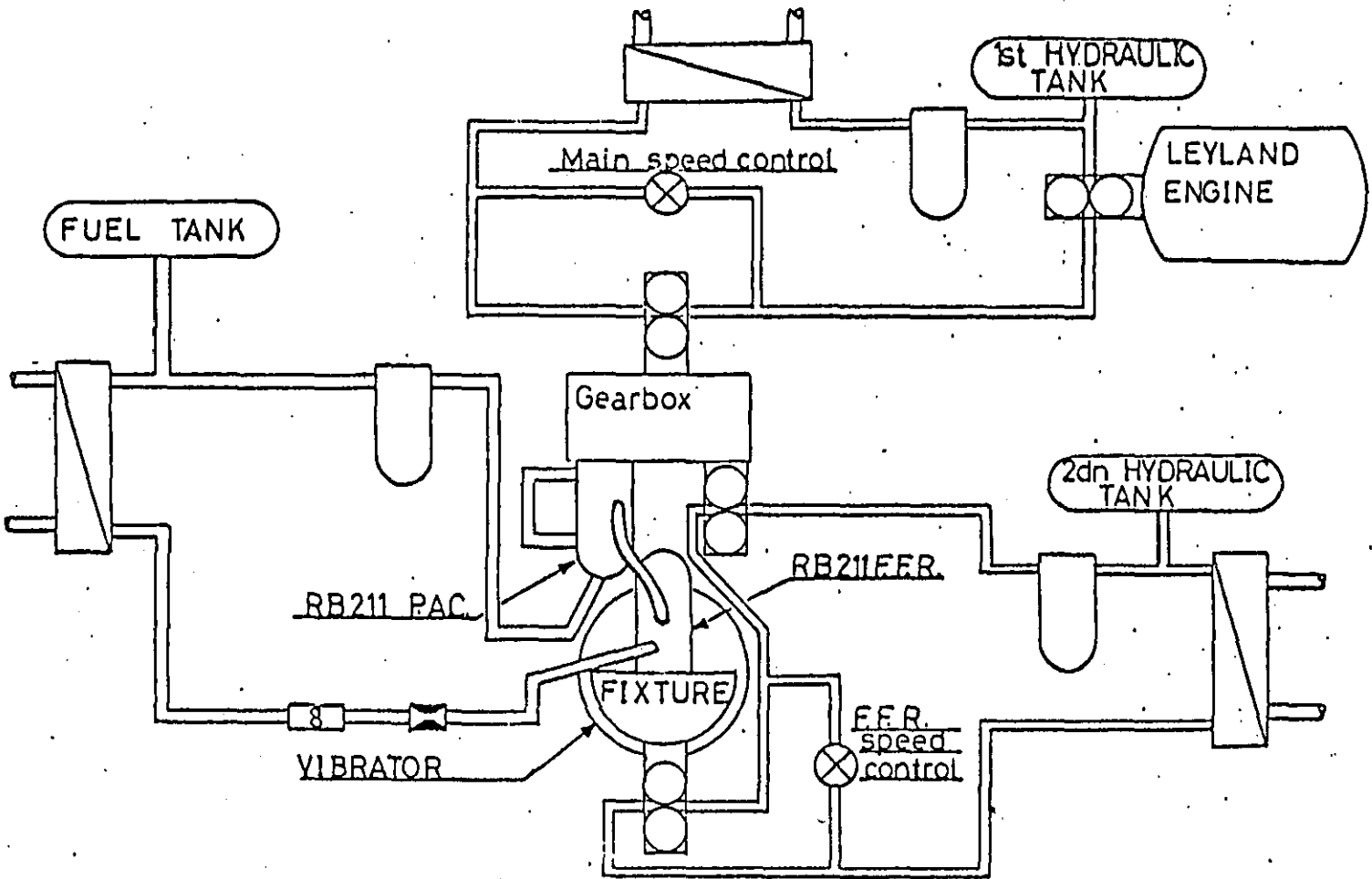
J52752/KD

DRAWN BY: D P WHATLEY

DATE: 4/1/79

DRG. No. HR 695

LUCAS AEROSPACE LIMITED



DRAWN BY: S. COOK.	DATE: 31/5/79.	DRG. No. HR 703.
--------------------	----------------	------------------

REPORT No J52752/KJ

20kW VIBRATION RIG

Fig B5

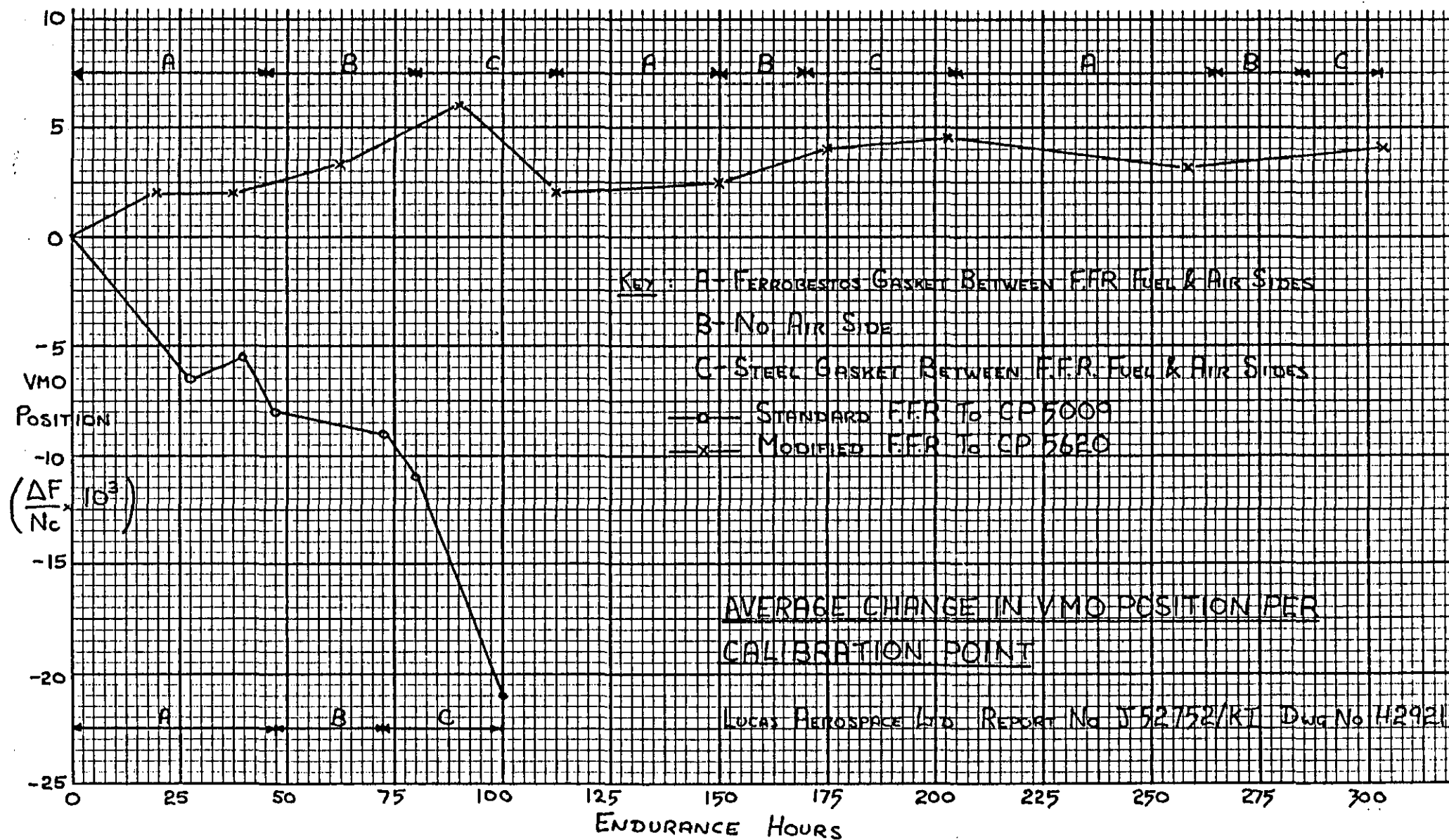


Fig B6

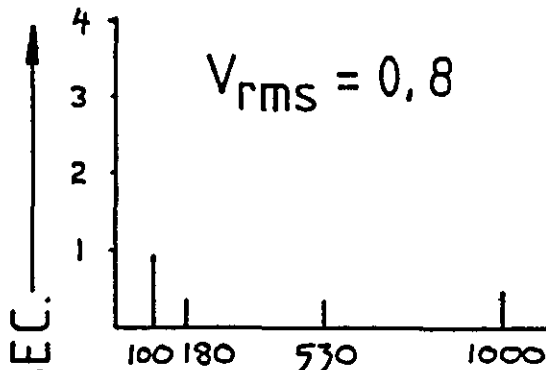
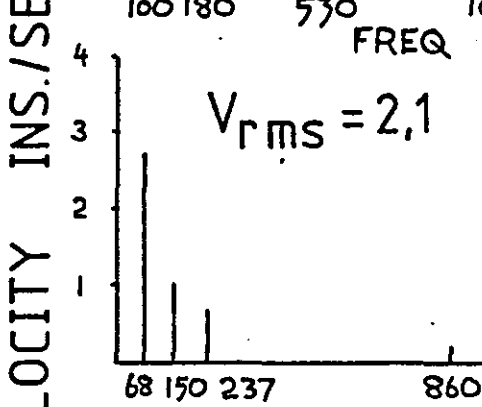
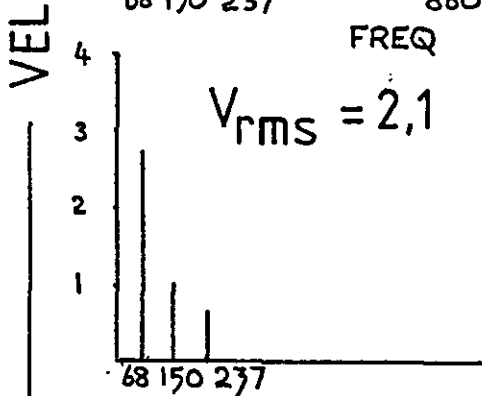
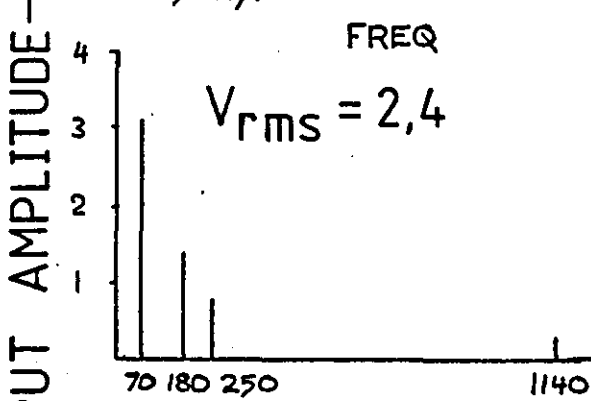
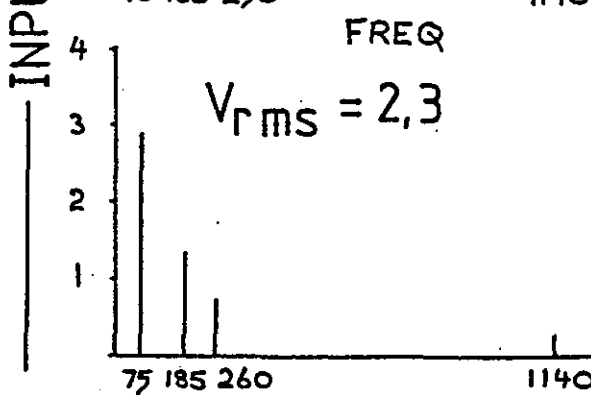

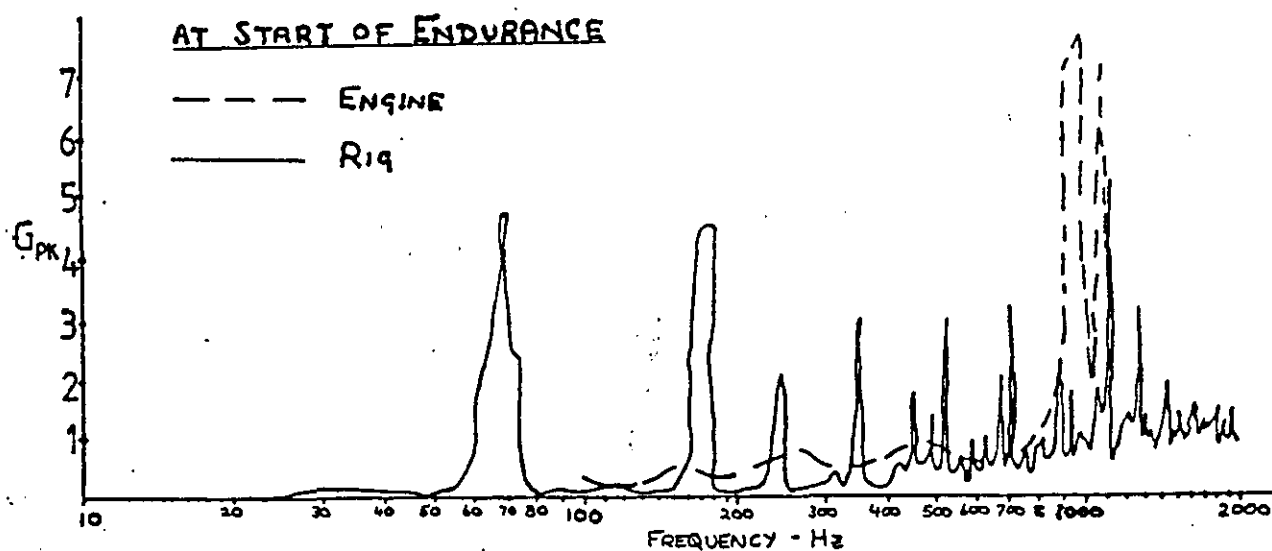
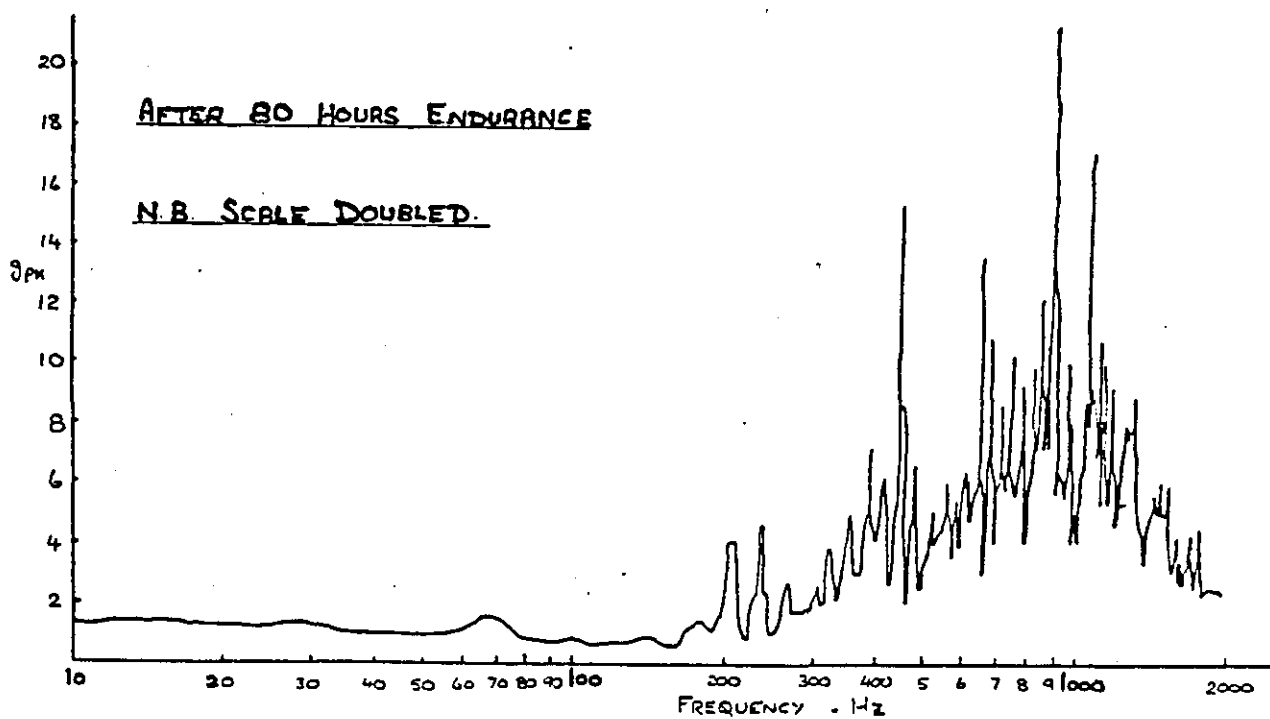
EXCITATION	DIREC ^N	EFFECT
 <p>$V_{rms} = 0,8$</p>	Y	No DETERIORATION AFTER 323 HRS. ON 3 kW SHAKER.
 <p>$V_{rms} = 2,1$</p>	Y	INCREASED INPUT LEVELS POSSIBLE WITH 10KW SHAKER SHOWED NO WEAR AFTER 214 HRS (537 HRS TOTAL)
 <p>$V_{rms} = 2,1$</p>	$Y + 45^\circ$	SHAKING IN ENGINE RADIAL DIR ^N INCREASED LEVER RESPONSE BUT NO WEAR AFTER 38 HRS (575 HRS TOTAL)
 <p>$V_{rms} = 2,4$</p>	Y	SMALL INCREASE TO 'ROUGH' ENGINE LEVELS PRODUCED SERVICE WEAR IN 100 HRS (675 HRS TOTAL)
 <p>$V_{rms} = 2,3$</p>	Y	MODIFIED UNIT SHOWED NO WEAR AFTER 303 HOURS.
 <p>$V_{rms} = 2,3$</p>		

Fig B7



Lucas Aerospace Ltd
Drg Nos XY 912/919



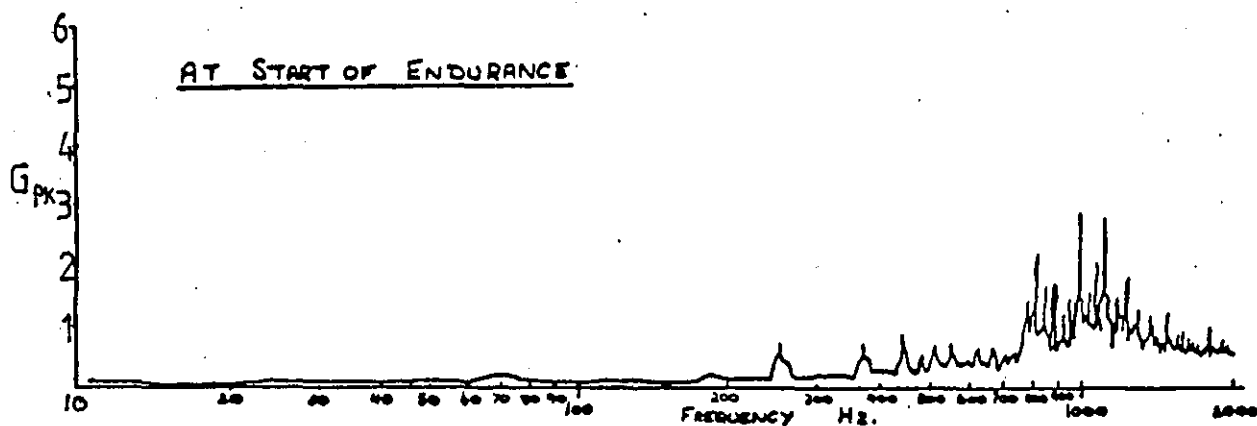
Transducer Location

VMO Y

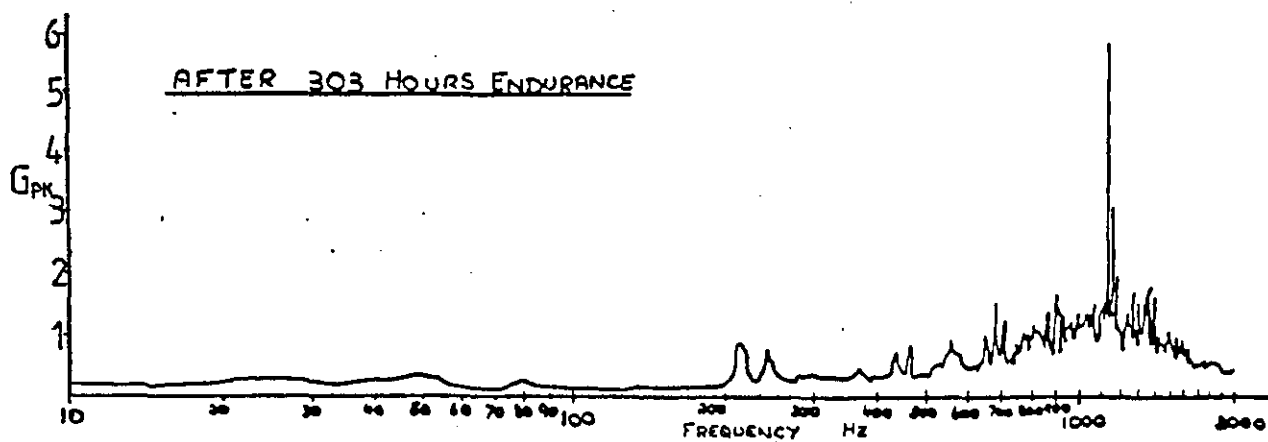
ORIGINAL VMO STIRRUP ASSEMBLY

TO CP 5009

Fig B8



Lucas Aerospace Ltd
Drg. Nos. XY 949/1002



Transducer Location

VMO Y

MODIFIED VMO STIRRUP ASSEMBLY

TO CP 5620

Fig B9

APPENDIX C - Fuel Flow Regulator Modelling

C 1 Modal Test Method

A complete FFR was suspended from a bar by means of elastic bands to simulate a free-free suspension system as shown in figure 5.1. The test results indicated that this suspension worked well with an initial mass-like response on the Mobility (Velocity/Force) plots.

In service this unit is fastened at one end by a Vee-clamping Quick Attach/Detach (QAD) ring to a mating flange on the engine external gearbox which drives the various shafts inside the unit. A throttle control rod and various fuel and air pipes provide the only other unit attachments. In order to represent to some extent this service environment it was decided to input the forcing function into a convenient flat face adjacent to the mounting flange.

An electromagnetic shaker was used to supply the forcing function. It was connected to the unit via a thin steel rod which ensured that the input force was basically uni-directional with no lateral or torsional component. A Bruel and Kjaer (B and K) type 8200 piezo-electric force transducer of sensitivity 4.04p C/N was placed between the drive rod and unit to measure the force. The response of the unit to the input force was measured immediately adjacent to the forcing position using a B and K Type 8344 miniature piezo-electric accelerometer of sensitivity 0.337 p C/ms⁻².

This enabled a nominal point transfer function measurement to be made on the unit. This measurement was taken using a Spectral Dynamics SD 1002E Transfer Analyser System (figure 5.2) and expressed in terms of the units' Mobility. A detailed description of this analyser is given in 7.5.7 but briefly it may be summarised as follows in conjunction with figure 5.2 and the block diagram in figure C.1.

The conditioned force and accelerometer signals are fed into the input channels of an SD 112-1-H Rms Voltmeter/Frequency Log Converter which gives a D C voltage output proportional to the logarithm of the force and acceleration signals. These signals however are first enhanced by passing them through the narrow band tracking filters of an SD 122 filter to eliminate all spurious data except for the signal fundamental. This filtered DC voltage is then processed by the SD 127 MZ/TFA Transfer Function Analyser controller to give the desired input/output ratio, in this instance Mobility, as well as the signal phase relationship.

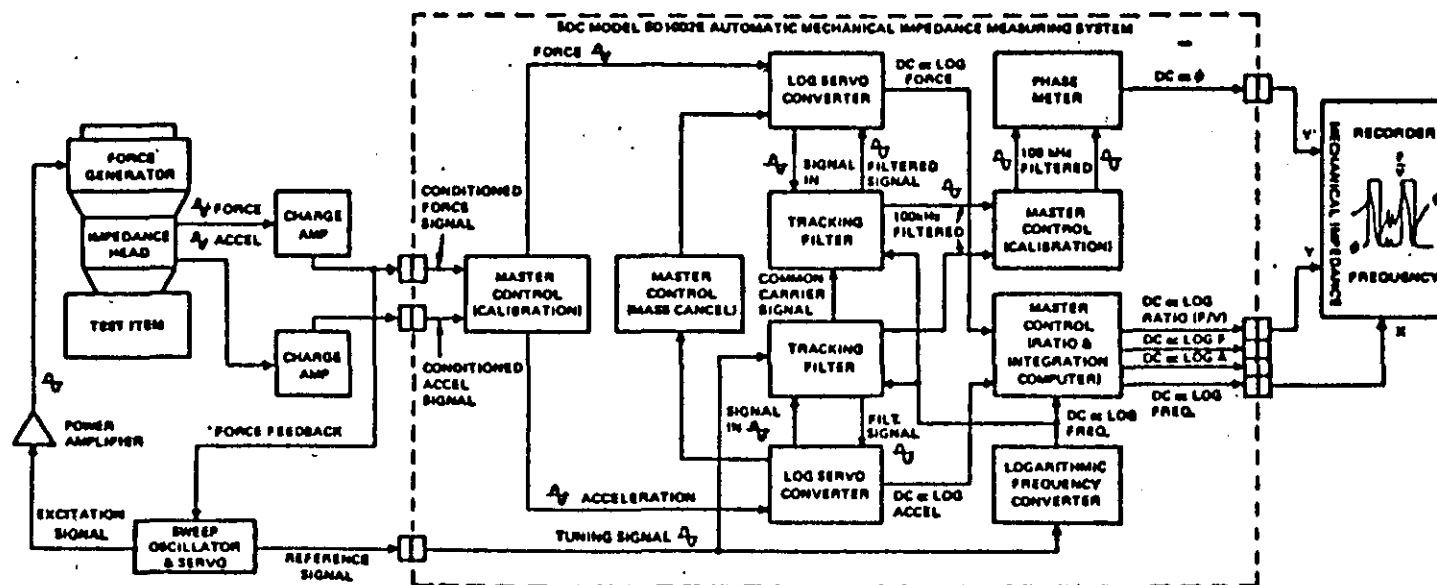
The SD 1002E also contains an SD 104-A Sweep Oscillator which is used to supply the input forcing function to the shaker power amplifier. For this testing a logarithmically swept sine wave was used.

No servo was used in conjunction with the sweep oscillator as shown in figure C.1 Hence the force feed back shown in this figure was not used. Suitable signal levels were maintained for the Analyser by manually altering the charge amplifier level settings. This worked well apart from occasional glitches in the Mobility plots, although particular care had to be taken at anti-resonances when the response signal reduced to very low levels.

C 2 Partially Assembled FFR (Air Side and Fuel Side less its internal shafts etc) Results

This assembly was tested as indicated above and the driving point Mobility measured adjacent to the mounting flange is shown in figure C.2

As before after an initial body mode the driving point response is basically mass-like although this time rotational effects have resulted in a dynamic mass varying from 13.9 lbs (6.3 kg) at 20 Hz to 16 lbs (7.25 kg) at 110 Hz compared with an actual mass of 44 lbs (20 kg).



SD1002E System Block Diagram

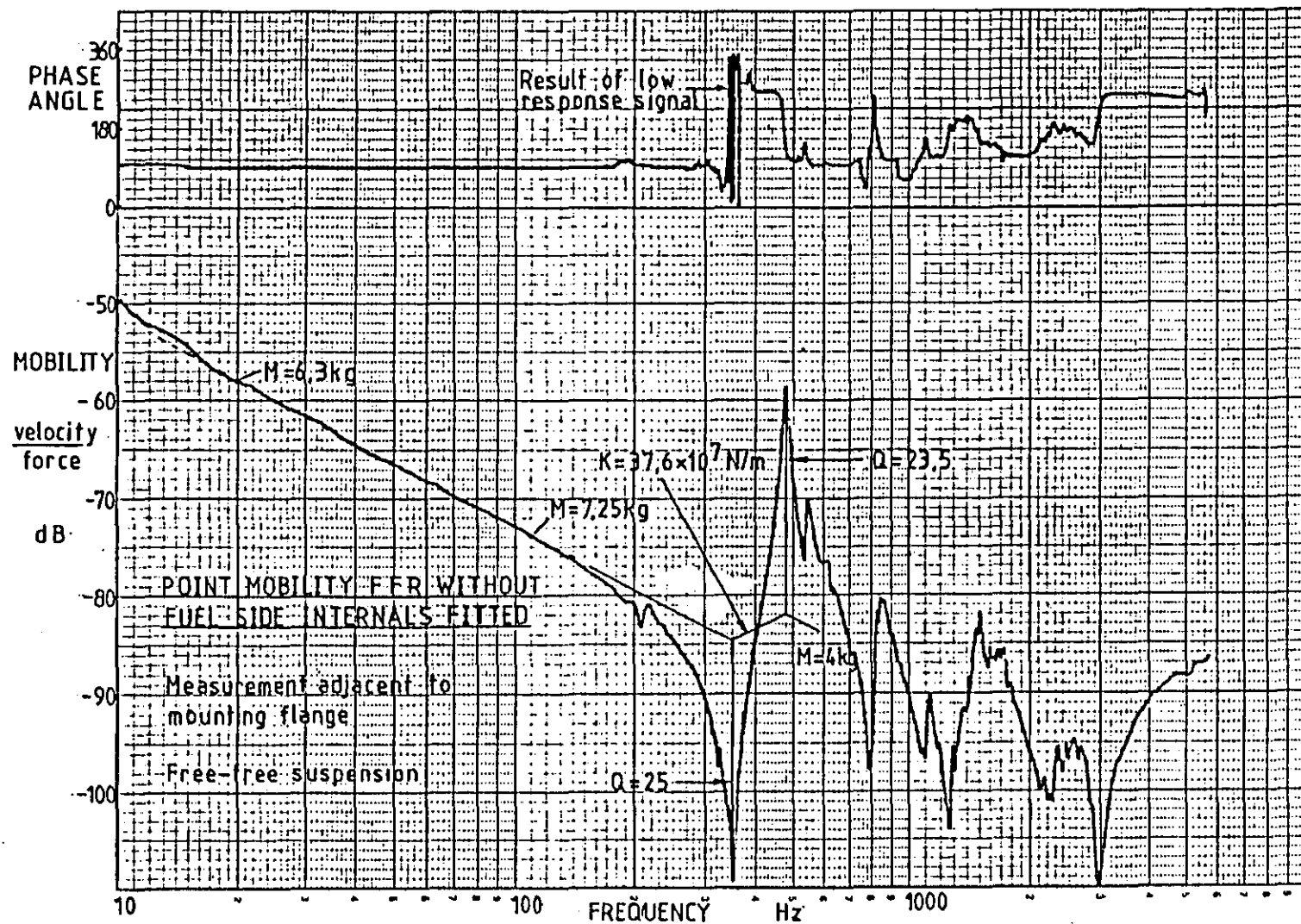


Fig C2

As damping begins to effect the response the mobility plot begins to deviate from the mass line until at 340 - 350 Hz an anti-resonance of the drive point is observed. This is followed by a resonance at 466-469 Hz with associated 180° phase change. The stiffness line between anti-resonance and resonance corresponds to 2.15×10^3 lbf/ins (3.76×10^8 N/m) and the subsequent mass line 8.8 lbs (4 kg).

After this point the Mobility plot shows several modes but since these are not accompanied by distinct 180° phase changes they are presumably natural frequencies of various air side components. It seems unlikely that they represent strongly coupled modes of structure.

In order to investigate the structural response of the unit itself without the effects of internal sub-system natural frequencies the test was repeated with the fuel side body alone.

C 3

FFR Fuel Side Body Results

The results of this test are shown in the driving point mobility plot of figure C.3. The initial mass line is now present to above 600 Hz varying from 7.5 lbs (3.4 kg) at 20 Hz to 8.8 lbs (4 kg) at 600 Hz. This compared with an actual mass of 19.3 lbs (8.75 kg), again the differences being explained by rotation about the centroid.

The initial drive point anti-resonance now occurs at 1500 Hz and has an associated stiffness of 6.4×10^3 lbf/ins (3.0×10^8 N/m) and a quality factor Q of 20 based on $\frac{1}{2}$ power points. This value has been quoted from the increased resolution obtained with figure C.4.

This anti-resonance is followed by what appears to be two small modes with some degree of coupling at 1675 and 1825 Hz. A clearer estimate of these would be obtained by varying the excitation input position.

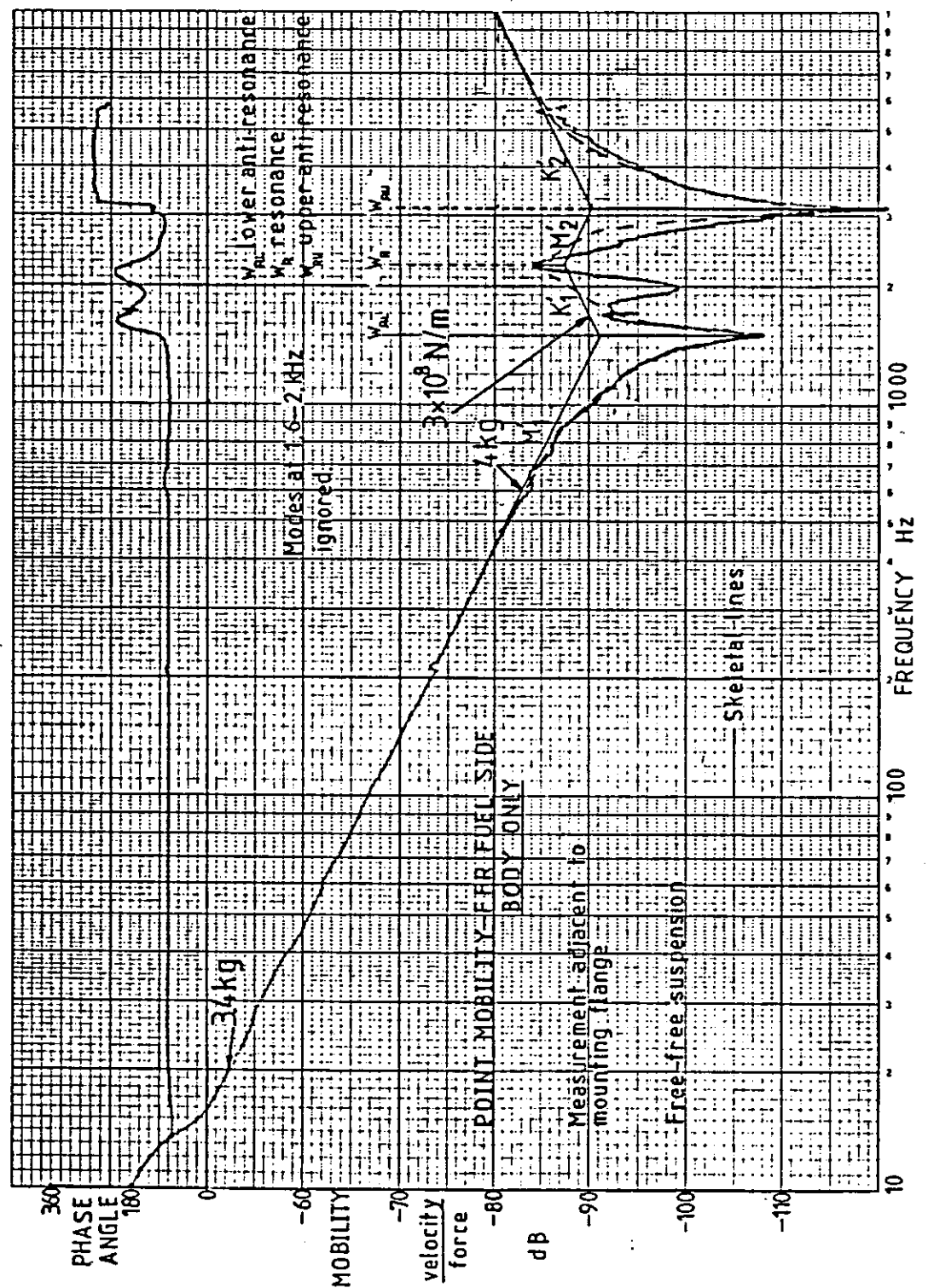


Fig. C.3

CHART
WELL

Graph Data Ref. 5511

Log 1 Cycle = mm, $\frac{1}{2}$ and 1 cm

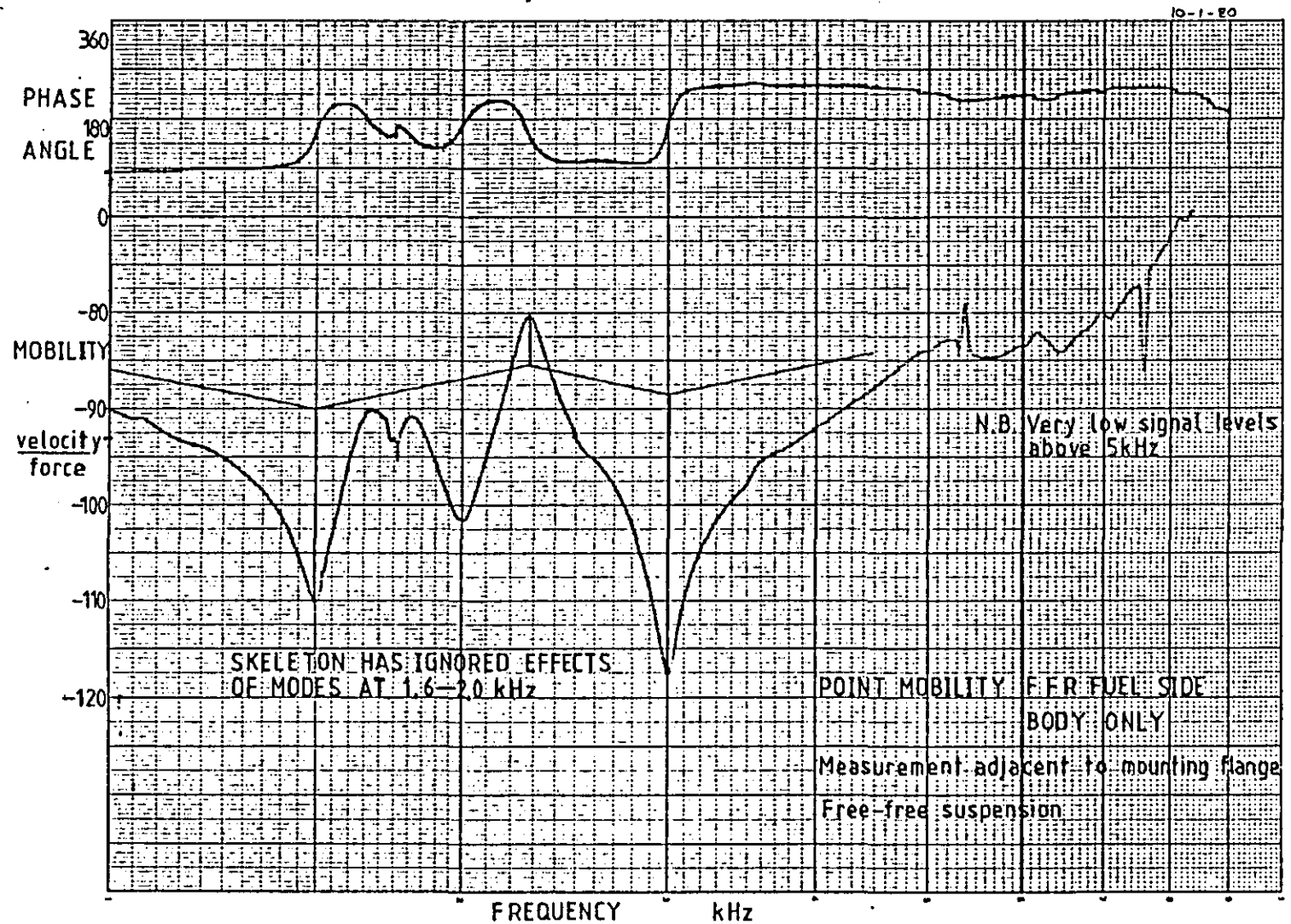


Fig. C4

At 2000 Hz is an anti-resonance with a Q of 10.75 and associated mass and stiffness of 2.6 lbs (2.7 Kg) and 9.2×10^3 lbf/ins (4.3×10^8 N/m). There is a strong resonance at 2270 Hz with a Q of 9 followed by a mass line of 2.1 lbs (2.1 kg).

A final anti-resonance is seen at 3000 Hz before the response changes to basically spring-like above this frequency.

C 4 Since drawing dimensions are given in metres, metric values only are shown here for clarity.

SCHEMATIC OF FFR—EFFECT OF EXCITATION AT MOUNTING FLANGE

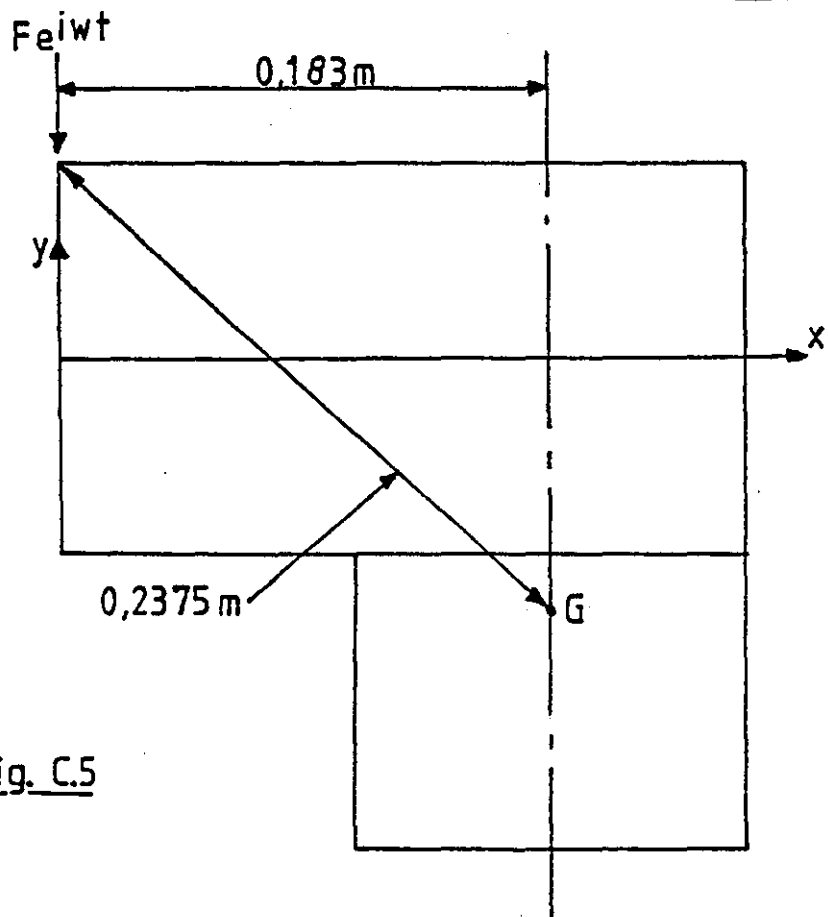


Fig. C.5

Total Unit Mass(m) acting through G = 24,3kg

For FFR Moment of Inertia about G(Ia) = mass (m) x
radius gyration (k)²

$$I_g = m.k^2$$

$$= 24.3 \times 0.183^2$$

Equating forces for small rotations about G we have for
a general displacement Y*

$$F e^{i\omega t} = 24.3 \times (-\omega^2 Y^* e^{i\omega t})$$

and

$$-F \cdot 0.2375 e^{i\omega t} = 24.3 \times 0.183^2 \times (-\omega^2 \frac{(Y^* - Y_o)}{0.2375} e^{i\omega t})$$

where Y_o is the displacement at the origin.

$$\frac{F}{\omega^2} \left(\frac{1}{14.427} + \frac{1}{24.3} \right) = -Y_o$$

$$Y_o/F = - 1/9.05 \omega^2$$

Hence the dynamic mass seen at the flange = 9.05 kg

This compares with a measured level of 7.5 to 8.5 kg.

```

LIST
1.  /*THIS PROGRAM IS CALLED 'CIRCLE' */
2.  /* THIS PROGRAM CAN BE EXECUTED FROM 'PLOT' IN TSO MODE */
3.  /* THIS PROGRAM PUTS A BEST FIT CIRCLE THROUGH A SET OF */
4.  /* EXPERIMENTAL DATA POINTS AND CALCULATES THE NATURAL */
5.  /* FREQUENCY, LOSS FACTOR, FLEXIBILITY AND RESIDUAL. */
10. DECLARE WHEN FILE ENV( F(80) SPACE(80,100) );
20. DECLARE default ENTRY EXT;
30. DECLARE X(75) CONTROLLED ,Y(75) CONTROLLED ,FREQ(75) CONTROLLED ;
40. DECLARE EX(75) CONTROLLED ,EY(75) CONTROLLED ;
50. DECLARE ES(75) CONTROLLED ,THETA(75) CONTROLLED ;
60. DECLARE CIRPLO ENTRY EXT;
70. PUT LIST('');
80. PUT LIST('CIRCLE FIT OF EXPERIMENTAL DATA');
90. PUT LIST('NUMBER OF DATA POINTS = ?');
100. GET LIST(N);
110. IF allocate(X)=1 THEN FREE X,Y,FREQ,EX,EY;
120. ALLOCATE X(N),Y(N),FREQ(N),EX(N),EY(N);
130. DO I=1 TO N;
140. GET LIST(FREQ(I),X(I),Y(I));
150. END ;
160. LET SIDE(X1,X2,Y1,Y2)=(X2-X1)**2+(Y2-Y1)**2;
170. LET ACOS(R,Q)=ATAN(SORT(R**2-Q**2)/Q);
180. /* COMPUTE SUMMATION TERMS */
190. X2,Y2,XV,X3,Y3,XV2,YX2, SX,SY=0;
200. DO I=1 TO N;
210. X2=X(I)**2+X2;
220. Y2=Y(I)**2+Y2;
230. XV=X(I)*Y(I)+XV;
240. X3=X(I)**3+X3;
250. Y3=Y(I)**3+Y3;
260. XV2=X(I)*Y(I)**2+XV2;
270. YX2=Y(I)**2*YX2+YX2;
280. SX=X(I)+SX;
290. SY=Y(I)+SY;
300. END ;
310. /* CALCULATION OF CIRCLE PROPERTIES */
320. /*
330. S=9X**2-N**2;
340. T=5X**2-N**2;
350. U=5Y**2-N**2;
360. U=5X**2+Y2)-N*(X3+XV2);
370. Z=5Y*(Y2+X2)-N*(Y3+YX2);
380. A=(U*U-T**2)/(U**2-S**2)*.5;
390. B=(U*T-S**2)/(T**2-S**2)*.5;
400. C=SORT(A**2+B**2+(X2+Y2)/N-2*(A*SX+B*SY)/N);
410. PUT LIST('');
420. PUT LIST('CENTRE COORDS. OF CIRCLE= ',A,B);
430. PUT LIST('');
440. PUT LIST('RADIUS= ',C);
450. /* CALCULATION OF FREQUENCY COORDINATES ON FITTED CIRCLE */
460. /*
470. DO I=1 TO N;
480. Z=sqrt((X(I)-A)**2+(Y(I)-B)**2);
490. EX(I)=(C*(X(I)-A)+Z*A)/Z;
500. EY(I)=(C*(Y(I)-B)+Z*B)/Z;
510. END ;
520. /* RESONANT FREQUENCY CALCULATION */
530. /*
540. IF ALLOCATE(ES)=1 THEN FREE ES,THETA;
550.

```

```

560. ALLOCATE THETA(N),ES(N);
570. DO I=1 TO N-1;
580. A1=SIDE(EX(I),EX(I+1),EY(I),EY(I+1));
590. B1=SIDE(EX(I),A,EY(I),B);
600. C1=SIDE(EX(I+1),A,EY(I+1),B);
610. Q1=B1+C1-A1;
620. R1=2*B1*C1;
630. THETA(I)=ACOS(R1,Q1);
640. ES(I)=2*B1*C1*THETA(I)/1260;
650. END ;
660. DARC=0;
670. K=0;
680. PUT LIST('I,DS1,DS2,DS3');
690. DO I=1 TO N-1;
700. PUT LIST(I,DS1,DS2,DS3);
710. DS1=ES(I)/(FREQ(I+1)-FREQ(I));
720. IF I=1 THEN DS2=0; ELSE DS2=ES(I-1)/(FREQ(I)-FREQ(I-1));
730. IF I=N-1 THEN DS3=0; ELSE DS3=ES(I+1)/(FREQ(I+1)-FREQ(I));
740. IF DS2=0|DS3=0 THEN GO TO LA;
750. IF DS1>DS2&DS1>DS3 THEN GO TO LD; ELSE GO TO LA;
760. IF I=N-1 THEN GO TO LA;
770. IF DS1<DARC THEN GO TO LA;
780. DARC=DS1;
790. K=I;
800. END ;
810. LAI
820. PUT LIST('K,DARC');
830. PUT LIST(K,DARC);
840. F=(FREQ(K+1)+FREQ(K))/2;
850. PUT LIST('');
860. PUT LIST('RESONANT FREQUENCY = ',F,'HERTZ');
870. PUT LIST('');
880. /* DAMPING CALCULATION */
890. /*
900. IF K>30 THEN FREQ(K+1)=FREQ(K+10)&FREQ(K)=FREQ(K-10);
910. IF K>30 THEN EX(K+1)=EX(K+10)&EX(K)=EX(K-10);
920. IF K>30 THEN EY(K+1)=EY(K+10)&EY(K)=EY(K-10);
930. FT=(FREQ(K+1)**2-FREQ(K)**2)/F**2;
940. H1=(EX(K+1)**2+EY(K+1)**2-EX(K)**2-EY(K)**2)/(2*(EY(K+1)-EY(K)));
950. H2=(EX(K+1)-EX(K))/(EY(K+1)-EY(K));
960. H3=1+H2**2;
970. H4=A+H2*(H1-B);
980. H5=A**2-C**2+(H1-B)**2;
990. EXF1=(H4+SORT(H4**2-H5*H3))/H3;
1000. EXF2=(H4-SORT(H4**2-H5*H3))/H3;
1010. PUT LIST('EXF1','EXF1','EXF2','EXF2');
1020. IF EX(K+1)&EX(K) THEN GO TO LB;
1030. IF EXF1>EX(K)&EXF1>EX(K+1) THEN EXF=EXF1;
1040. IF EXF2>EX(K)&EXF2>EX(K+1) THEN EXF=EXF2;
1050. IF EXF1<EX(K)&EXF1<EX(K+1) THEN EXF=EXF1;
1060. IF EXF2<EX(K)&EXF2<EX(K+1) THEN EXF=EXF2;
1070. EYF=H1-H2*EXF;
1080. PUT LIST('');
1090. PUT LIST('COORDINATES OF RESONANT FREQUENCY=?');
1100. PUT LIST(EXF,EYF);
1110. PUT LIST('');
1120. LET TAN(X)=SIN(X)/COS(X);
1130. A2=SIDE(EX(K),EXF,EY(K),EYF);
1140. B2=SIDE(EX(K),A,EY(K),B);
1150. C2=SIDE(EX(K+1),A,EY(K+1),B);
1160. Q2=B2+C2-A2;
1170.
1180.
1190.
1200.
1210.
1220.
1230.
1240.
1250.
1260.
1270.
1280.
1290.
1300.
1310.
1320.
1330.
1340.
1350.
1360.
1370.
1380.
1390.
1400.
1410.
1420.
1430.
1440.
1450.
1460.
1470.
1480.
1490.
1500.
1510.
1520.
1530.
1540.
1550.
1560.
1570.
1580.
1590.
1600.
1610.
1620.
1630.
1640.
1650.
1660.
1670.
1680.
1690.
1700.
1710.
1720.
1730.
1740.
1750.
1760.
1770.
1780.
1790.
1800.
1810.
1820.
1830.
1840.
1850.
1860.
1870.
1880.
1890.
1900.
1910.
1920.
1930.
1940.
1950.
1960.
1970.
1980.
1990.
2000.
2010.
2020.
2030.
2040.
2050.
2060.
2070.
2080.
2090.
2100.
2110.
2120.
2130.
2140.
2150.
2160.
2170.
2180.
2190.
2200.
2210.
2220.
2230.
2240.
2250.
2260.
2270.
2280.
2290.
2300.
2310.
2320.
2330.
2340.
2350.
2360.
2370.
2380.
2390.
2400.
2410.
2420.
2430.
2440.
2450.
2460.
2470.
2480.
2490.
2500.
2510.
2520.
2530.
2540.
2550.
2560.
2570.
2580.
2590.
2600.
2610.
2620.
2630.
2640.
2650.
2660.
2670.
2680.
2690.
2700.
2710.
2720.
2730.
2740.
2750.
2760.
2770.
2780.
2790.
2800.
2810.
2820.
2830.
2840.
2850.
2860.
2870.
2880.
2890.
2900.
2910.
2920.
2930.
2940.
2950.
2960.
2970.
2980.
2990.
3000.
3010.
3020.
3030.
3040.
3050.
3060.
3070.
3080.
3090.
3100.
3110.
3120.
3130.
3140.
3150.
3160.
3170.
3180.
3190.
3200.
3210.
3220.
3230.
3240.
3250.
3260.
3270.
3280.
3290.
3300.
3310.
3320.
3330.
3340.
3350.
3360.
3370.
3380.
3390.
3400.
3410.
3420.
3430.
3440.
3450.
3460.
3470.
3480.
3490.
3500.
3510.
3520.
3530.
3540.
3550.
3560.
3570.
3580.
3590.
3600.
3610.
3620.
3630.
3640.
3650.
3660.
3670.
3680.
3690.
3700.
3710.
3720.
3730.
3740.
3750.
3760.
3770.
3780.
3790.
3800.
3810.
3820.
3830.
3840.
3850.
3860.
3870.
3880.
3890.
3900.
3910.
3920.
3930.
3940.
3950.
3960.
3970.
3980.
3990.
4000.
4010.
4020.
4030.
4040.
4050.
4060.
4070.
4080.
4090.
4100.
4110.
4120.
4130.
4140.
4150.
4160.
4170.
4180.
4190.
4200.
4210.
4220.
4230.
4240.
4250.
4260.
4270.
4280.
4290.
4300.
4310.
4320.
4330.
4340.
4350.
4360.
4370.
4380.
4390.
4400.
4410.
4420.
4430.
4440.
4450.
4460.
4470.
4480.
4490.
4500.
4510.
4520.
4530.
4540.
4550.
4560.
4570.
4580.
4590.
4600.
4610.
4620.
4630.
4640.
4650.
4660.
4670.
4680.
4690.
4700.
4710.
4720.
4730.
4740.
4750.
4760.
4770.
4780.
4790.
4800.
4810.
4820.
4830.
4840.
4850.
4860.
4870.
4880.
4890.
4900.
4910.
4920.
4930.
4940.
4950.
4960.
4970.
4980.
4990.
5000.
5010.
5020.
5030.
5040.
5050.
5060.
5070.
5080.
5090.
5100.
5110.
5120.
5130.
5140.
5150.
5160.
5170.
5180.
5190.
5200.
5210.
5220.
5230.
5240.
5250.
5260.
5270.
5280.
5290.
5300.
5310.
5320.
5330.
5340.
5350.
5360.
5370.
5380.
5390.
5400.
5410.
5420.
5430.
5440.
5450.
5460.
5470.
5480.
5490.
5500.
5510.
5520.
5530.
5540.
5550.
5560.
5570.
5580.
5590.
5600.
5610.
5620.
5630.
5640.
5650.
5660.
5670.
5680.
5690.
5700.
5710.
5720.
5730.
5740.
5750.
5760.
5770.
5780.
5790.
5800.
5810.
5820.
5830.
5840.
5850.
5860.
5870.
5880.
5890.
5900.
5910.
5920.
5930.
5940.
5950.
5960.
5970.
5980.
5990.
6000.
6010.
6020.
6030.
6040.
6050.
6060.
6070.
6080.
6090.
6100.
6110.
6120.
6130.
6140.
6150.
6160.
6170.
6180.
6190.
6200.
6210.
6220.
6230.
6240.
6250.
6260.
6270.
6280.
6290.
6300.
6310.
6320.
6330.
6340.
6350.
6360.
6370.
6380.
6390.
6400.
6410.
6420.
6430.
6440.
6450.
6460.
6470.
6480.
6490.
6500.
6510.
6520.
6530.
6540.
6550.
6560.
6570.
6580.
6590.
6600.
6610.
6620.
6630.
6640.
6650.
6660.
6670.
6680.
6690.
6700.
6710.
6720.
6730.
6740.
6750.
6760.
6770.
6780.
6790.
6800.
6810.
6820.
6830.
6840.
6850.
6860.
6870.
6880.
6890.
6900.
6910.
6920.
6930.
6940.
6950.
6960.
6970.
6980.
6990.
7000.
7010.
7020.
7030.
7040.
7050.
7060.
7070.
7080.
7090.
7100.
7110.
7120.
7130.
7140.
7150.
7160.
7170.
7180.
7190.
7200.
7210.
7220.
7230.
7240.
7250.
7260.
7270.
7280.
7290.
7300.
7310.
7320.
7330.
7340.
7350.
7360.
7370.
7380.
7390.
7400.
7410.
7420.
7430.
7440.
7450.
7460.
7470.
7480.
7490.
7500.
7510.
7520.
7530.
7540.
7550.
7560.
7570.
7580.
7590.
7600.
7610.
7620.
7630.
7640.
7650.
7660.
7670.
7680.
7690.
7700.
7710.
7720.
7730.
7740.
7750.
7760.
7770.
7780.
7790.
7800.
7810.
7820.
7830.
7840.
7850.
7860.
7870.
7880.
7890.
7900.
7910.
7920.
7930.
7940.
7950.
7960.
7970.
7980.
7990.
8000.
8010.
8020.
8030.
8040.
8050.
8060.
8070.
8080.
8090.
8100.
8110.
8120.
8130.
8140.
8150.
8160.
8170.
8180.
8190.
8200.
8210.
8220.
8230.
8240.
8250.
8260.
8270.
8280.
8290.
8300.
8310.
8320.
8330.
8340.
8350.
8360.
8370.
8380.
8390.
8400.
8410.
8420.
8430.
8440.
8450.
8460.
8470.
8480.
8490.
8500.
8510.
8520.
8530.
8540.
8550.
8560.
8570.
8580.
8590.
8600.
8610.
8620.
8630.
8640.
8650.
8660.
8670.
8680.
8690.
8700.
8710.
8720.
8730.
8740.
8750.
8760.
8770.
8780.
8790.
8800.
8810.
8820.
8830.
8840.
8850.
8860.
8870.
8880.
8890.
8900.
8910.
8920.
8930.
8940.
8950.
8960.
8970.
8980.
8990.
9000.
9010.
9020.
9030.
9040.
9050.
9060.
9070.
9080.
9090.
9100.
9110.
9120.
9130.
9140.
9150.
9160.
9170.
9180.
9190.
9200.
9210.
9220.
9230.
9240.
9250.
9260.
9270.
9280.
9290.
9300.
9310.
9320.
9330.
9340.
9350.
9360.
9370.
9380.
9390.
9400.
9410.
9420.
9430.
9440.
9450.
9460.
9470.
9480.
9490.
9500.
9510.
9520.
9530.
9540.
9550.
9560.
9570.
9580.
9590.
9600.
9610.
9620.
9630.
9640.
9650.
9660.
9670.
9680.
9690.
9700.
9710.
9720.
9730.
9740.
9750.
9760.
9770.
9780.
9790.
9800.
9810.
9820.
9830.
9840.
9850.
9860.
9870.
9880.
9890.
9900.
9910.
9920.
9930.
9940.
9950.
9960.
9970.
9980.
9990.
1000.

```

```

1110.      RB=2*RB2*CB;
1120.      PHI1=ACOS(RB,OB);
1130.      A3=SIDE(EXF,EX(K+1),EYF,EY(K+1));
1140.      B3=SIDE(EXF,A,EYF,B);
1150.      C3=SIDE(EX(K+1),A,EY(K+1),B);
1160.      Q3=B3+C3-A3;
1170.      R3=2*B3*C3;
1180.      PHI2=ACOS(R3,Q3);
1190.      PHI=ATAN(TAN(PHI1*.5)+TAN(PHI2*.5));
1200.      PUT LIST('FT,PHI1,PHI2,PHI');
1210.      PUT LIST('FT,PHI1,PHI2,PHI');
1220.      NETA=FT/PHI;
1230.      PUT LIST('');
1240.      PUT LIST('DAMPING = ',NETA);
1250.      PUT LIST('');
1260.      /* FLEXIBILITY CALCULATION */;
1261.      /*
1270.      CR=2*CR*NETA;
1280.      PUT LIST('FLEXIBILITY = ',CR,'10**6 m/N');
1290.      PUT LIST('');
1300.      /* CALCULATION OF CONTRIBUTION OF OTHER MODES */;
1301.      /*
1310.      EXF1=2*A-EXF;
1320.      EYF1=2*B-EYF;
1330.      DR=SQRT(EXF1**2+EYF1**2);
1340.      PUT LIST('CONTRIBUTION OF OTHER MODES=',DR);
1350.      PUT LIST('');
1360.      STORE FILE AHEH COPY;
1361.      /* COMPLETION OF COMPUTATION */;
1370.      /* K540 PLOTTING INSTRUCTIONS */;
1371.      /*
1380.      PUT LIST('INIT,2,Q1,,CHAR 1,FREQ.,REAL,DEF;PAR Y.,REAL 2;PAR X,PAR EX,PAR EY');
1390.      PUT LIST('ADD Q1 A');
1400.      PUT LIST('DIM',N,'ARR');
1410.      PUT LIST('ADD X +');
1420.      CALL datout(X,N,AHEH);
1430.      PUT LIST('ADD Y +');
1440.      CALL datout(Y,N,AHEH);
1450.      PUT LIST('ADD FREQ +');
1460.      CALL datout(FREQ,N,AHEH);
1470.      PUT LIST('MERGE');
1480.      PUT LIST('ADD Q1 C');
1490.      PUT LIST('DIM',N,'ARR');
1500.      PUT LIST('ADD EX +');
1510.      CALL datout(EX,N,AHEH);
1520.      PUT LIST('ADD EY +');
1530.      CALL datout(EY,N,AHEH);
1540.      PUT LIST('ADD FREQ +');
1550.      CALL datout(FREQ,N,AHEH);
1560.      PUT LIST('MERGE');
1570.      PUT LIST('ADD Q1 B');
1580.      CALL CIRPLO(A,B,C,AHEH);
1590.      PUT LIST('DISPLAY,X X,Y Y,SYM,CURVE C2 NEU,X XPLOT,Y YPLOT,LINE ITP 2,EQUAL,');
1600.      PUT LIST('CURVE C3 NEU,X EX,Y EY,SYM,NOLINE,NOLEG,');
1610.      PUT LIST('SEL S1=Q1.EQ.'B',Y,CURVE C2,USE SEL S1,');
1620.      PUT LIST('CURVE C3,NOLEG,GR 1,60');
1630.      STORE *;
1640.      CLOSE FILE(AHEH);
1641.      /* END OF PLOTTING ROUTINE */;

```


APPENDIX D

Signal Processing Techniques

Fig 1.2 showed a Campbell Diagram (Frequency to 10Kz v Time, expressed as shaft speed) derived from an accelerometer measurement on an external gearbox. This particular plot and the similar one shown in figure D1 were both obtained from a mini-computer display of the output obtained from a Real Time Spectrum Analyser (RTA), in this instance a Nicolet UA - 500 A and Nova 422 computer. A block diagram of the system is shown in figure D2 and detailed description in 7.6.1.

The RTA acts as 500 bandpass filters arranged in parallel so that the amplitude of that portion of the incoming waveform which falls within a given frequency band is obtained at the analyser output. However, since the time taken to reach the true amplitude in each filter is inversely proportioned to the filter bandwidth it would take 0.05 seconds for the 10 KHz signal to reach the correct amplitude with a resolution of 20 Hz. If better resolution is required this can only be achieved at the expense of time i.e. 0.1 Hz resolution requires 10 seconds.

In fact the RTA only has one filter and this is effectively slid across the whole frequency range at high speed to give a frequency expansion of the actual signal and hence time compression. With reference to the block diagram in figure D2 this is achieved by first low-pass filtering the input signal to prevent aliasing of the input signal when sampling it at a rate determined by the analysis range set. The sampled signals are then digitised and passed into a recirculating digital memory. The loading of the data blocks is accomplished during hundreds of circulations of the memory but the readout is completed during only one recirculation. The relationship between the load and readout time (500 : 1 on the UA-500) gives the amount of time compression occurring. The digital output from the memory is converted back to analogue and the recreated

input signal is observed but with an expanded frequency range (e.g 5 MHz for the 10 KHz range of figure 1.2). This analogue signal is then spectrum analysed with a sweeping filter (10 KHz nominal).

Hence each memory recirculation, which takes 100 μ sec, produces one line of the 500 line spectrum and the full spectrum is produced in just 0.05 secs as with the 500 parallel band-pass filters. Hence the one filter is producing the same result as 500 in parallel.

This time compressed signal is then again digitised and either stored in a memory if signal averaging is being performed, or fed directly to the computer input for storage on disc, or it can be converted back to analogue for direct display on some output device such as described in 7.6.2 and 7.6.3. It is apparent from all this A/D conversion why more recent analysers work purely with digital data.

In actual operation the recirculating digital memory is continually being updated with new blocks of data and hence the output spectrum represents a continually changing period of time, the storage of which is purely limited by the size of the computer disc store something like 8000 spectra for the equipment used in this work.

In fact the UA-500 analyser can analyse frequency ranges above 10 KHz but it then has to store data and send the output out in batches i.e. it is no longer operating in real time.

Returning to figure D2 it should be noted that the shaft speeds corresponding to the particular instantaneous spectra are sampled and stored by the mini-computer.

On completion of the data acquisition stage the stored spectra and speeds can be recalled and manipulated within the computer to give the required annotated display format.

The Campbell Diagram displayed in figure D1 has an 'X' symbol plotted at every 50 rpm increments to represent an amplitude above a preset threshold level which in this case is 0.2"/s. Also to be seen are circles scaled relative to the standard circle near the origin of the plot. This standard circle is given the calibration level indicated to the right of the plot. These circles are plotted when an amplitude peak is reached or can be plotted if a certain threshold level is exceed depending on the input instructions.

To ease identification of the spectral data presented above, integer engine shaft speed harmonics (or orders) are also drawn on the diagram, with the spacing and number controlled by the input instructions. These shaft orders are relative to the particular abscissa scale shaft speed chosen. In figure D1 this is the high speed shaft N3. Spectral orders which do not vary linearly with increasing engine speed can either be caused by another shaft or if basically parallel to the abscissa usually indicate the presence of a resonance of the structure.

Also shown in figure D1 (b) and (c) is another output option which has tracked a predetermined integer or non-integer engine order and displayed the amplitude variation of the signal as it varies with speed. Fig D.1.d represents a three dimensional display of the above data and shows the views used to obtain the plots a - c.

With accelerometer data it is also possible to integrate (or double integrate) the data as necessary, although for most testing in order to obtain a reasonable dynamic range in the recording, the accelerometer signal is integrated to give velocity at the conditioning stage (Ref 7.6.4 for further details).

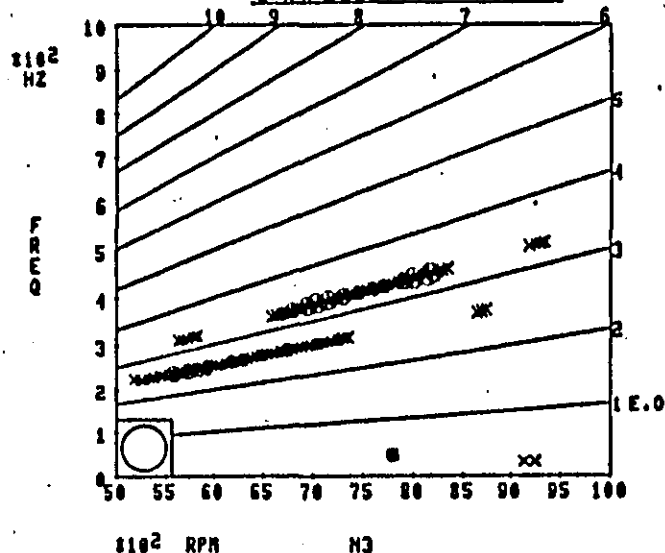
The computer can be used to obtain the rms velocity (V_{rms}) content in the signal under analysis between predetermined frequency boundaries and above a certain threshold.

Unfortunately, the system currently available can only analyse single data channels and it is not therefore possible to store different data tracks to obtain the resultant velocity (VRES) required for the severity criteria described in Section 4.1. For this thesis this has had to be done by hand looking at the peak levels.

It is probable that with new equipment under review it will be possible to perform multi-channel analysis and hence compute VRES directly and apply the appropriate flight weightings.

PROBLEM TITLE: FANCASE MOUNTED ACCESSORY - VIBRATION SURVEY
 CONFIGURATION: ACCEL - HIGH LOAD
 TRANSDUCER: FFR END AX THRESHOLDS: 0.20 IN/S

CAMPBELL DIAGRAM (A)



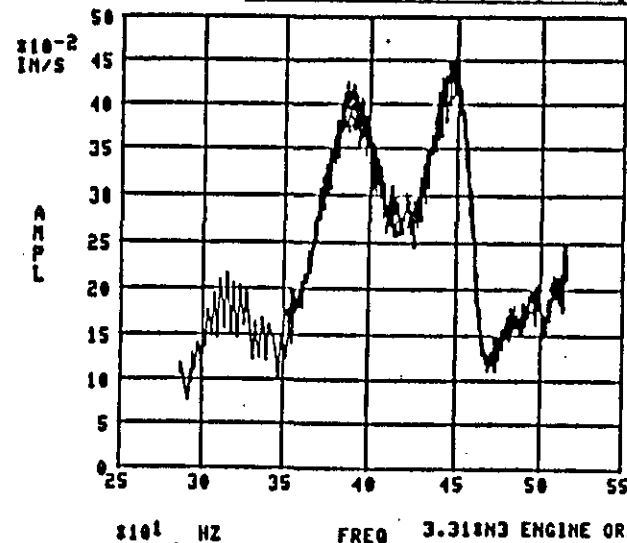
MET NO: 58139
 RB211-535
 ENG NO: 17/1
 DATE: 20-4-80
 PLOT NO: 1

AR 1000
 AA -20
 CA 4
 TT 6
 TI 32
 INC RRM150

CAL CIRCLE:
 1.0 IN/S

PROBLEM TITLE: FANCASE MOUNTED ACCESSORY - VIBRATION SURVEY
 CONFIGURATION: ACCEL - HIGH LOAD
 TRANSDUCER: FFR END AX

TRACKED ORDER v. FREQUENCY (C)

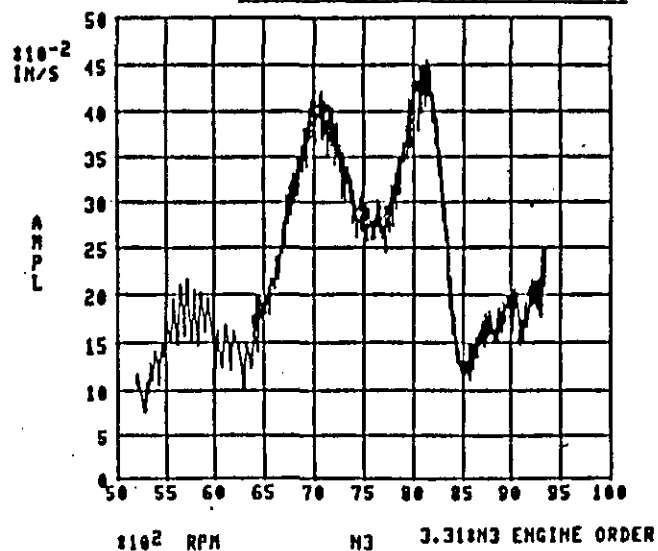


MET NO: 58139
 RB211-535
 ENG NO: 17/1
 DATE: 20-4-80
 PLOT NO: 3-1

AR 1000
 AA -20
 CA 4
 TT 6
 TI 32

PROBLEM TITLE: FANCASE MOUNTED ACCESSORY - VIBRATION SURVEY
 CONFIGURATION: ACCEL - HIGH LOAD
 TRANSDUCER: FFR END AX

TRACKED ORDER v. SPEED (B)



MET NO: 58139
 RB211-535
 ENG NO: 17/1
 DATE: 20-4-80
 PLOT NO: 2

AR 1000
 AA -20
 CA 4
 TT 6
 TI 32

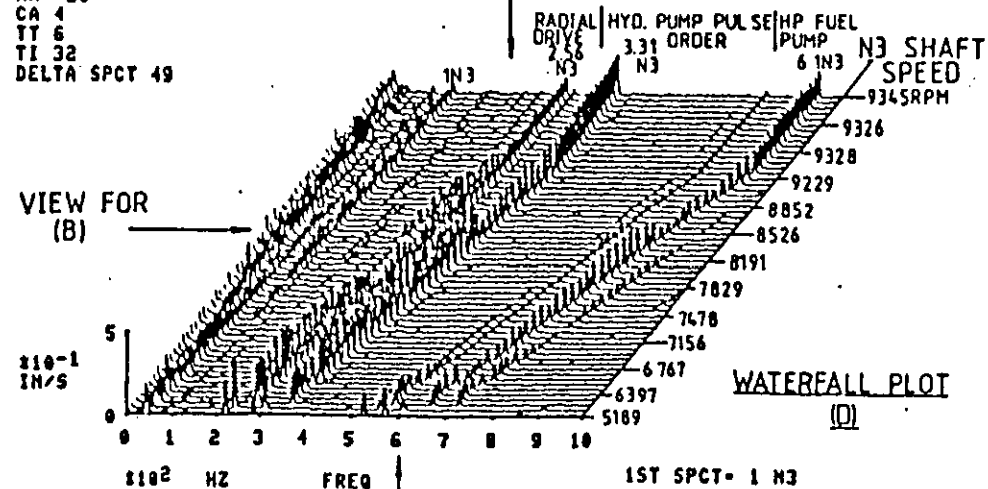
PROBLEM TITLE: FANCASE MOUNTED ACCESSORY - VIBRATION SURVEY
 CONFIGURATION: ACCEL - HIGH LOAD
 TRANSDUCER: FFR END AX

MET NO: 58139
 RB211-535
 ENG NO: 17/1
 DATE: 20-4-80
 PLOT NO: 1

AR 1000
 AA -20
 CA 4
 TT 6
 TI 32
 DELTA SPCT 49

VIEW FOR
 CAMPBELL DIAGRAM (A)

VIEW FOR
 (B)



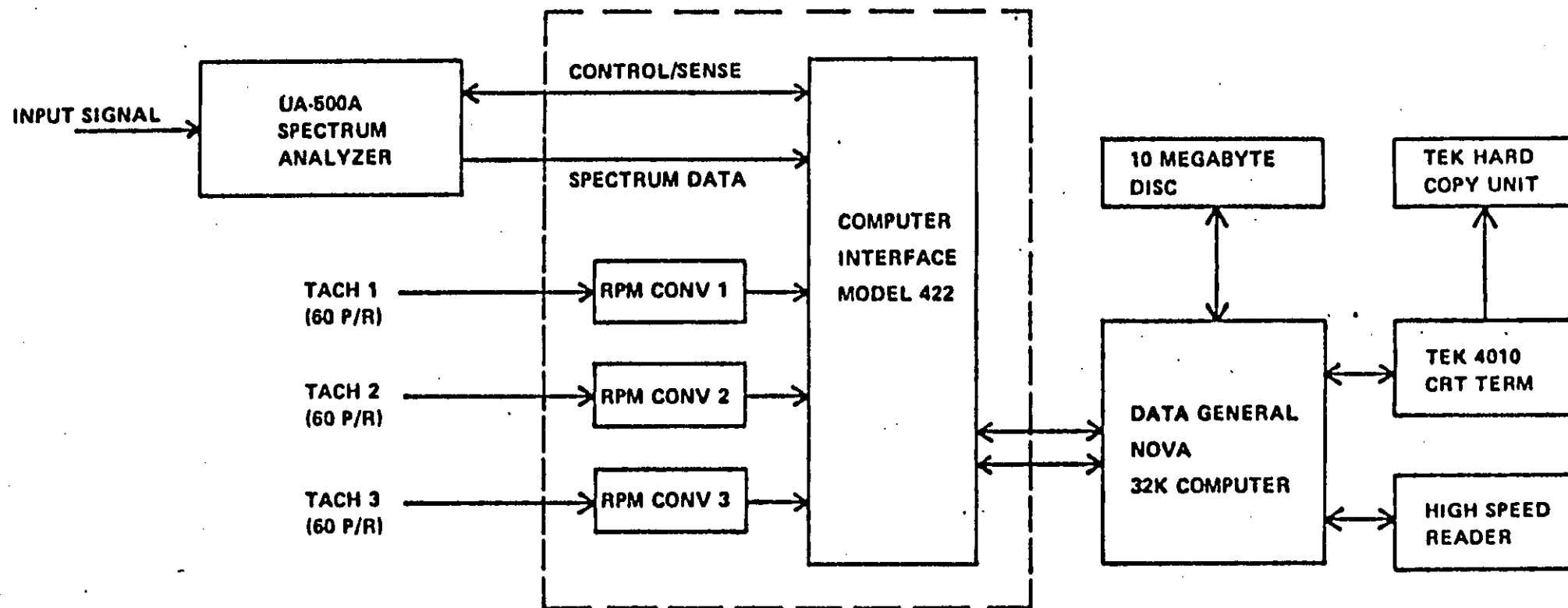


Fig. D.2

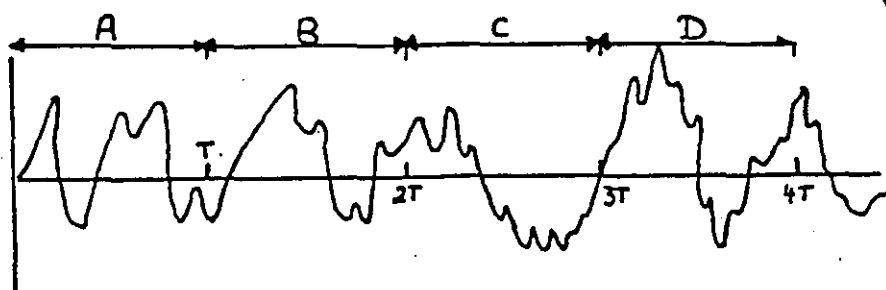
CAMPBELL DIAGRAM SYSTEM

APPENDIX E - Excitation Techniques

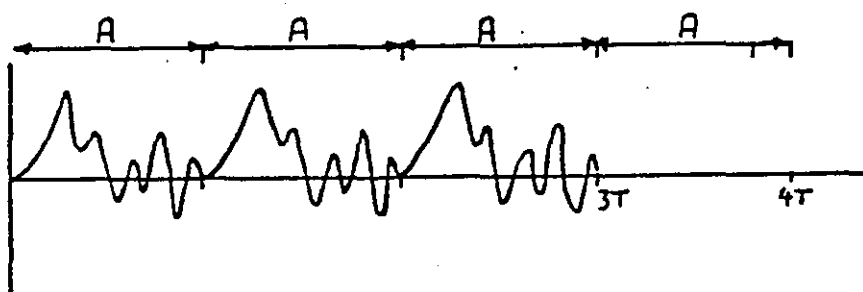
In this work and during the course of the research various excitation techniques have been mentioned or tried. The advantages and disadvantages of the various techniques are well known being detailed in such works as 7.6.5 to 7.6.19.

1. The main excitation technique used has been Swept Sine. This approximates to the steady state vibration excitation condition giving good results although somewhat time consuming.
2. Also investigated were the various forms of Random Excitation. The basic techniques used are summarised in figure E.1 as is a typical problem in figure E.2. These techniques gave acceptable results in a far shorter timescale but required a Fast Fourier Transform analyser to carry out the analysis. An analyser of this type was not available until late in the project.
3. The final excitation formats tested fall under the heading of Transient techniques. In particular based on the work at Southampton University the Chirp (or Fast Sine Sweep) was investigated (7.6.13 - 15). This technique is summarised in figure E.3 and appeared useful. However, it was found that it was necessary to disconnect the exciter in some way to ensure that the mass and damping of the exciter system did not corrupt the accessory's response characteristics. Reference 7.6.19 gives a summary of the practicalities of using 'chirp' excitation.

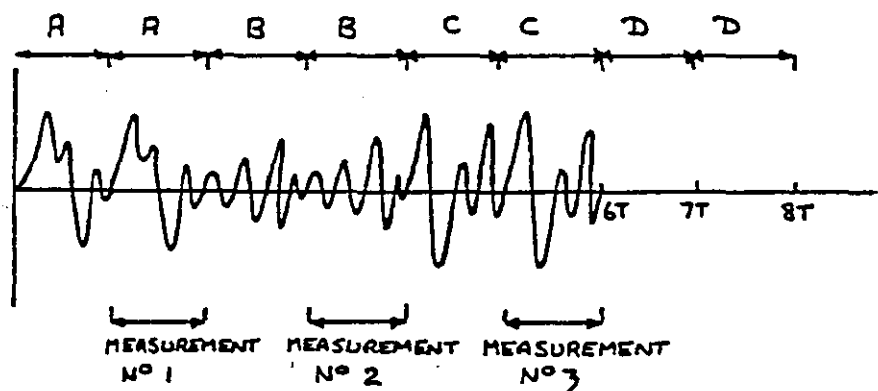
A. PURE RANDOM



B. PSEUDO RANDOM



C. PERIODIC RANDOM

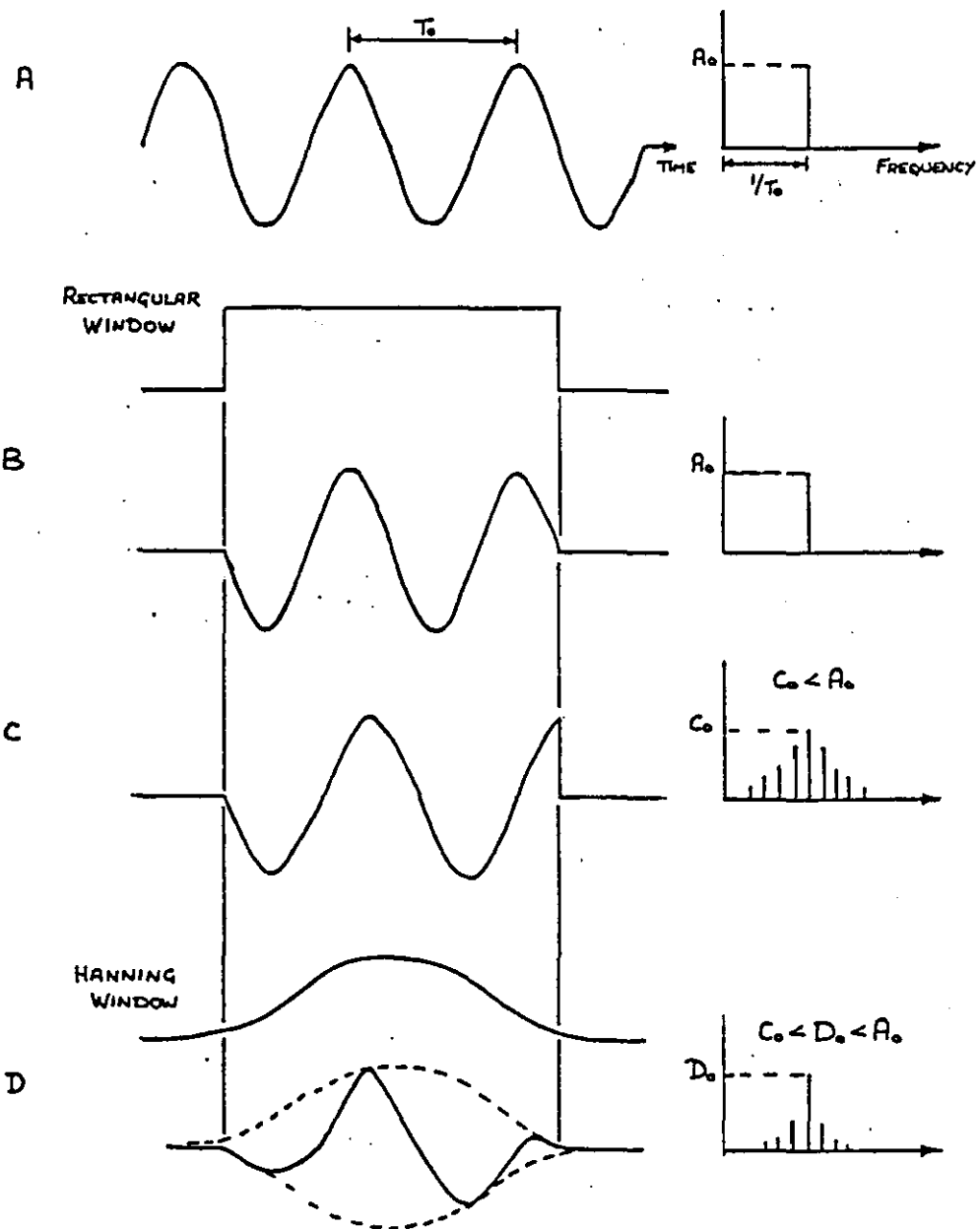


A. PURE RANDOM IS NEVER PERIODIC.

B. PSEUDO RANDOM IS EXACTLY PERIODIC EVERY T SECONDS.

C. PERIODIC RANDOM IS A PSEUDO RANDOM SIGNAL THAT IS CHANGED FOR EVERY ENSEMBLE AVERAGE.

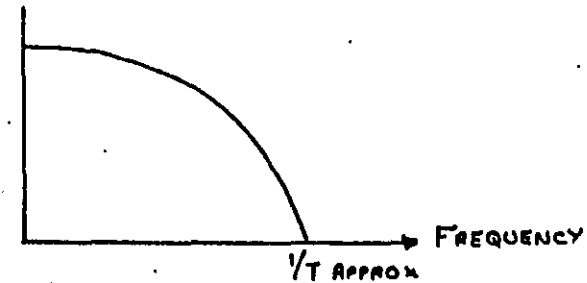
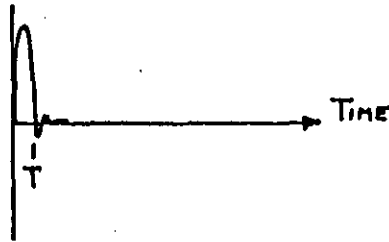
FIG E.1



- A. A CONTINUOUS TIME-VARYING SINEWAVE IS REPRESENTED BY A SINGLE LINE OF AMPLITUDE A_0 SAY, IN THE FREQUENCY DOMAIN.
- B. WHEN OBSERVED THROUGH A STANDARD RECTANGULAR WINDOW IT IS STILL A SINGLE SPECTRAL LINE IF EXACTLY PERIODIC WITHIN THE WINDOW.
- C. IF IT IS NOT EXACTLY PERIODIC 'LEAKAGE' OCCURS AND ENERGY IS SEEN IN ADJACENT FREQUENCY CHANNELS.
- D. MULTIPLYING THE SIGNAL BY SUCH WINDOWS AS THE HANNING RESTORES SOME OF THE PERIODICITY REQUIREMENT REDUCING LEAKAGE EFFECTS.

FIG E.2

A. IMPACT (OR STEP RELAXATION)



B. 'CHIRP'

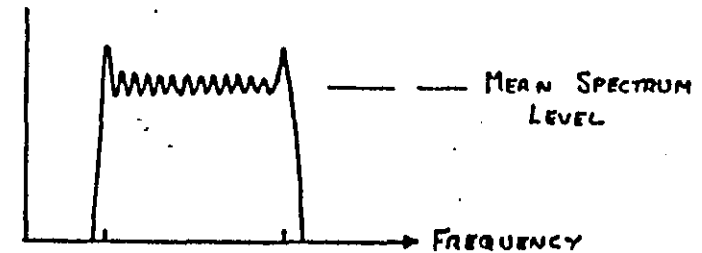
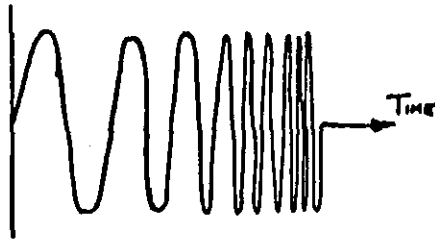


FIG B.3

FOR SWEPT SINEWAVE

$$x(t) = \sin(at^2 + bt) \quad 0 \leq t \leq T$$

IF INITIAL FREQUENCY IS F_1

FINAL FREQUENCY IS F_2

$$a = \frac{\pi}{T^2}(F_2 - F_1), \quad b = 2\pi F_1$$

PROPERTIES OF POWER SPECTRUM:-

1. MEAN VALUE OF SPECTRUM = $\pi/4a$
2. THE SPECTRUM IS NOT FLAT BUT HAS TWO PEAKS, $1.4 \times$ MEAN SPECTRUM LEVEL IN HEIGHT (APPROX), AT $F_1 + 1.2\sqrt{a/2\pi}$ AND $F_2 - 1.2\sqrt{a/2\pi}$ Hz.
3. THE AMPLITUDE RIPPLE IS PROPORTIONAL TO $1/\sqrt{T}$.
4. THE CUT-OFF RATE AT F_1 AND F_2 IS HIGH.

APPENDIX F - Use of Rms Velocity

In 3.2 it was stated that for accessories the vibration response spectra amplitudes should be expressed in velocity and root mean square (rms) velocity in particular. The reasons for this are based on the following considerations:-

- C 1) All practical structures contain some form of damping which dissipates the Kinetic Energy of the vibration as heat. This dissipation can be the result of friction between adjacent surfaces, or air or fluid resistance, or electrical damping or impacts between sub-systems. It may also result from the imperfect elastic properties of the vibrating material.

For an accessory of mass m and vibrating at a velocity v , the kinetic energy present is given by

$$\text{Kinetic Energy} = \frac{1}{2} m v^2$$

Hence the energy dissipation for a given structure is proportional to the square of the vibration velocity.

The above damping sources can result in fretting or wear on mechanical parts, or general operational problems. Therefore it has been common practice to relate the velocity measurement of vibration to its destructive ability.

- C 2) Consider a piece of equipment which when subject to a certain excitation shows resonances responding to $1''/s$ at 10 and 1000 Hz. From the above the energy dissipation is similar being independent of frequency and hence equal velocity amplitudes have been associated with equal vibration severity.

In addition for a sinusoid velocity is related simply by frequency to both displacement and acceleration, which results in velocity giving a very reasonable dynamic

range for analysis.

Considering the above example

1"/s is equivalent to 0.032" at 10 Hz and 0.00032" at 1000 Hz, or 0.163g at 10 Hz and 16.3g at 1000 Hz if expressed in acceleration.

Hence for displacement or acceleration measurements both analysis systems would require a dynamic range of at least 100 : 1 (or 40 dB).

- C 3) In reference 7.2.5 it is stated that the general intensity of any random data may be described in rudimentary terms by a mean square value which is simply the average of the squared values of the time history. In physical terms the mean square value is a measure of the total area under a power spectral density plot and hence is a measure of the signal energy content. The root mean square value is by definition the positive root of the mean square value and hence the rms value X_{rms} may be defined at

$$X_{rms} = \sqrt{(1/T \cdot \int_0^T x^2(t) \cdot dt)}$$

In Appendix A of reference 7.6.18 it is shown that this is a statement of the standard derivation of the time history $x(t)$ about its mean. Hence measuring rms velocity not only gives a direct estimate of the power involved in a process but also gives a direct estimate of the process statistics.

- C 4) Recent electronic advances have meant that true rms measurements are now easy to make.

